Order Number 9405593

SEM and FTIR investigation of bulk crystallized TPI and its epoxidized copolymers

Vasanthan, Nadarajah, Ph.D.

City University of New York, 1993

U·M·I
300 N. Zeeb Rd.
Ann Arbor, MI 48106

SEM AND FTIR INVESTIGATION OF BULK CRYSTALLIZED TPI AND ITS EPOXIDIZED COPOLYMERS

by

NADARAJAH VASANTHAN

A dissertation submitted to the Graduate Faculty in Chemistry in partial fulfillment of the requirements for the degree of Doctor of Philosophy, The City University of New York

1993

This manuscript has been read and accepted for the Graduate Faculty in Chemistry in satisfaction of the dissertation requirement for the degree of Dooctor of Philosophy.

9/7/93
date

Arthur E Woodward
Chairman of Examining Committee

9/7/93
date

Executive Officer

Supervisory Committee

The City University of New York

Abstract

FTIR AND SEM INVESTIGATION OF BULK CRYSTALLIZED TPI AND SOLUTION EPOXIDIZED TPI

by

NADARAJAH VASANTHAN

Adviser: Professor Arthur E. Woodward

Trans-1,4- polyisoprene structures in the alpha and the beta crystal forms with different morphologies were prepared by various crystallization methods such as direct method, annealing method, cast method and prenucleation method. The morphology of bulk crystallized unfractionated TPI and two fraction therefrom were studied using SEM for either the alpha or the beta crystal forms. The morphology generally studied was isothermal crystallization, carried to equlibrium, followed by cooling to room temperature. However some samples was studied at crystallization temperature. The morphology of bulk crystallized TPI, as observed using SEM, is a function of molecular weight, crystal form, crystallization temperature and post-crystallization cooling. The morphology is found to be lamellar and the organization depends on molecular weight, paticularly for samples in the beta crystal form. For the alpha crystal form the size of the structures observed increases with increasing temperature. The melt crystallization of trans-1,4-polyisoprene was followed using FTIR spectroscopy. The spectral

subtraction factor versus time was obtained at the crystallization temperature and after cooling to 25°C for fractions and parent material. Crystallization of the beta crystal form was followed at 36 and 43°C and the alpha form at 43 and 51°C. Samples crystallized at 25°C and annealed at 43°C were also investigated. The effect of molecular weight on the crystalline/ amorphous content depend on the crystal form/ morphology, the crystallization temperature and the thermal history. The amorphous fraction for prenucleated melt crystallized alpha form containing samples increased with molecular weight at the crystallization temperature and after cooling to 25°C. Samples containing the beta crystal form showed a molecular weight dependence at crystallization temperature/ annealing temperature that disappears upon cooling the sample to 25°C. Bulk crystallization of solution epoxidized TPI also was investigated using SEM and FTIR spectroscopy. The effect of amount of epoxidation and crystallization temperature on final crystallinity, morphology and crystallization rate was investigated. The morphology is less dependent on the epoxidation amount, only showing a marked changes at 9.8% epoxidation. The subtraction factor was plotted against the time for various solution epoxidized samples crystallized from the bulk. The rate of crystallization was observed from the slope of the plot. A decrease in rate occurs with increasing epoxi content or with increasing crystallization temperature. The crystallinity decreases linearly with increasing epoxi content at Tc = 25°C and 36°C and shows marked deviations from linearity at Tc = 36°C. The differences in crystallinty between solution and melt crystallized samples are discussed.

Acknowledgment

At this point I feel I should thank those people who have contributed to my educational achievements. This research owes a great dept to teachers, friends and family who have encouraged me become as a chemist. I am especially grateful to my mentor, Prof. A. E. Woodward for his untiring guidness, his excellent leadership and friendship throughout this research. Next I would like to thank my parents, sisters and relatives with out their love, encouragement and support this would not be possible. However my parents who shared the dream but did not see it completed.

I also would like to thank to the members of the thesis committee; Prof. David Lock and Prof. N. L. Yang for their valuable guidness and suggestions to make this thesis success. Thanks are due to Jack Downy for helping me to use SEM. Acknowledgment is made gratefully to the department of chemistry at City College for the teaching assistantship and the graduate school of the City University of New York for the fellowships which help me financially throughout this period. Finally I would like to thank my closest friend, Sheila for the support and encouragement she has given me during the last year of my graduate work.

TABLE OF CONTENTS

Page

Page

LIST OF TABLES

LIST OF FIGURES

Page

Page

Page

Page

Page

1. INTRODUCTION

1.1. Morphologies of semicrystalline polymers

It has been known for many years that polymer molecules possess the ability to crystallize. The extent to which this occurs varies with the type of polymer and the molecular microstructure[1]. Solid polymers differ from ordinary, low molecular weight compounds in the nature of their physical state or morphology. The main difference between polymers and small molecules, is that polymers show characteristic of both crystalline solids and viscous liquids. This has been shown by various authors (Keller[2], Sharples[3], Sperling[4], Woodward[5]).

Flexible chain polymers crystallize from solution to form single lamellas or multilamellar structures with a lamellar thickness that depends on the solvent, the polymer composition and the crystallization temperature[6]. Single lamellas are only partially crystalline and contain a surface component that includes chain folds, chain ends and lateral surfaces[7]. In multi lamellar structures such as hedrites and spherulites, there is an interlamellar component containing chain folds, chain ends[8] and interlamellar traverses which are part of one chain common to two adjacent lamellas. In multi lamellar structures there is usually considerable branching, twisting and interlamellar penetration. Bulk crystallization by cooling a polymer melt usually leads to spherulite formation[9-10].

Most crystallizable thermoplastic polymers of technological importance are processed above the melting temperature in bulk, which is well above room temperature, and then cooled bringing about crystallization. The usual polymer sample crystallized from the bulk is polycrystalline[11]. The individual crystals are small and difficult to see by optical microscopy. The texture of the bulk crystallized material has been studied with the polarizing microscope before the results on chain folded crystallization were known. These studies established that the essential mode of crystallization is spherulitic. All observations of the bulk system were handicapped because crystalline units cannot be obtained in isolation without seriously disturbing the sample[12].

Single crystals obtained from solution can be studied most readily whether or not such studies are relevant to the technologically important problem of crystallization from the bulk. The general belief, however, is that there is no difference in the basic principle. It is obvious a priori that the lamella grown from the melt would be expected to be less regular, in view of competion among molecules at growth faces[13], than when molecules crystallize more or less independently from solution. In particular, evidence for regularity in folding of chains crystallized from solution has come from electron microscopy. A fundamental understanding of many important properties of crystalline polymers depends upon an adequate knowledge of their lamellar morphologies[14]. For example, the Young's modulus along the chain axis is much less for a series lamellar arrangement than for parallel one which constrains the soft

interlamellar region[15]. Also the electric strength of crystalline polymers fall as spherulite size increases because of the changing nature of interspherulite boundaries and the consequent facilitation of breakdown[16]. Detailed morphological studies are still lacking. The primary reason for the lack of detailed morphological knowledge is that this should have been provided by electron microscopy but transmission of electrons through polymers causes radiation damage and limits direct studies[17]. Therefore scanning electron microscopy is used to observe polymer surfaces.

The modern concept of polymer crystals started from the careful work of Keller[18] in 1957, followed by the work of Jaccordine[19] who showed that polyethylene molecules could form single crystals from dilute solution. The dimension of a single crystal is about 10000A° x 100A°. X ray diffraction patterns showed the polymer chain axis is parallel to the smaller dimension of the crystal. Since polymer molecules are much longer than 100A°, Keller concluded that in the crystal it had to be folded back and forth upon itself. Keller's conclusion was immediately confirmed by the independent observation of Fisher[20] and Till[21]. Chain folding is unexpected, since the most thermodynamically stable crystal is one involving completely extended chains. Various models of the fold surface on polymer lamellas have been proposed.

A large number of morphological studies have been carried out on polymer materials to date. It has been shown that the size, shape and complexity of these structures depend on the polymer and the

crystallization conditions[22]. These investigations were carried out on various type of samples including solution crystallized materials and bulk crystallized materials. When polymers are crystallized from a dilute solution (< 0.1% W/V) they give a single lamella type morphology[23-24]. These lamellas can have a variety of shapes and sizes depending on the polymer. For example, polyethylene yields single crystals in xylene and more concentrated solution in the same solvent generally yield multilayer aggregates. More complex crystalline morphologies such as hedrites and spherulites can be observed when polymers are crystallized from concentrated solution[25]. When polymer samples are crystallized from the bulk, the most obvious structures are spherulites. On cooling from the bulk, the first structures that form are single crystals. These are rapidly transformed into sheaflike structures called hedrites or axialites. These transitional multilayered structures represent an intermediate stage in the formation of spherulites. Gradually the lamella in the hedrite fan outward in a splaying motion[26-28]. This leads to a spherically shaped object called a spherulite. The formation of spherulites from single crystals through the transitional state is shown in the Figure1.1. Usually the spherulites are in spherical shape only during the intermediate stage of crystallization. During the latter stages of crystallization, the spherulites impinge upon their neighbors. When the spherulites are nucleated simultaneously, the boundaries between them are straight. However when the spherulites have been nucleated at different times, so that they are of different sizes when impinging on one another, their boundaries form a hyperbola[4]. Detailed examination of spherulitic structures

show that the spherulites are composed of individual lamellar crystalline plates. The lamellar structures sometimes resemble stair cases, being composed of nearly parallel but slightly diverging lamellas of equal thickness[29].

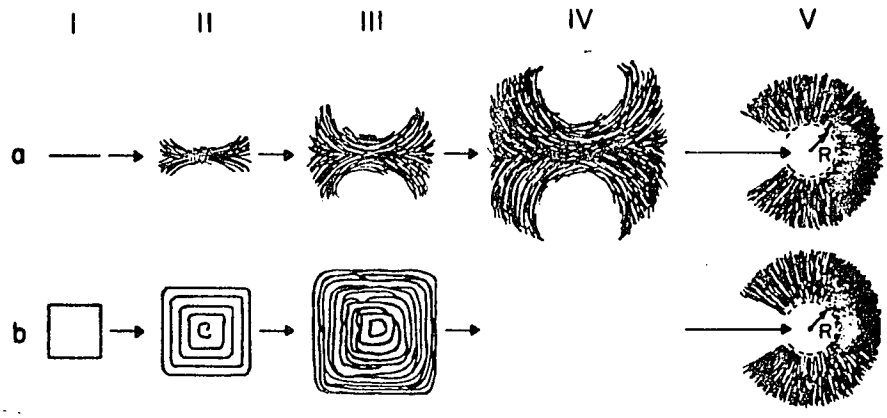

Figure 1.1. Schematic development of a spherulite from a chain folded precursor crystal

Rows (a) and (b) represent, respectively, edge-on and flat-on views of the evolution of the spherulite

It has been established that all properties from bulk crystallized or solution crystallized polymers are dependent on the molecular weight, solvent, crystallization temperature and method of crystallization. A wide range of properties can be achieved by varying the molecular weight and crystallization temperature. The effect of molecular weight on the morphology has been investigated for polyethylene fractions(1×10^4 to 8×10^6) crystallized from the melt[30]. Well developed spherulites were observed at low molecular weight (less than 8.5×10^5) but the higher molecular weight samples fail to give a well defined morphology.

A single lamellar type morphology is obtained when the poly-ethylene oxide with a narrow molecular weight distribution is crystallized from the melt. Allen and Mandelkern[31] also reported the crystalline morphology of poly(ethylene oxide) as function of molecular weight and crystallization temperature. Fractions with molecular weights in the range 6×10^3 to 1×10^7 were used. Three different types of morphology were observed; spherulites, intermediate structures and hedrites.

Crystallization of trans-1,4-polyisoprene using synthetic and naturally occurring(Gutta percha, Balata) has been carried out with unfractionated materials and sharp fractions. It has been shown by Kuo and Woodward[32] that the morphology of trans-1,4-polyisoprene structures grown directly from solution depends on crystallization temperature, molecular weight and solvent. Three structural types were observed: hedrites, spherulites and aggregates of curved

lamellas. Under isothermal crystallization conditions the hedrites formed become larger and more complex as the crystallization temperature decreases and/or molecular weight increases. In that work Gutta percha fractions with molecular weights from 4.7 x 10^3 to 2.5 x 10^5 were used. Xu and Woodward[33] studied the effect of morphology on molecular weight and crystallization time for trans-1,4-polyisoprene directly crystallized from 1% amyl acetate solution at 20°C using scanning electron microscopy. The change with molecular weight was observed from stacks to overgrown lamellas that are curved and interpenetrating to spherically shaped structures containing twisted and curved lamellar ribbons. A high degree of curvature was evidenced for TPI sheaves obtained at 20°C. Sperulitic structures were obtained for TPI with Mv= 5.9 x 10^5 at crystallization temperature of 20°C. These structures appear to be less tightly packed due to branching and twisting and are made up of ribbons smaller in width than for the structures found using low molecular weight material.

Melt crystallization of trans-1,4-polyisoprene was carried out by Davies[34-35] et al and two types of spherulites were observed under the optical microscope. At crystallization temperatures below 35°C, the spherulites displaying a characteristic maltese cross were identified with the beta form, while dendritic type spherulites were observed at above 45°C (alpha form). The rate of spherulitic growth of TPI have been studied previously using optical microscopy by Henderson, Fisher and Lovering[36]. They have shown that alpha form

spherulites grew faster than beta form spherulites at the same crystallization temperature.

The supermolecular structures of melt crystallized TPI have been studied by transmission electron microscopy at early stages of crystallization and low angle X-ray diffraction at latter stages. These methods measure the lamellar thickness and allow the calculation of lamellar surface energies. The values of fold surface energy agree very well with those energies determined for solution grown crystals[37].

1.2.Crystallinity and reentry problem

Many polymers are known to be semicrystalline, consisting of crystalline and non crystalline or amorphous components. It is well known that most of the physical properties and mechanical behavior of the partially crystalline materials depend on the crystallinity[38]. A number of studies on the variation of molecular weight and crystallization temperature were reported by many researchers. It is well summarized in the books of Wunderlich[39] and Geil[40].

Keller[18], Till[20] and Fisher[21] independently proposed a chain folding hypothesis from electron diffraction studies of polyethylene in 1957. However the configuration of the fold remained incompletely solved. A number of models of the fold surface have been proposed and experimental evidence to support these models also has been given for various polymers. These include tight

adjacent, loose adjacent, and non adjacent or switch board model[41]. All these models are shown in the Figure 1.2. In single lamellas, the amorphous component is expected to be at the lamellar surfaces as chain folds and chain ends, for multilamellar structures interlamellar traverses may also be present.

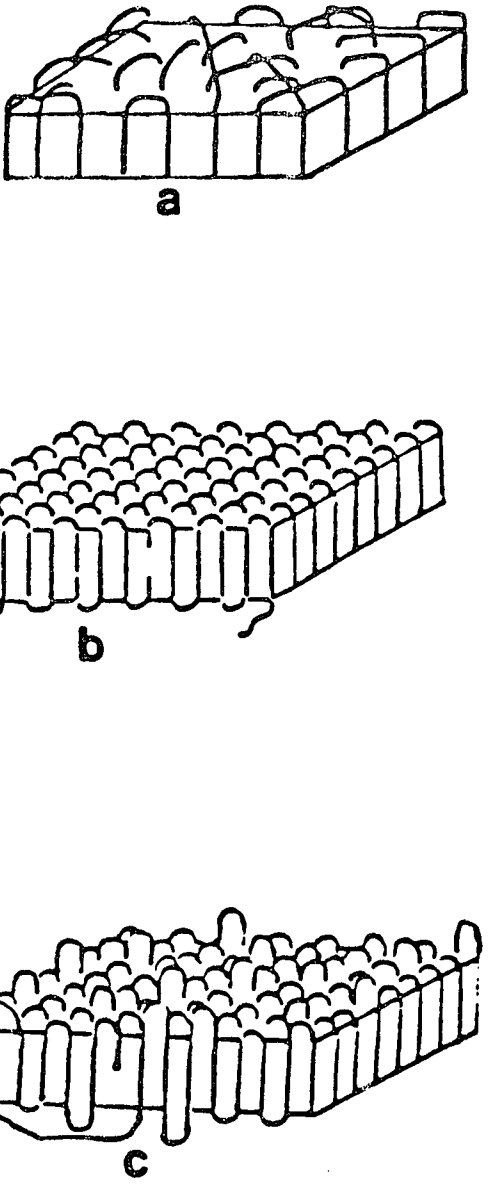

Figure 1.2. Schematic drawing of the conformation models of poly isoprene

a) switch board model b) tight adjacent model c)loose adjacent model

One method of evaluating the folding model is by measurement of the average number of monomer units in the fold. This has been done indirectly by measuring the noncrystalline fraction using physical methods such as density, heat of fusion, IR, Raman and solid state NMR spectroscopies and coupling this with lamellar thickness measurements. A large number of these investigations were made on linear polyethylene[42-45]. Crystallinities derived from various physical methods such as density, heat of fusion and wide angle X-ray diffraction(WAXS) were found to be excellent agreement. It has been reported that when the molecular weight of linear polyethylene is in the region of 2 X 10^4 to 2 x 10^6 , the crystalline thickness is independent of chain length and depends only the crystallization temperature for the given solvent.

Krimm et al used a mixed crystal infrared spectroscopic technique to prove the type of folding for solution crystallized poly ethylene. Mixed single crystals of protonated and deuterated polymer were made by precipitation from dilute solution. Analyzing the characteristic crystal field splitting in the infrared spectrum, Krimm has shown that the predominant type folding involves adjacent reentry[46-47]. Melt crystallized polyethylene was shown to be organized differently with a much lower extent of adjacent reentry. However, a significant undercooling is required to prevent segregation of deuteriated species from the ordinary hydrogen bearing species. Recently Iso Ando[48] et al have used solid state NMR spectroscopy and microscopy to demonstrate that polyethylene

mainly forms a sharply folded structure during melt crystallization. However, small angle neutron scattering results for melt crystallized polyethylene and polypropylene[49] (using a small amount of deutrated polymer) strongly suggest random reentry to be predominant.

Dilute solution grown lamellas of TPBD of high trans content have been investigated by various researchers. A number of studies have shown that the lamellas can have a sizable noncrystalline component, the amount of which depends on crystallization conditions. The crystallinity has been measured by various physical methods such as density and X-ray diffraction. Hendrix, Whiting and Woodward[50] obtained IR spectra of TPBD crystal mats in the range of 1000 to 1400 cm^{-1}. It was found that the ratio of intensity of the IR band at 1350 cm^{-1}, an amorphous band, to that intensity of the band at 1335 cm^{-1}, a regularity band, varies from 1.3 to 0.1 depending on the solvent used for crystal preparation, the TPBD used and the thermal history.

Most physical methods used to evaluate the amorphous fraction of the polymer measure the total amorphous fraction and provide little information about the nature of the chain folds. In order to get more information about the location of the amorphous component, a number of chemical reactions, including substitution, elimination and addition were carried out on various polymer lamellas[51-55].

Attempts have been made to study the fold region of polyethylene lamellas directly by chemical assay, but the degradative chemical reaction employed resulted in destruction of the crystal core it self, and the results are difficult to interpret[56]. Digestion with a strong oxidizing agent such as HNO_3 and destructive reaction with ozone coupled with gel permeation chromatography has been used by Keller and coworkers to obtain the information about distribution of fold length in polyethylene lamellas[57]. The results were interpreted as confirming the model of adjacent reentrant folds of various lengths. However, the degradation method cannot be used for quantitative determination because it has little selectivity between crystalline and amorphous components.

Substitution of bromine atoms onto polyethylene lamellas using ultraviolet or visible light activation of Br_2 in solution at room temperature and above has been studied by various authors. Harrison and Baer[58] report an initial fast reaction with a changing rate corresponding to about 2-3% bromine by weight; following that, the rate of bromine addition remain constant up to at least 7% bromine by weight. Assuming tight reentry folding, it was estimated that 4.5% bromine by weight corresponds to 1 Br atom per fold.

A different approach, developed by Woodward and coworkers, is to carry out a nondestructive chemical reaction on the chain units at the lamellar surfaces of solution crystallized polymers in suspension. Trans-1,4-polybutadiene and trans-1,4-polyisoprene were chosen for this work since they crystallize easily and can

undergo quantitative addition reaction at low temperatures. These reactions have included epoxidation with metachloro perbenzoicacid(MCPBA) and Markownikoff addition of HCl in nonaqueous solution.

Epoxidation of TPBD was carried out by Wichacheeva and Woodward[59]. The fraction of double bonds reacted with the epoxidizing agent was obtained by observing the IR intensity ratio of the carbonyl absorption for MCPBA and MCBA. The number of monomer units per fold was calculated for heptane and toluene grown crystals. By comparing with the theoretically estimated values for possible tightest reentrant folds it was concluded that TPBD crystals grown from heptane, principally contain regular reentrant folds and TPBD crystals grown from toluene contain irregular adjacent reentrant folds.

Surface modification of trans-1,4-polybutadiene was carried out by Stellman and Woodward[60-61]. The reaction used was epoxidation of the double bonds at the surface with MCPBA in suspension. It was found in benzene suspension at 6°C, it took 4-5 days to reach equilibrium and that above 14-27% of the double bond were epoxidized leading to an average value of the fold length 2.5 to 5 monomer units. Tseng and Woodward[62] followed epoxidation in suspension by proton NMR spectroscopy. Combining the proton NMR results with lamellar thickness from small angle Xray scattering or electron microscopy. The fold length of TPBD lamellar crystals from heptane was determined to be 3-5 monomer units. More recently an

experimental method was developed by Wang and Woodward[63] to determine crystalline/amorphous fraction quantitatively. This involves surface epoxidation of TPBD crystals in suspension followed by C-13 NMR analysis, allowing the simultaneous determination of both crystalline stem length and the fold length. This results strongly favored adjacent reentry folding.

Crystallization of trans-1,4-polyisoprene from solution studies was carried out by Woodward and coworkers[64-67]. During these studies considerable amount of quantitative knowledge was obtained about these structures. This was also carried out by using various physical and chemical methods.

Epoxidation reaction on solution crystallized TPI (Balata and Gutta percha) lamellas in suspension at 0°C using MCPA was reported by Anandakumaran and Woodward[64]. The number of monomer units per fold was calculated from the fraction epoxidized and lamella thickness obtained from electron microscopy. Six to 10 monomer units were calculated, the number increasing with increasing molecular weight and T_c. More recently C-13 NMR method was used to determine the average reacted and unreacted block lengths. The effect of reaction medium on the epoxidation of beta TPI structures crystallized from solution was investigated using 16 different liquids including alcohols, ketones and esters[65]. The apparent average reacted sequence length varied four-fold depending on the suspension liquid used, being lowest for alcohol, while the average unreacted sequence length remain constant. The variation in the

average reacted length with the unreacted length remaining constant suggest that a peeling off or loosening of reacted chains at the lateral edges takes place to a degree depending on the suspending liquid leading to epoxidation of the exposed double bonds.

Surface hydrochlorination of TPI followed by C-13 NMR analysis was carried out by Tischler and Woodward[66]. They found that only half of the amount of the noncrystalline fraction obtained from density measurements can be hydrochlorinated. The average fold length was obtained as 5 monomer units. This result was not in agreement with epoxidation results obtained for the same material. However recent studies showed that the hydrochlorination done by Tischler was not complete[14].

Density measurements were used in order to quantitatively determine the amounts of crystalline and the amorphous components of trans-1,4-polyisoprene by Kuo and Woodward using a density gradient column. The crystallinity was calculated from the measured density and from values for the totally amorphous and totally crystalline TPI samples. These results were compared with crystallinities obtained by other methods. Since there was some disagreement in the value of the crystalline density for beta TPI, an alternative method using FTIR was employed to determine the crystallinity[67]. FTIR has several advantages compare to the other physical methods, including 1) experimental simplicity; 2) sensitivty to conformational changes; 3) Various manipulation such as subtraction and deconvolution.

FTIR spectral subtraction, developed by Koenig[68], is extremely useful for the analysis and under standing of semicrystalline polymer spectra. This method can be used to obtain a 100% crystalline spectrum from a semicrystalline spectrum. Subtraction is carried out using a 100% amorphous spectrum obtained at temperatures above the melting point. The 100% amorphous spectrum has been shown to exhibit essentially the same conformational distribution and the same infrared spectrum as the lamellar surface component[69]. Subtraction has been carried out in this way for many polymers[70-72]. The resulting spectrum for the crystalline component usually contains a good base line with sharp and separate by distinct peaks. The broad bands which are usually associated with the amorphous component disappear from the spectrum upon subtraction.

One method to study conformation of polymer chains in the lamellar surface was carried out by Koenig and coworkers for poly (vinyl chloride)[73] by assigning separate components of a broad amorphous band to different conformations. These separate components appear and disappear upon heating the sample to temperature above Tm. Poly(ethylene terephthalate) was also studied at temperatures up to 468K[74-75]. The trans and gauche conformations were identified in the infrared band contours. The effect of temperature change in atactic polystyrene was studied and two transitions were found. The higher one involved conformational changes that can be seen by changes in the band contours.

Conformational changes at low temperatures were studied for a number of polymers[76-77]. In all the studies an increase in band intensity is observed as the sample temperature is decreased. In work using polyethylene and polystyrene it was shown that there is a linear change in peak height with temperature. The authors of these studies attributed these changes to intermolecular contraction which leads to an increase in the dipole moment interaction and therefore to an increase in the intensity. This phenomenon was found to be more pronounced for highly polar groups. The changes in the slope of the plot of temperature versus intensity indicated the occurence of a transition. Similar studies was carried out by K.W.Frank and coworkers for polyethylene, polyethylene teraphthalate and some polyurethanes[78-79]. They explained the increase in absorbance peaks intensity as resulting from anharmonicity that occurs as the lattice potential decreases and the vibrational force constant increases. Another work showed that small frequency shifts are expected at low temperatures. Boerio[80] found an increase in intensity as the temperature is lowered. He also showed that some narrowing of the crystalline bands occurs.

FTIR spectra were obtained for solvent cast TPI film (alpha form), the same sample melted and quenched(beta form)[81] and for solution crystallized lamellas(alpha and beta form)[82]. Normal coordinate single chain calculations were carried out and band assignments given with some differences being found in the two studies. A correlation between the spectra for the two forms was shown to exist with each vibrational band for the beta form being correlated to a

singlet or a doublet in the alpha form; additional bands appear in the alpha spectrum attributed to groups of atoms from two adjacent monomer units in the chain.

FTIR spectroscopy was used in the past to determine the crystallinity for solution crystallized trans-1,4-polyisoprene. One method for the quantitative determination of the crystalline fraction in semicrystalline TPI was developed by Gavish and Woodward using a conformationally independent band, attributed mainly to C=C stretching vibration. Another FTIR method developed to measure the crystalline/amorphous ratio involves subtraction of spectrum just above the melting point from that same sample in the semicrystalline state. FTIR were also taken at temperatures from -170°C to 110°C and the changes relative to spectra at 30°C followed. A decrease in amorphous content with decreasing temperature down to about -30°C and an increase in amorphous fraction with temperature to 60°C were quantitatively determined[83]. Crystal field splitting of a CH_2 scissoring band was observed at -145°C. Changes in conformationally sensitive amorphous bands at temperatures above 65°C were used for tentative assignments of the components of these bands.

1.3.Crystallization kinetics

During the crystallization from the bulk, polymers form lamellas, which in turn are organized into spherulites or their precursors, hedrites[81]. If a polymer melt is allowed to crystallize the

crystallinity increases and so the analysis of crystallization kinetics is important to understand structure/property relationships. The rate of crystallization is expected to be a function of temperature, molecular weight and method of crystallization[82-84].

Crystallization kinetics of various homopolymers and copolymers were studied using dilatometry[84-86], DSC[87-89] and electron microscopy[91-92]. The experimental observations of crystallization kinetics are based on three theories of polymer crystallization kinetics. The first is the Avrami theory[92-94]. The second theory was developed by Keith and Paddden[27-28], providing a qualitative understanding of spherulite growth. The third theory was developed by Hoffman and coworkers[95-97]and is called kinetic nucleation theory of chain folding; this provides an understanding of how lamellar structures form from the melt.

Crystallization kinetics of poly(ethylene oxide) was studied by Hay and Sabin[98] using dilatometry. Melting temperature of PEO is 66°C where the rate of crystallization is zero. They have shown that the rate of crystallization increases as the temperature is decreased. The crystallization kinetics of gutta percha and synthetic trans-1,4-polyisoprene was also investigated by Cooper and Vaughan[99] using dilatometry. In this study rate constants were obtained from the crystallization from the melt and for interconversion of isomorphous forms.

Crystallization rates were obtained microscopically, by measuring the growth of sphrulites as function of time. This was done using both optical microscopy and transmission electron microscopy of thin sections. The crystallization kinetics for an isotactic and atactic polypropylene blend was studied by measuring the radius of the spherulites as function of time using optical microscopy[100]. When the spherulite radius was plotted against the time, a linear relationship was obtained. This implies that the concentration of foreign units at the growing tips of the lamella remain constant through the growth process. Introducing more foreign units caused growth rate to slow. However, the linearity of the growth rate was maintained. The crystallization kinetics of poly (ethylene terephthlate) was studied by Philips and coworkers[101] using TEM. When the radial growth rate was plotted as a function of crystallization temperature, a maximum was observed. The increase in rate of crystallization as the temperature is lowered is controlled by the increase in driving force. As the temperature is lowered further, molecular motion become sluggish as Tg is approached, and the crystallization rate decreases again. Below Tg, molecular motion is so sluggish, the rate of crystallization effectively becomes zero.

The crystallization kinetics of low molecular weight polyethylene fractions have been studied by Mandelkern and coworkers using differential scanning calorimetry. This study showed that crystallization kinetics obey nucleation theory appropriate to chains of finite length. All the fractions displayed three distinct regimes[102].

1.4. Crystallization of copolymers

When a small amount of comonomer unit is introduced into a linear homopolymer, one obtains a copolymer which still crystallizes into a semicrystalline structure resembling that of the homopolymer. A large number of experiments were carried out in the past to determine the role of comonomer units in crystallization, annealing and melting. Frequently, WAXS is used to study the structure of semicrystalline copolymers. The effects of copolymer composition on unit cell parameters were investigated by several workers[103-110]. Baker and Mandelkern analyzed two sets of branched polyethylene samples using WAXS. An increase in the 'a' dimension of polyethylene unit cell was observed as the number of methyl and propyl branches along the polyethylene chain was increased. This effect was attributed to a lower concentration of propyl branches in the crystalline phase of the sample.

Roe and Greniwiski[107] studied the effects of chlorination on the crystallization of polyethylene. They found that as the concentration of Cl atoms along the back bone become larger, the 'a' dimension of the for polyethylene unit cell increases. This behavior was attributed to greater levels of Cl incorporation into the crystalline phase of polyethylene. This trend was consistent with their experimentally determined heat of fusion values. Hf was observed to decrease as the degree of chlorination increased.

A detailed structural analysis of ethylene/propylene and ethylene/butene copolymer was made by Holdsworth and Keller[109] using a nitric acid etching technique. For increasing etching time the 'a' dimension of the unit cell was observed to decrease and approach that for the pure polyethylene. Since etching presumably primarily attacks the amorphous region, it was postulated that many of the comonomer units are in this region. Birber and Thomas investigated the crystallization behavior of a condensation type segmented block copolymer of polybutylene teraphthalate(4GT) and poly (tetra-methylene ether glycol) (PTMEG)[111-112]. In this study single crystals of the copolymer were grown in thin films crystallized from the melt. It was found that the resulting crystals consist of a relatively pure 4GT crystal core with the PTMEG sequence and short 4GT segments being rejected.

Several workers have studied model copolymer systems to determine the effects of primarily excluded comonomer units on observed structural data. These materials were prepared by chemically modifying the fold surface of single crystals held in suspension. Harrison and Baer[58, 110] studied single crystals of poly-ethylene which were halogenated in suspension. Results obtained from kinetic, thermal and infrared studies indicated that the halogenation reaction was selective to the fold surface of the crystals. No changes were observed in the ΔH_f values for each of the halogenated crystals. However after these crystals melted and recrystallized, a significant drop in ΔH_f was observed. Similar behavior was observed by Marchatti and Martuscelli[113] for single

crystals of polybutadiene brominated in suspension. From SAXS measurements it was found that the ability of the crystals to anneal was inhabited by the presence of Br atoms on the fold surface. The fold period of these materials did not change significantly after annealing.

Crystallization of trans-1,4-polybutadiene containing up to 10% cis units was carried out by Wang and Woodward[63]. They showed that most of the cis units are rejected from the crystal core. Recently, the crystallization of segmented block copolymer prepared by surface hydrochlorination and epoxidation of solution crystallized trans-1,4-polyisoprene lamellas were carried out from 2-octanol, 2-pentanol and 2-pentanone[114,115]. The resulting precipitates were studied by SEM, DSC and FTIR and in some cases by the suspension epoxidation/C-13 NMR method. It was shown that there is no incorporation of modified TPI in the crystal core.

1.5. Melt crystallization of TPI and rationale for further study

The crystallization of trans-1,4-poly isoprene from the melt has been the subject of a number of earlier studies. This earlier work includes the use of dilatometry[116], differential scanning calorimetry[117], low and wide angle X-ray diffraction[118-119], solid state C-13 NMR spectroscopy[120] and optical and transmission microscopy[34-37]. In part of earlier work the monoclinic crystal form(alpha) and the orthorhombic crystal form(beta) have been characterized by X-ray

diffraction. The work carried out previously in this laboratory was concerned with solution crystallized trans-1,4-polyisoprene. A considerable amount of new quantitative knowledge concerning the morphology of these structures has been obtained during these studies. The surface reaction/C-13 NMR method, which gives unique quantitative information about the average chain fold length and crystalline stem length in dilute solution-grown polymer lamellas, can not be used to obtain quantitative information for bulk crystallized TPI since all of the amorphous portion is not easily brought into contact with chemical reactant.

The effect of crystallization temperature on TPI crystallinity after quenching to 25°C was obtained using dilatometry[116]. The morphology was investigated using optical and transmission electron microscopy[32, 34-37]. All of these previous studies with morphology and crystallinity of TPI have been studied with unfractionated samples. Many studies of properties such as crystallinity and morphology have been made on crystallized polymers. Most of these investigations were carried out after quenching from the crystallization temperature to room temperature. This quenching process leads to morphological changes which complicate the interpretation of the original crystallization step. Therefore investigation of crystallization and the morphology at the crystallization temperature should simplify this interpretation. Infrared spectroscopy has been used to some extent to investigate melt crystallized homopolymers but detailed morphological study in which the effects of polymer molecular weight and the crystallization

temperature on the melt crystallized polymer as obtained by this method is lacking. By carrying out the crystallization process in an IR cell, it should be possible to evaluate the effects of post crystallization quenching on the spectrum and the crystallinity as derived therefrom. Crystallization from the melt of polyisoprene and random copolymers has received little attention to date. FTIR spectroscopy has not been applied to study such materials.

1.6. Goals of current research

The principle goal of this research was to quantitatively investigate the bulk crystallization of trans-1,4 -polyisoprene and its random epoxidized copolymer. The dependence of the morphology, the crystallinity, and the melting characterstics of these samples on the molecular weight, crystal form, crystallization temperature and method of crystallization were investigated. The crystalline/amorphous nature of these materials was studied quantitatively as a function of temperature using FTIR. The dependence of the crystallization rate, crystallinity, morphology and melting temperature on the amount of epoxidation and the crystallization temperature were also studied for solution epoxidized TPI.

2. EXPERIMENTAL SECTION

2.1. Samples

Synthetic trans 1,4 polyisoprene obtained from Poly Sci Inc was used in these studies. The molecular weight distribution of unfractionated synthetic trans-1,4-polyisoprene was determined earlier using a Water Associates 200 analytical gel permeiation chromatograph with toluene as the solvent at 85°C. The Mn and Mw/Mn values are $3.5X10^4$ and 4.8 respectively. The trans 1,4 content was previously determined to be 100%. These determinations were made by F.A. Bovey and F.C. Schilling at Bell Laboratories by C^{13} NMR spectroscopy. Three samples of solution epoxidized TPI, prepared by J. Xu were also used in this study. The three random copolymers were prepared by carrying out a reaction with m-chloro perbenzoic acid in 1% chloroform solution using unfractionated TPI having Mn = 3.5 x 10^4 and Mw/Mn = 4.8. The degree of oxirane content were determined previously using C-13 solution NMR and found to be 2.2, 5, and 9.8 mole%.

2.2. Fractionation

Fractionation of synthetic trans 1,4 polyisoprene was carried out by fractional precipitation from toluene/MeOH mixtures. 10 grams of TPI and 0.2g of antioxidant 2246, 2,2-Methelene-bis -(4 methyl-6-tertiary-butyl phenol) was dissolved in one liter of toluene at 50°C. Then methanol was added until cloudiness appeared. After heating the solution to a temperature at which it became clear, the solution

was placed in a water bath at 30°C overnight for precipitation. Then the precipitate and supernatant are separated by filtration. The precipitate was dissolved in toluene keeping the concentration approximately 1%. The fractionation procedure was repeated for both solutions obtained above using the scheme shown in the Figure2.1. The fractions, used for this research, labelled P_5, P_6 and P_{15}, were collected after complete precipitation and dried under vacuum.

2.3. Molecular weight determination

Viscosity average molecular weights, M_v, of the fractions were determined by solution viscosity measurement using an Ubbelohde viscometer.

The Ubbelhode dilution viscometer is shown in Figure 2.2. Successive dilution are made on the same starting solution. The viscosity of the solution depends on the solute concentration, the solute molecular weight and the shape of the solute molecule. The specific viscosity is obtained from the following equation.

$$\eta_{sp} = (\eta_c - \eta_o) / \eta_o = (t_c - t_o)/ t_o$$

η_{sp} =Specific viscosity

η_c =Viscosity of the solution

η_o =Viscosity of the pure solvent

t_c =Flow time of the solution

t_o=Flow time of the pure solvent

Intrinsic viscosity, [η] was obtained by plotting the ratio of the specific viscosity to the concentration of the solution against the concentration of solution. The emprical relationship between M_v and intrinsic viscosity was given by the Mark, Houwink and Sakundra equation shown below.

$$[\eta] = KM^a$$

K and a are constants characteristics of the solvent - solute system. The values used here were obtained by J. Xu[33]. They are $3.34X10^{-2}$ and 0.686 respectively. These values were used to calculate the molecular weight of the fractions.

The viscosity average molecular weight of fractions P_5, P_6 and P_{15} shown in figure 2.1 were found to be $8.3x\ 10^4$, $2.8x\ 10^5$ and $6.1x10^5$ respectively.

2.4. Crystallization techniques

Five different crystallization methods were employed, using the unfractionated sample and four fractions with M_v's of $8.3x10^4$, $2.8x10^5$, $4.9x10^5$ and $6.1x\ 10^5$ derived therefrom.

a) Solution crystallization

For solution crystallization of TPI a prenucleation method was used. One gram of trans-1,4-polyisoprene and 0.2grams of antioxidant were dissolved in 100ml of hexane at 60°C for about one hour. Then the solutions was filtered at that temperature and cooled down to 0°C in an ice bath. After the precipitation was complete the solution was heated to the redissolution temperature, resulting in a clear solution. This was placed in a constant temperature bath at 30°C overnight. This method yields the alpha crystal form. The beta crystal form was prepared by heating the precipitated solution from 0°C to room temperature very slowly.

b) Casting method

Unfractionated and fractionated samples of synthetic TPI were crystallized by casting a 1% hexane solution onto a water surface at crystallization temperatures from 30°C to 50°C. After crystallization was complete, the system was cooled down to 25°C.

c) Melt crystallization

The solution crystallized mats were prepared by filtering the solution using Teflon filters. The solution crystallized mats were heated for one hour at 75°C on a water surface, and then the temperature was reduced the desired crystallization temperature: 25°C, 36°C and 43°C

for 12 hours, 3days and 7 days respectively. After the requisite crystallization time at 36°C and 43°C, the sample was cooled down to room temperature. In another procedure solution crystallized mats were heated between NaCl plates inside the FTIR heating cell or on a glass plate in the vacumn to 75°C for about one hour; then it was brought down to the desired crystallization temperature. After crystallization was complete the sample was cooled to room temperaturte.

d) Annealing treatment

Annealing was done by heating the room temperature melt crystallized beta samples to 43°C between NaCl plates in the FTIR heating cell. After crystallization was complete the samples was taken to room temprature. This experiments also has been carried out on a water surface. This experiment yields only the beta form of TPI.

e) Prenucleation method

The alpha crystal form was prepared by this method. Melt crystallized alpha crystals prepared at 55°C, were heated to 65°C inside the FTIR heating cell for about 15 minutes; then the solution was cooled to the desired crystallization temperatures, either 43°C or 51°C. After crystallization is complete, the sample was cooled down to room temperature.

2.5. Morphological studies

a) Optical microscopy

Preliminary morphological studies were made for various samples prepared by the direct melt crystallization method, the annealing method using a Zeiss optical microscope fitted with interference contrast optics. The birefringence pattern of these structures was viewed using ordinary optics with cross Polaroids.

b) Scanning electron microscopy

Bulk crystallized trans-1,4-polyisoprene samples were stained by OsO_4 vapor for at least overnight. A peice of sample was placed on the sample holder and then coated with gold. A Cambridge S4 scanning electron microscope was used to study these preparations.

2.6. Crystal form

The crystal forms were determined by infrared spectroscopy. Trans-1,4-polyisoprene has two crystal forms. Crystallization can occur either in one or the other or both crystal forms. The bands due to =CH out of plane deformation are strongly characteristic of the alpha, beta and amorphous spectrum with a sharp doublet at $882cm^{-1}$ and $862cm^{-1}$ for alpha TPI, a sharp singlet at $877cm^{-1}$ for beta TPI and a broad band at $842cm^{-1}$ with a shoulder at $860cm^{-1}$ for amorphous TPI. Spectra for alpha, beta and amorphous TPI are shown in the Figure 2.3.

2.7. Differential scanning calorimetry

Heat of fusion, the melting endotherm and melting temperature measurements were made using a Dupont 1090 thermal analyzer with a sample weight of approximately 3mg to 5mg. The temperature indicated by the analysis was checked by comparing the melting point of Indium into its literature values. A scanning speed of 10°C/min or 20°C/min was used for these experiments. This speed is high enough to avoid recrystallization of trans-1,4-polyisoprene.

2.8. FTIR spectroscopy at temperatures above 25°C

FTIR spectroscopic measurements were carried out using a DIGILAB FTS40 Fourier transform infrared spectrometer at 4 cm^{-1} resolution from 450 cm^{-1} to 4000 cm^{-1}. Crystallization at higher temperatures above 25°C were carried out using a thermostated heating cell (model 48) made by Control Corporation. FTIR spectra were recorded as a function of time after cooling from the melt at 75°C to constant crystallization temperature. When the FTIR spectrum showed no further change with time, the samples were cooled to room temperature.

2.9. FTIR spectroscopy at temperatures below 25°C

Solution crystallized and melt crystallized samples in either the alpha or beta form were used for the low temperature studies. A cooling cell, as shown in figure 2.4 was used for this experiment. The sample was placed between the copper holders with a thermocouple attached to the sample. Then the cell was cooled to one of temperatures of 0°C, -78°C, or -198°C. FTIR spectra were taken at those three temperatures and at room temperature. In order to see the changes in the spectrum at low temperature, the semicrystalline spectrum taken at room temperature was subtracted from the low temperature spectrum by using a subtraction factor of one.

2.10. Measurement of the amorphous fraction

Measurements of the amorphous fraction were carried out for all semicrystalline samples using two different FTIR methods. One was the subtraction factor method and the other the absorbance ratio method. The amorphous fraction obtained by the two different methods were not in agreement. However after a correction was made for contraction of the samples upon crystallization and cooling close agreement between the two methods was found.

a) Subtraction factor method

An amorphous spectrum was obtained at 65°C for all samples for which semicrystalline spectra were taken. A 100% crystalline spectrum for each sample is obtained by the subtraction of the amorphous spectrum from the semicrystalline spectrum by a reduction of the intensity of the amorphous spectrum to compensate for the crystallization that has occurred. This subtraction is carried out by watching the disappearance of the 842cm^{-1} band. The subtraction factor is equal to the uncorrected amorphous fraction.

b) Absorbance ratio method

Using this method stretching band at 1664-1670cm^{-1} was used to measure the crystallinity. This band has been shown to be independent of the overall crystalline and amorphous conformation due to the fixed configuration of the double bond. The crystallinity was calculated from the relative absorbance of the band 1664-1670cm^{-1} obtained in the computer before and after the subtraction described above. This procedure is illustrated in figure 2.5.

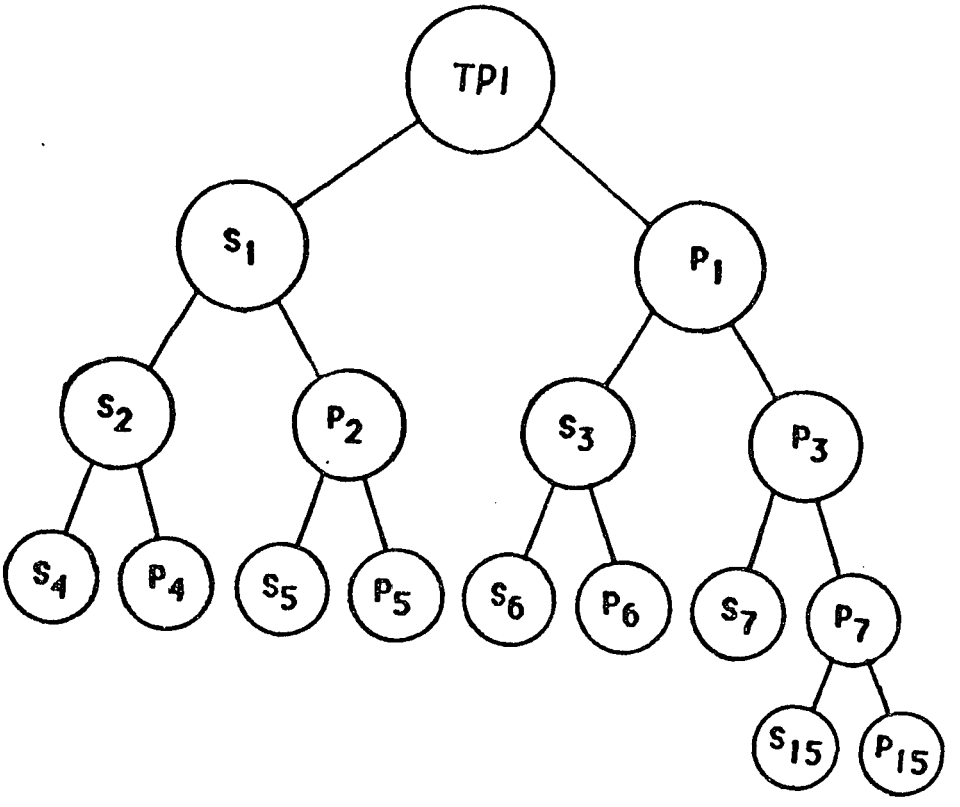

Figure 2.1. Trans-1,4-polyisoprene fractionated scheme

s. supernatent phase p. precipitate phase

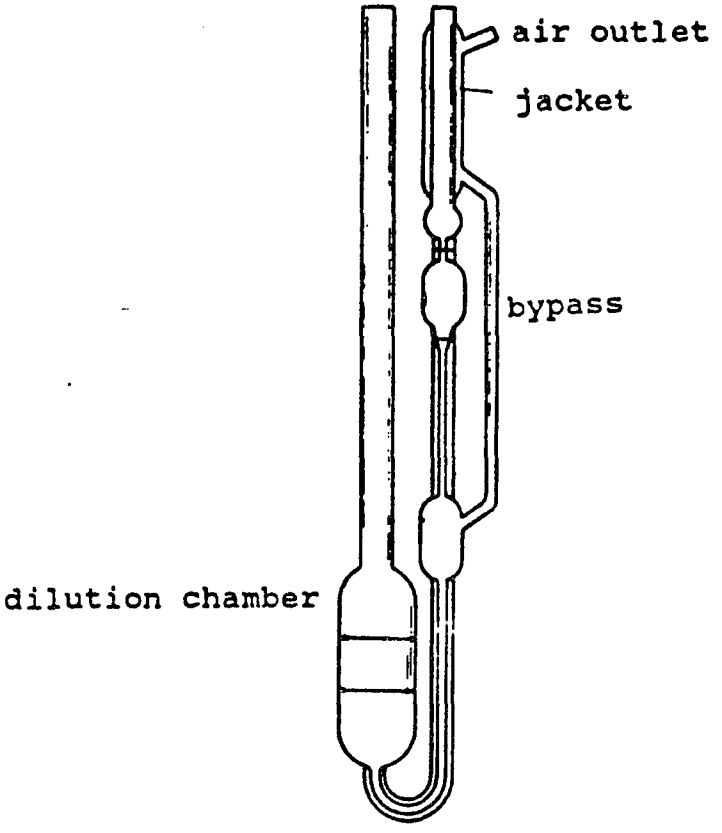

Figure 2.2. Ubbelohde dilution viscometer

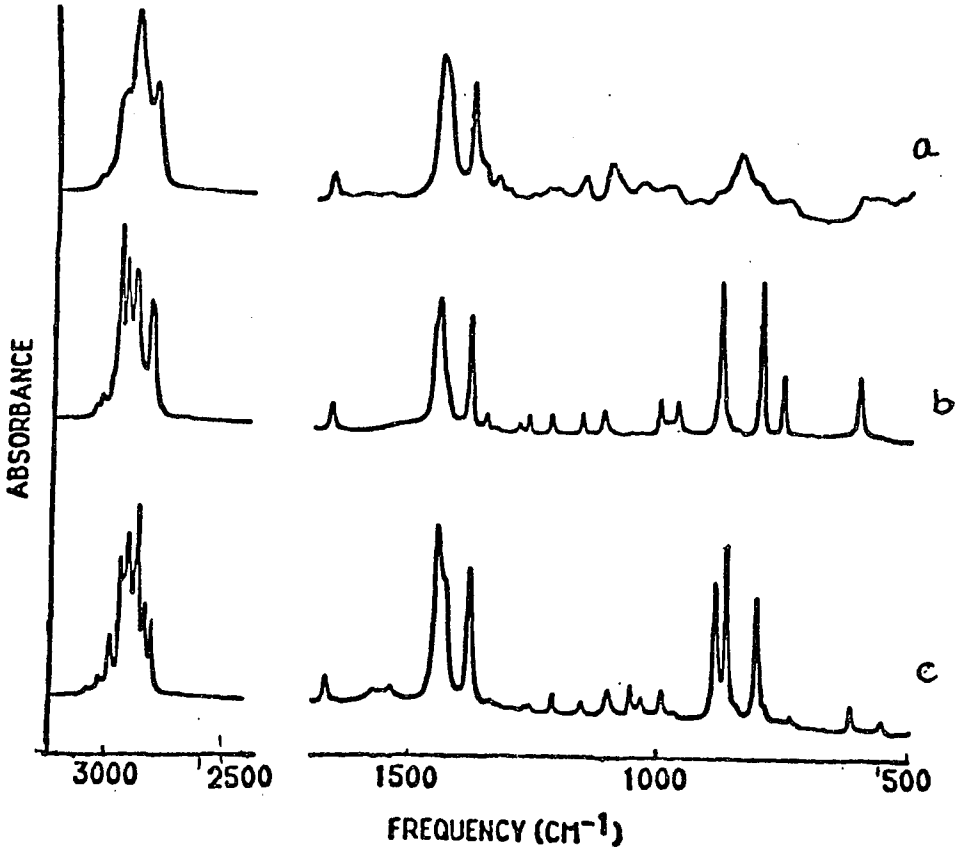

Figure 2.3. A typical FTIR Spectra of melt crystallized TPI
a) amorphous TPI b) beta TPI c) alpha TPI

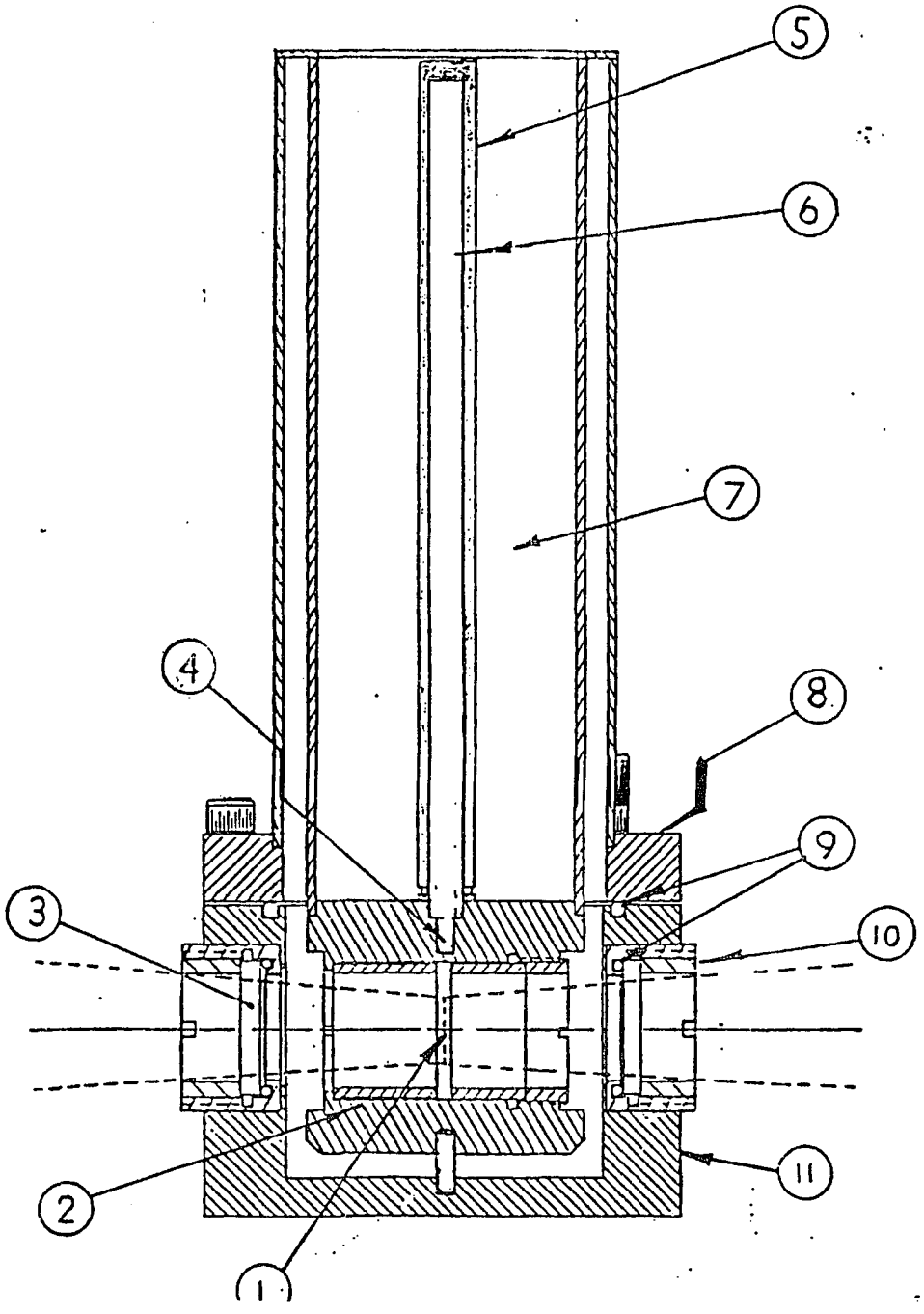

Figure 2.4. Cooling Cell

1. Sample Location 2. Sample Holder 3. Window 4. Themocouple

5. Heating Cartridge Location 6. Thermocouple Tube

7. Liquid N_2 Reservoir 8. Dewar Upper section 9. O-Ring

10. Dewar Lower section

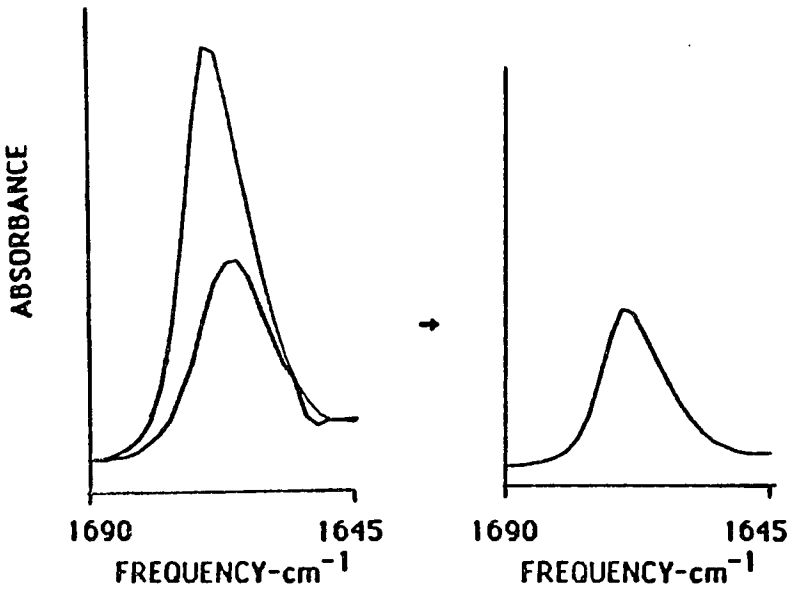

Figure 2.5. Illusration of Absorbance ratio method

3. RESULTS

3.1. Morphological investigation of bulk crystallized TPI

3.1.1. Morphologies of TPI in cast films

Unfractionated and fractionated samples of synthetic TPI were crystallized by casting a 1% solution in hexane onto a water surface at crystallization temperatures from 30 to 50°C. After cooling to 25°C and treating with OsO_4, the morphology was investigated with SEM.

Representative scanning electron micrographs of beta TPI structures crystallized at 40°C are shown in Figures 3.1 and 3.2. These are prespherulitic type lamellar structures with lengths of 5-8 microns containing interpenetrating lamellas. This type of structure is also obtained at 30°C. Alpha-spherulites with 30 - 60 microns are seen at 50°C. Although these structures show clear boundaries, inter lamellar penetration across the boundaries does occur as can be seen Figures 3.3 and 3.4.

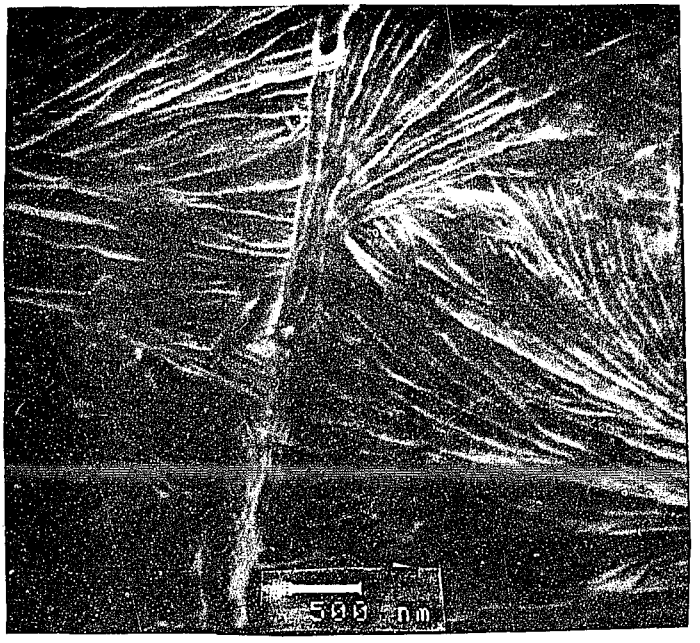

Figure 3.1. Scanning electronmicrograph of fractionated TPI ($Mv=6.1x10^5$) cast from 1% hexane solution at 40°C

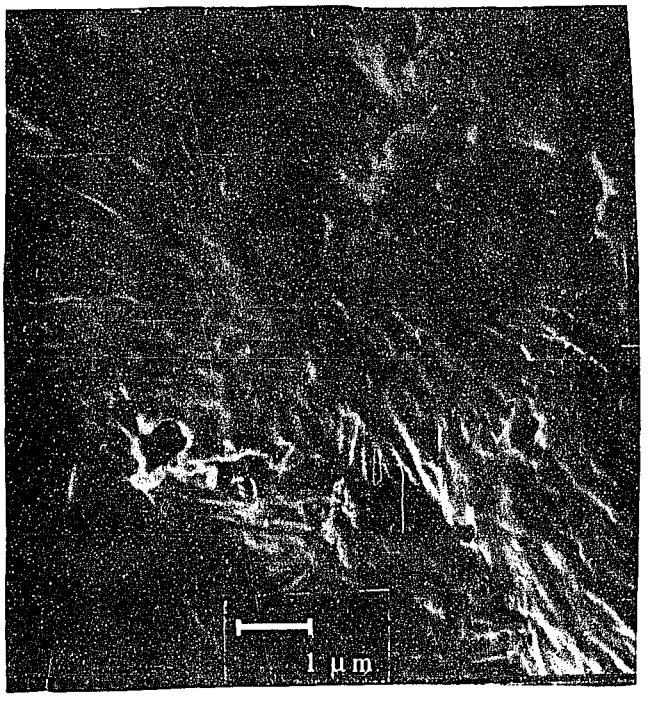

Figure 3.2. Scanning electron micrograph of unfractionated TPI cast from 1% hexane solution at 40°C

Figure 3.3. Scanning electron micrograph of unfractionated TPI cast from 1% hexane solution at 50°C

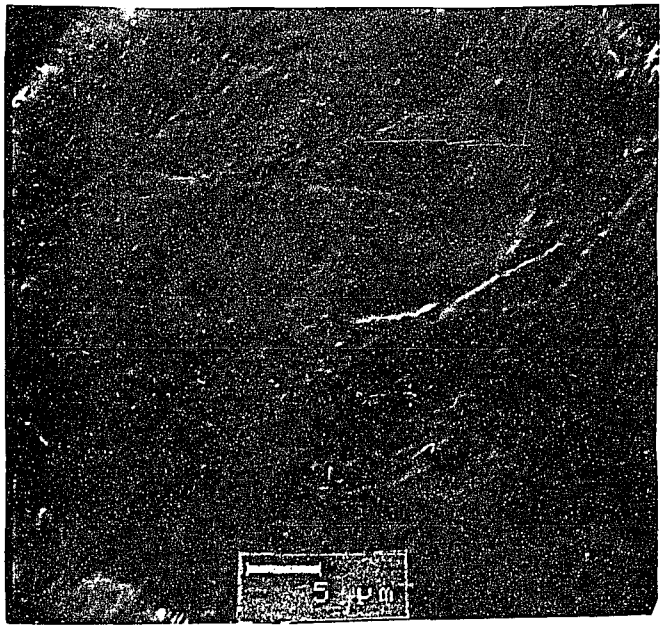

Figure 3.4. Scanning electron micrograph of unfractionated TPI cast from 1% hexane solution at 50°C

3.1.2. Morphologies of beta TPI crystallized from the melt

Unfractionated TPI (M_V=1.7 x 10^5) was crystallized in the beta form at 0°C, 25°C, 36°C, and 43°C. The two fractions, both obtained from the unfractionated sample, one with M_V= 6.1 x 10^5 and the other with 8.3 X 10^4 were also crystallized at 25°C, 36°C and 43°C. Morphological investigation was made after the crystallization was completed as confirmed by FTIR spectroscopy.

A scanning electron micrograph of unfractionated TPI cooled from the melt to 0°C then heated to 25°C and OsO_4 treated is shown in Figure 3.5. Sheaf-like structures are apparent. These sheafs are less developed as compared to the sheafs obtained at 25°C. Typical scanning electron micrographs of unfractionated TPI and two fractions crystallized at 25°C are shown in the Figures 3.6, 3.7 and 3.8. For the unfractionated sample interconnected sheaf-like structures, principally viewed edge-on, are observed in Figure 3.6a and 3.6b. Most of these structures are larger and more developed than those prepared at 0°C. The lengths of these structures ranges from 4 to 8 microns. Views principally of lamellar ends are also observed (Fig. 3.6c). Fraction with M_V = 8.3 x 10^4 shows connected sheaf-like structures, viewed both edge-on and face-on as shown in Fig 3.7. Many of these show less branching and are more asymmetric than those obtained from the unfractionated material. These structures range in length from 7 to 8 microns. An edge-on view of the lamellar structures from the M_V=6.1 X 10^5 sample (Fig. 3.8a) shows a relatively loose and disorganized, but connected, lamellar array; some lamellas were also viewed face-on (Figure 3.8b).

Typical scanning electron micrographs of samples crystallized at 36°C and OsO_4 treated at 25°C are given in Figures 3.9, 3.10, 3.11 . Sheaf structures with interconnecting lamellas are seen for the unfractionated TPI. The structures observed for the two fractions show considerable twisting and curvature perpendicular to the long direction of the sheafs. The lamellas comprising these structures, viewed edge-on, are less closely packed than those for the unfractionated sample .

SEM micrographs of beta crystal form samples prepared at 43°C using unfractionated TPI, treated with OsO_4 at T_c and cooled to 25°C are given in Figure 3.12. Various structures with lengths/ diameters of 4-5 microns are observed. Micrographs, obtained after crystallization at 43°C and cooling to 25°C followed by OsO_4 treatment, are given for unfractionated TPI in Figure 3.13. Sheaf-like lamellar structures are more clearly visible and, on the average, are larger than those observed for samples receiving the OsO_4 treatment at crystallization temperature. Micrographs, obtained for the two fractions crystallized at 43°C and OsO_4 treated at 25°C, are given in Figures 3.14 and 3.15. Morphological differences occur for the unfractionated TPI and the two fractions therefrom. For the M_V =8.3 X 10^4 sample face-on and edge-on structures are apparent; the latter contain few layers. At low magnification (Figure 3.15a) M_V=6.1 x 10^5 preparation shows a network of lamellar structures each about 5 microns in size; one of these is shown at higher magnification in Figure 3.15b in which many end-on lamellas are visible. Open sheaf-like structures containing fewer lamellas are also found, as shown in Figure 3.15c.

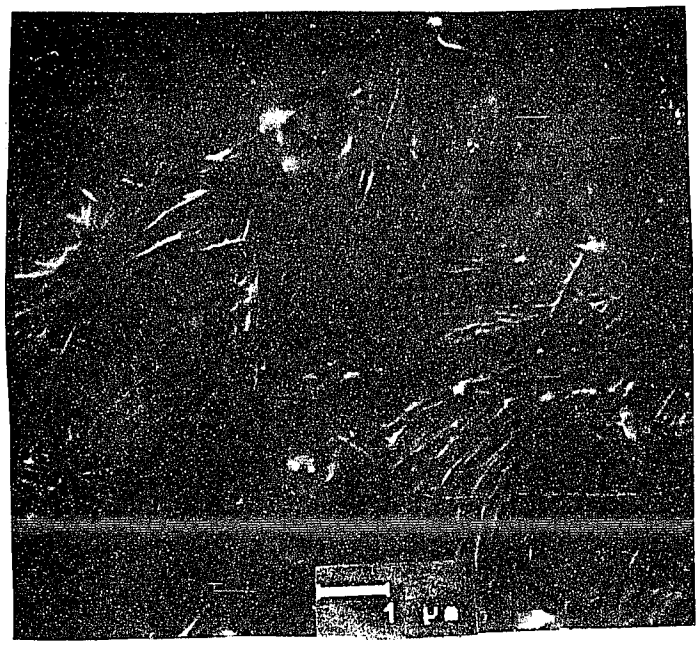

Figure 3.5. Scanning electron micrograph of unfractionated TPI crystallized from the melt at 0°C

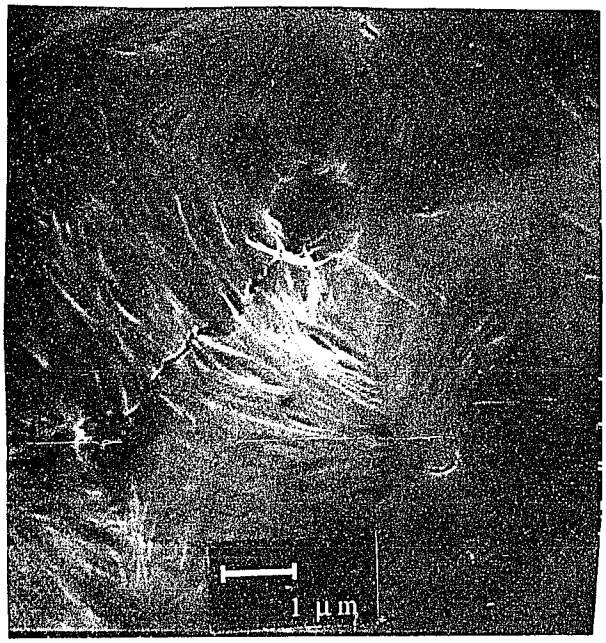

Figure 3.6a. Scanning electron micrograph of unfractionated TPI crystallized from the melt at 25°C

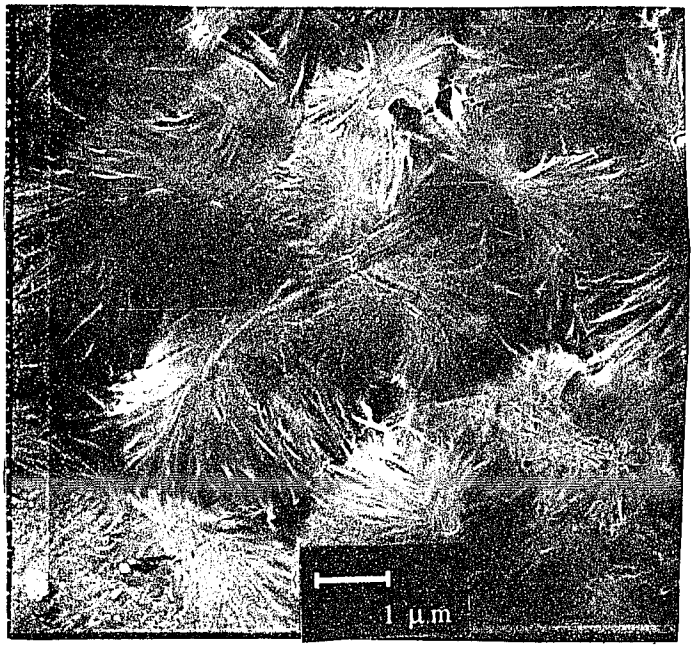

Figure 3.6b. Same as figure 3.6a but different field

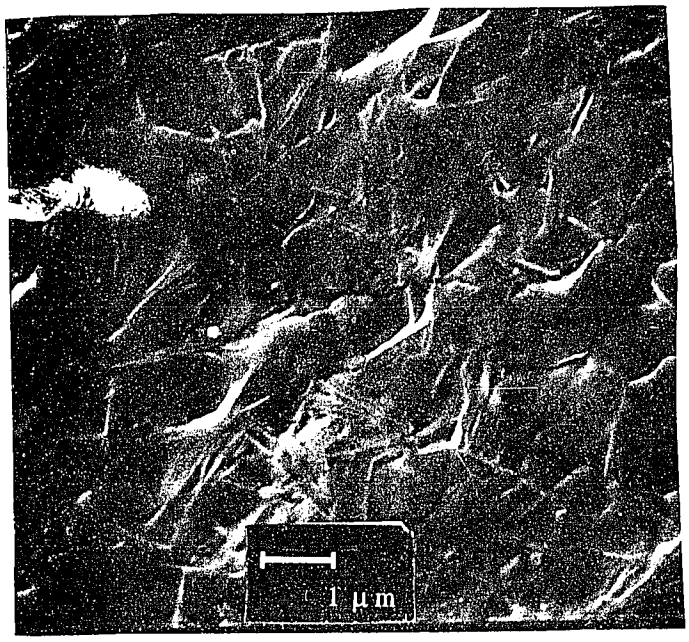

Figure 3.6c. Same as figure 3.6a but different field

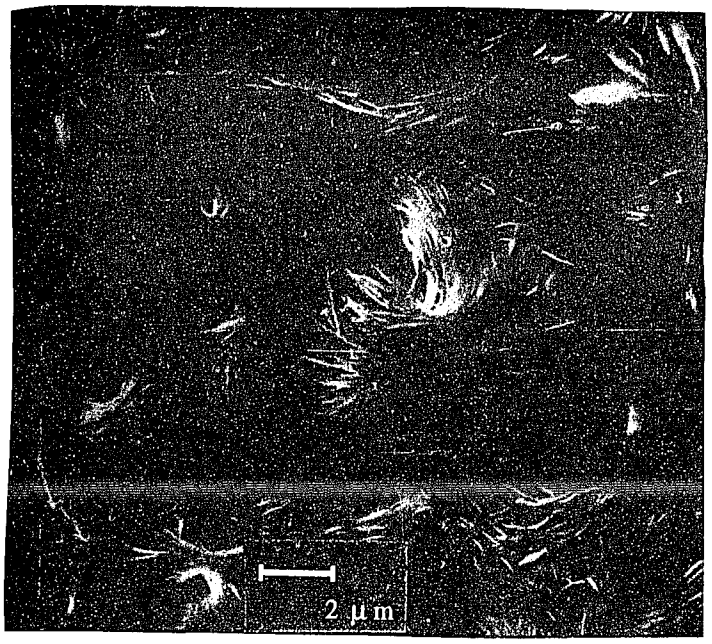

Figure 3.7a. Scanning electron micrograph of fractionated TPI (Mv=$8.3x10^4$) crystallized from the melt at 25°C

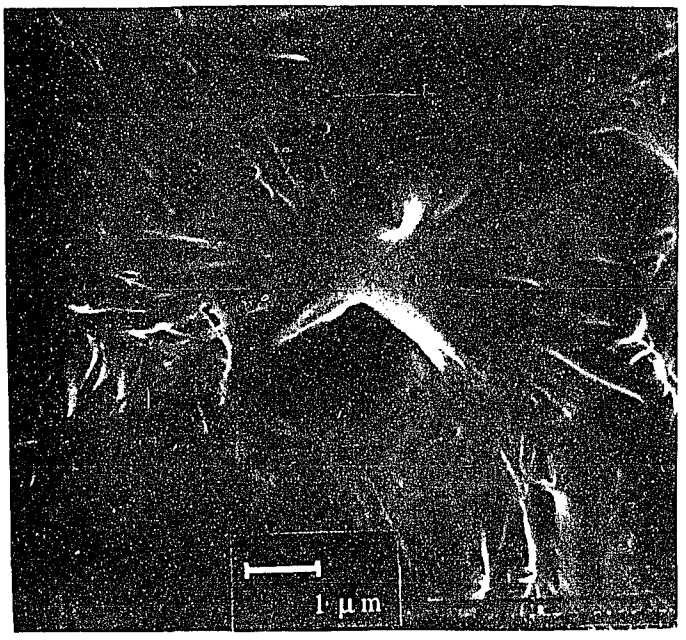

Figure 3.7b. Same as figure 3.7a but different field

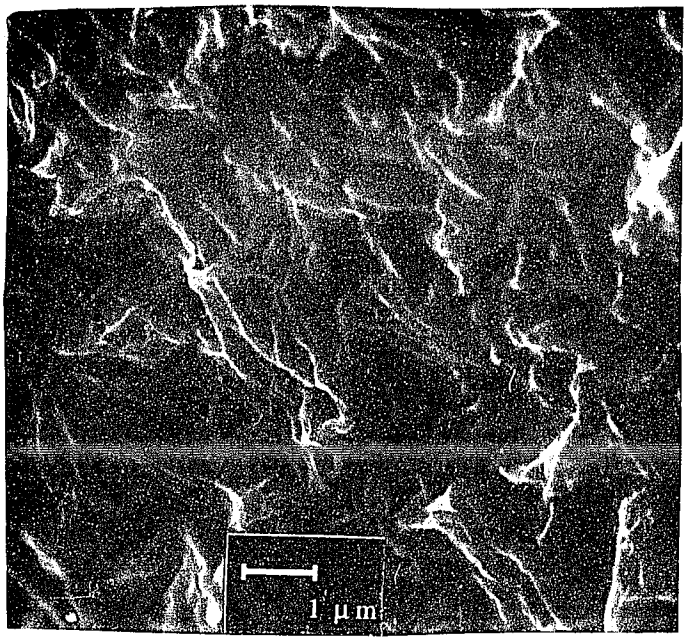

Figure 3.8a. Scanning electron micrograph of fractionated TPI (Mv=6.1×10^5) crystallized from the melt at 25°C

Figure 3.8b. Same as figure 3.8a but different field

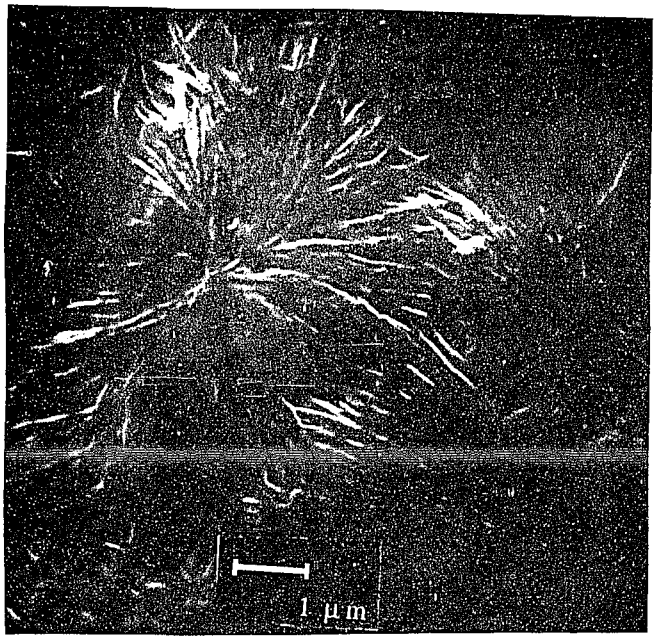

Figure3.9a. Scanning electron micrograph of unfractionated TPI crystallized from the melt at 36°C

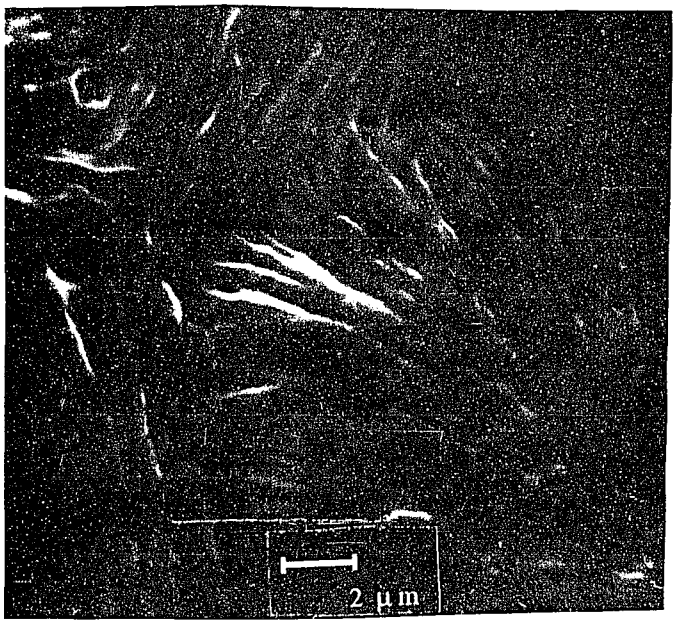

Figure 3.9b. Same as figure 3.9a but higher magnification

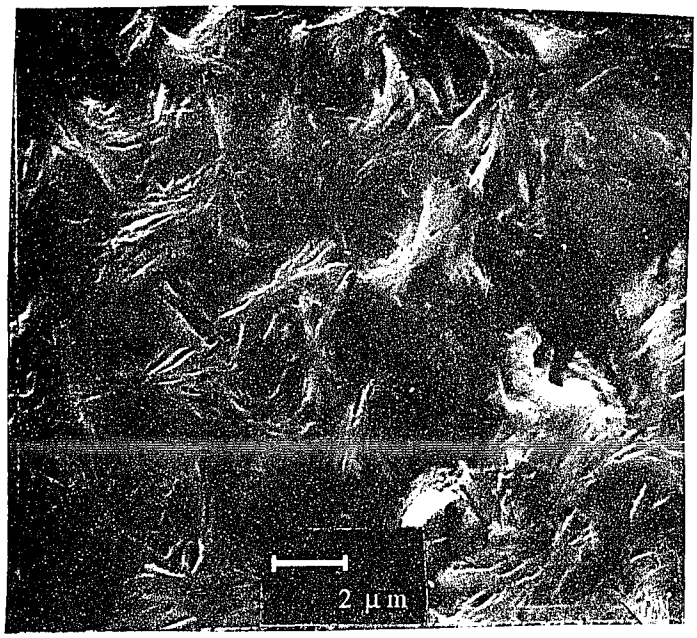

Figure 3.10a. Scanning electron micrograph of fractionated TPI ($Mv=8.3x10^4$) crystallized from the melt at 36°C

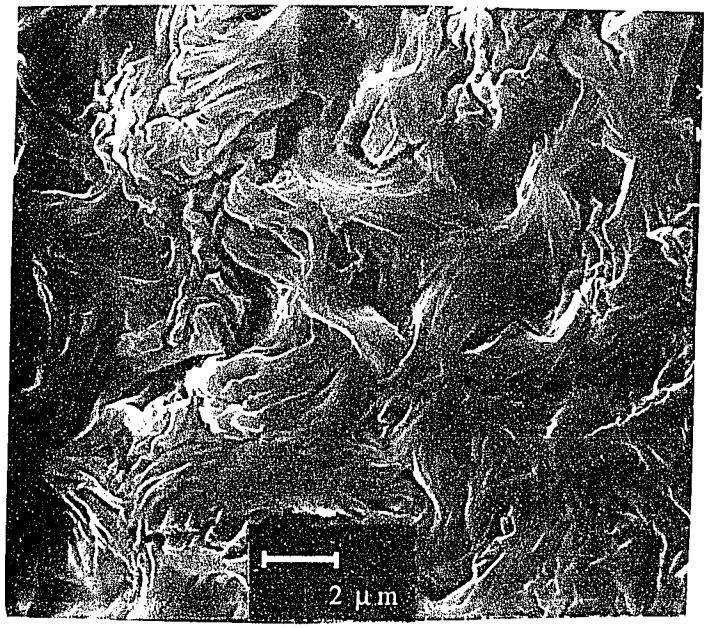

Figure 3.10b. Same as figure 3.10a but higher magnification

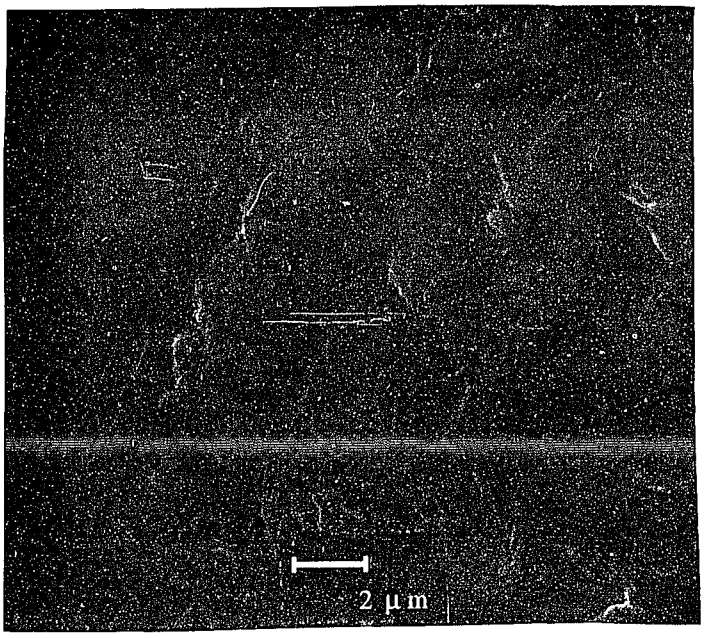

Figure 3.11a. Scanning electron micrograph of fractionated TPI (Mv=6.1x10^5) crystallized from the melt at 36°C

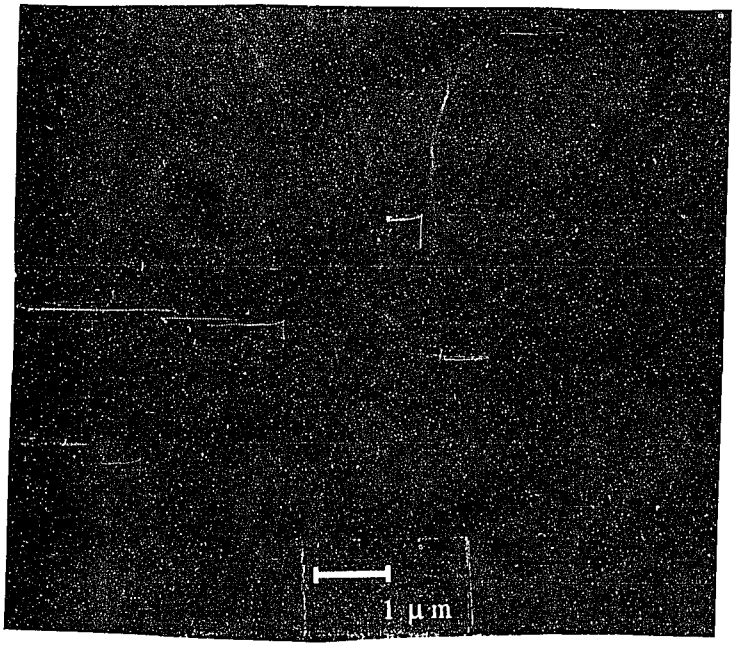

Figure 3.11b. Same as figure 3.11a but higher magnification

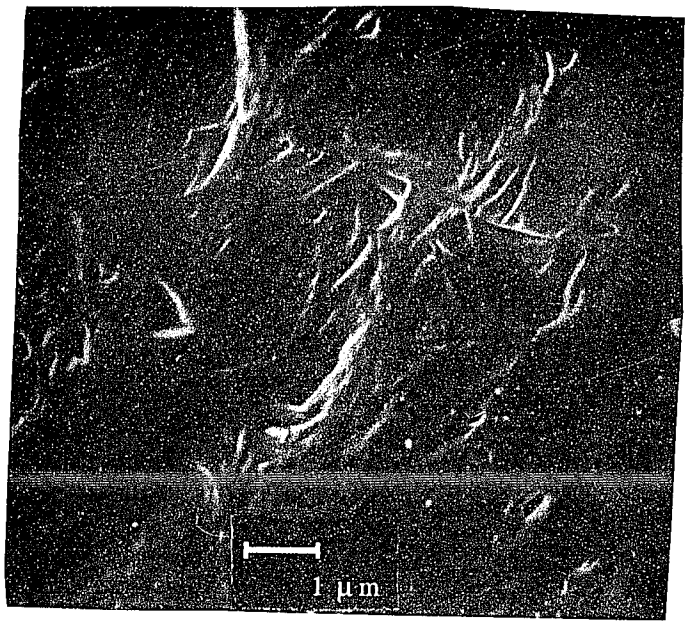

Figure 3.12a. Scanning electron micrograph of unfractionated TPIcrystallized from the melt at 43°C and reacted with OsO_4, cooled to 25°C

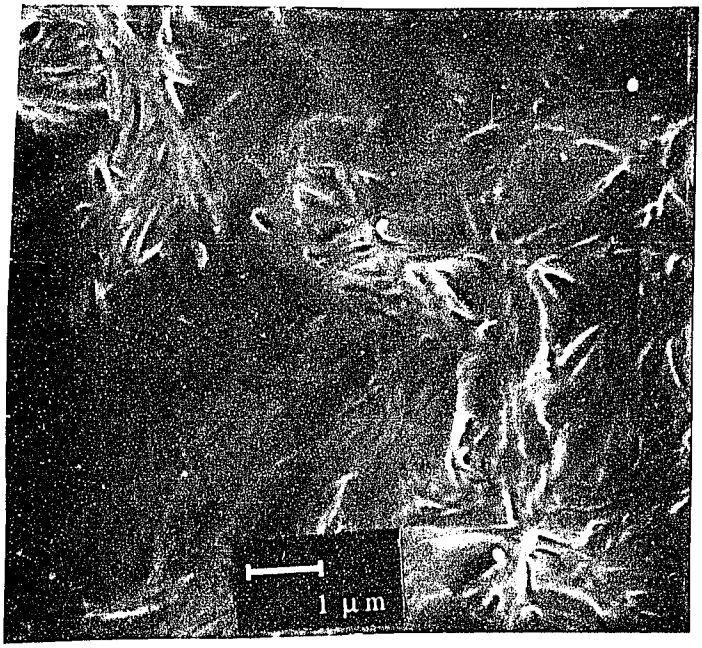

Figure 3.12b. Same as figure 3.12a but different field

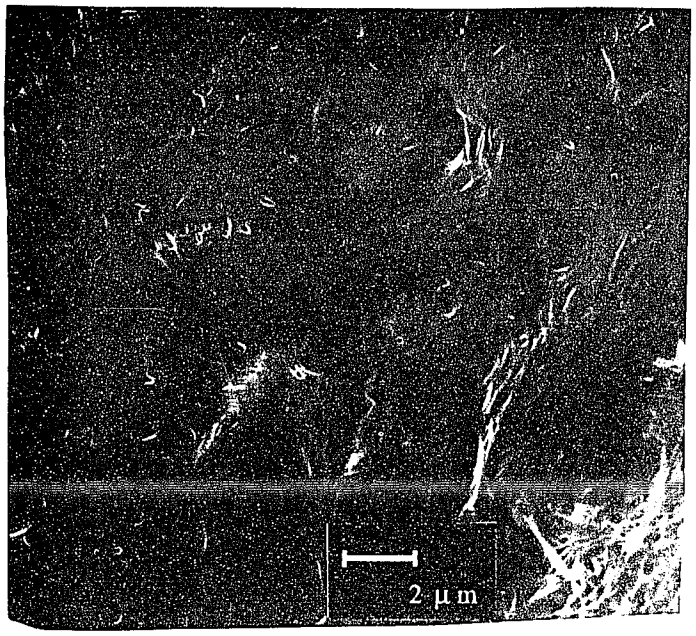

Figure 3.13a. Scanning electron micrograph of unfractionated TPI crystallized from the melt at 43°C, cooled to 25°C and reacted with OsO_4

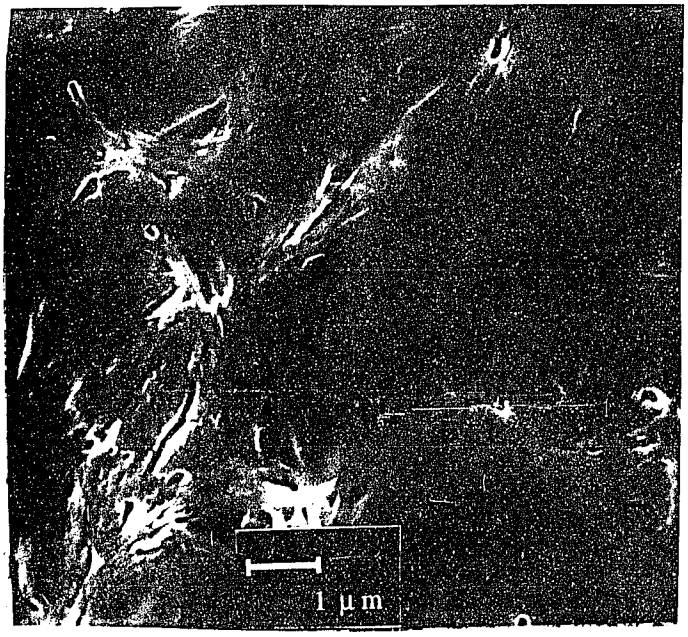

Figure 3.13b. Same as figure 3.13a but higher magnification

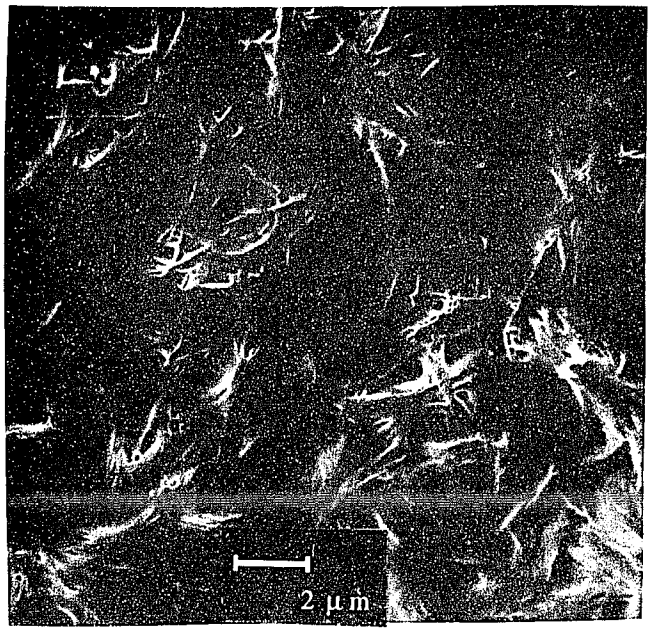

Figure 3.14a. Scanning electron micrograph of fractionated TPI($8.3x10^4$) crystallized from the melt at 43°C, cooled to 25°C and reacted with OsO_4

Figure 3.14b. Same as figure 3.14a but higher magnification

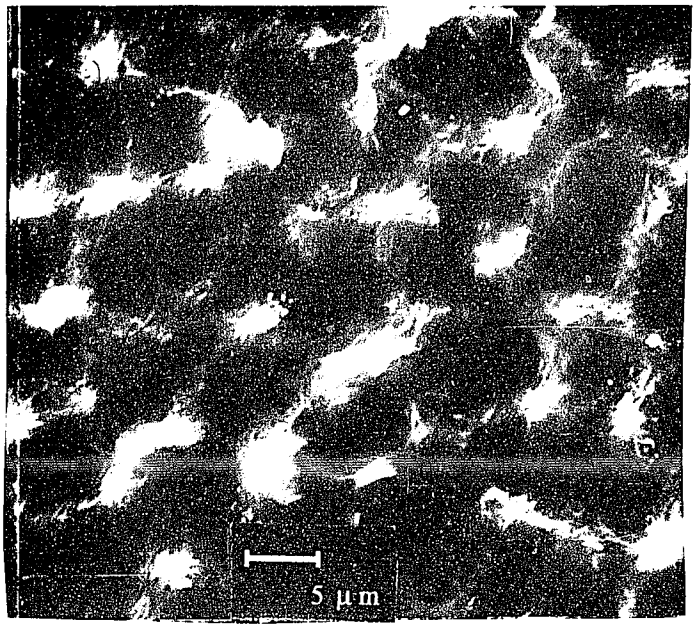

Figure 3.15a. Scanning electron micrograph of fractionated TPI(6.1×10^5) crystallized from the melt at 43°C, cooled to 25°C and reacted with OsO_4

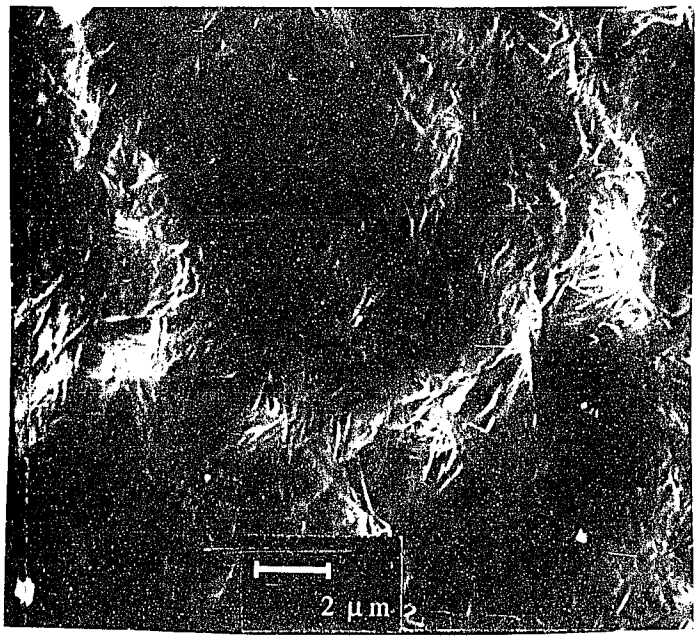

Figure 3.15b. Same as figure 3.15a but different field

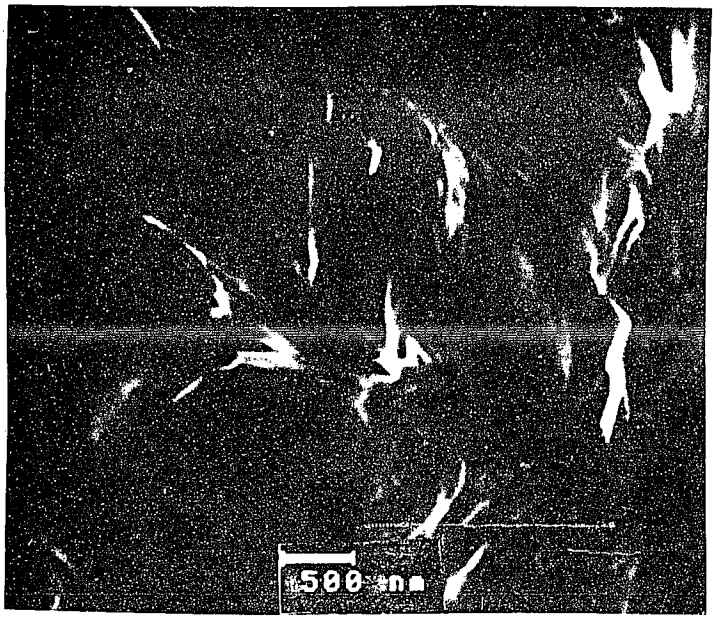

Figure 3.15c. Same as figure 3.15a but different field

3.1.3. Morphologies of alpha TPI

Alpha TPI structures were prepared by bulk crystallization at 43°C and 51°C in an FTIR heating cell using a seeding technique. These same samples were used for FTIR investigation. The structures obtained at T_c = 43°C for unfractionated TPI in the alpha form are smilar in size and appearance to those obtained at this temperature for the same material in the beta form, as seen in Figure 3.16. Crystallization of the high molecular weight fraction in the alpha form at 43°C leads to spherulitic structures, as shown in Figure 3.17 that are larger in average diameter than those from unfractionated TPI. Unlike those for unfractionated TPI, these spherulites differ markedly from the beta form structures appearing at 43°C for the two fractions. At T_c= 43°C the sizes observed for the alpha spherulite range from 3 to 6 microns for the unfractionated sample and 5-8 micrometer for those from the high molecular weight fraction.

A spherulitic morphology is obtained for the unfractionated TPI and for both fractions at T_c = 51°C as shown in Figures 3.18 - 3.20. When the OsO_4 treatment was carried out after cooling to 25°C, as was generally the case, smaller sheaf structures were observed in some fields of view at both T_c=43°C and 51°C . These were not found when a sample was crystallized at 43°C and OsO_4 treated at T_c, as shown in Figure 3.21.

Direct crystallization at 55°C on a glass plate in the alpha form was accomplished using the unfractionated sample. This yields spherulites with diameters of 40 to 60 microns as shown in Figure 3.22. In some cases regions between the spherulites contained multilamellar structures 2 to 5 microns in length (Figure 3.23).

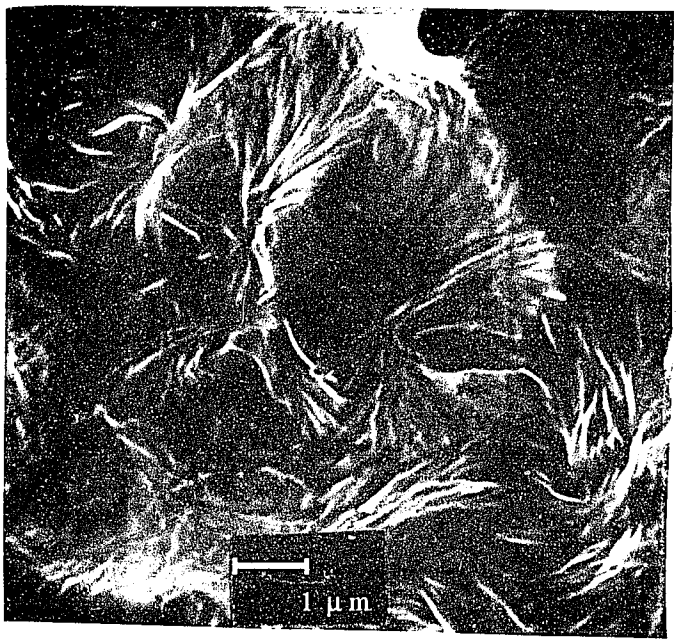

Figure 3.16. Scanning electron micrograph of unfractionated TPI crystallized from the melt using a prenucleation method at 43°C, cooled to 25°C and reacted with OsO_4

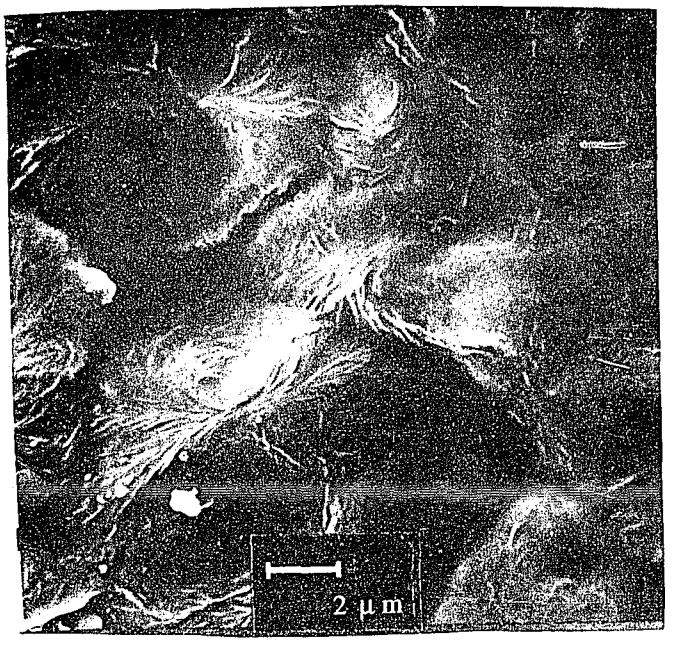

Figure 3.17. Scanning electron micrograph of fractionated TPI(M_V=6.1x10^5) crystallized from the melt using a prenucleation method at 43°C, cooled to 25°C and reacted with OsO_4

Figure 3.18. Scanning electron micrograph of unfractionated TPI crystallized from the melt using a prenucleation method at 50°C, cooled to 25°C and reacted with OsO_4

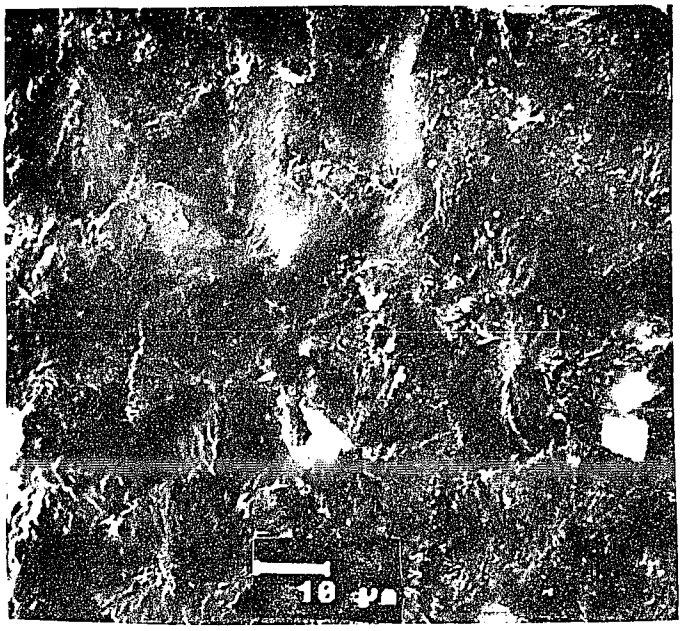

Figure 3.19a. Scanning electron micrograph of fractionated TPI(M_V=8.3x10^4) crystallized from the melt using a prenucleation method at 51°C, cooled to 25°C and reacted with OsO_4

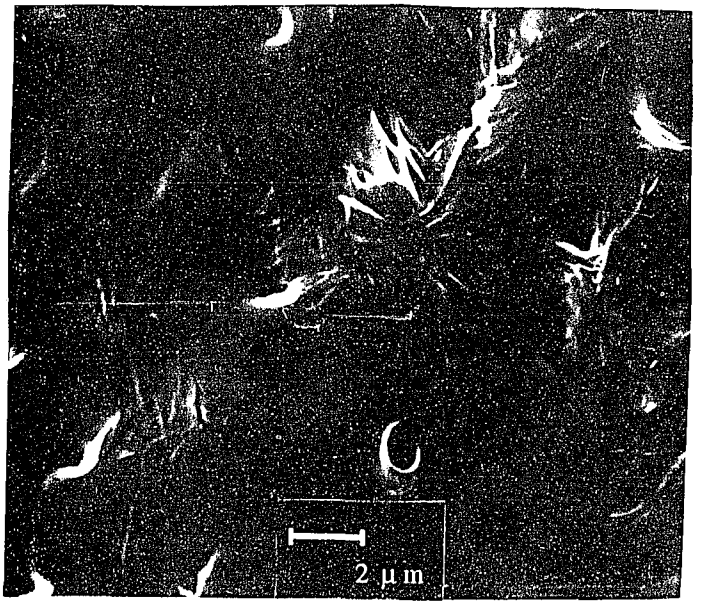

Figure 3.19b. Same as figure 3.19a but diffrent field

Figure 3.20. Scanning electron micrograph of fractionated TPI(M_V=6.1x10^5) crystallized from the melt using a prenucleation method at 51°C, cooled to 25°C and reacted with OsO_4

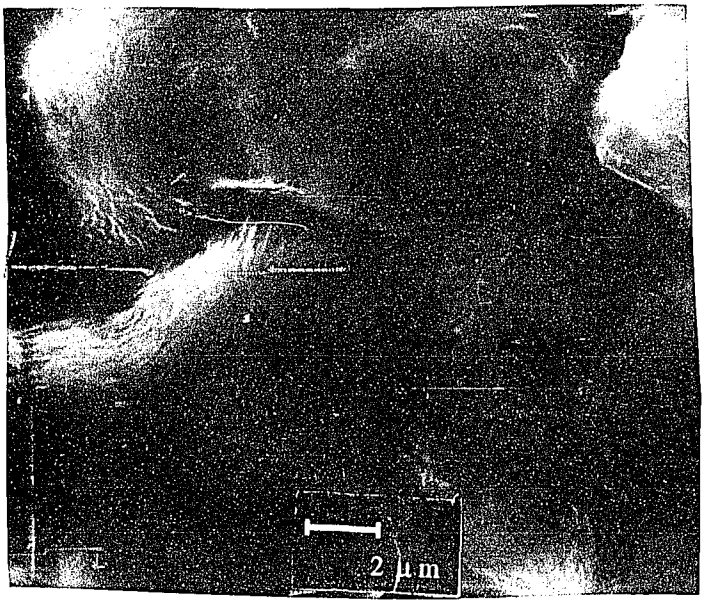

Figure 3.21. Scanning electron micrograph of fractionated TPI(M_V=6.1x10^5) crystallized from the melt using a prenucleation method at 43°C, reacted with OsO_4 and cooled to 25°C

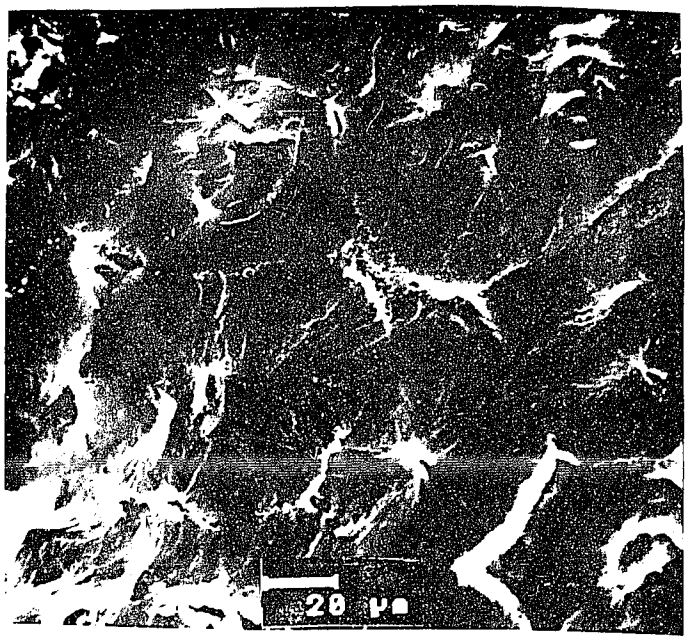

Figure 3.22. Scanning electron micrograph of unfractionated TPI crystallized from the melt at 55°C

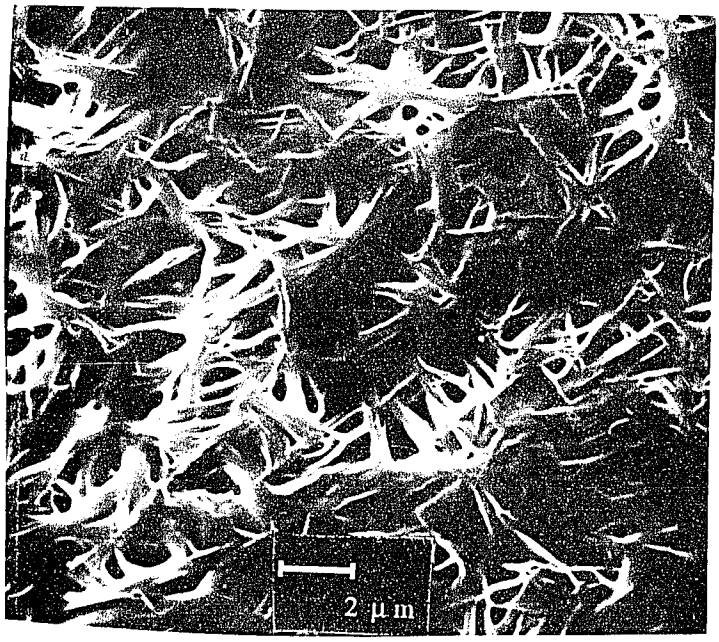

Figure 3.23. Same as figure 3.22 but different field and higher magnification.

3.1.4. Differential scanning calorimetry

Crystallization of unfractionated material and two fractions from the direct melt crystallization method at constant crystallization temperature, T_c of 25°C to 43°C, yields the beta crystal form only, as evidenced by FTIR spectroscopy. Crystallization of TPI by an annealing method at T_c=43°C also yields the beta form. Some representative melting endotherms are given in Figure 3.24. One clear endotherm is observed in each case. The melting temperatures were obtained by extrapolation. Melting temperatures and endotherms of all beta-TPI samples are given in Table 3.1 in terms of molecular weight and crystallization temperature.

DSC measurements were also carried out for samples in the alpha crystal form as obtained by a seeding technique. Some representative scans of alpha-TPI samples are also given in Figure 3.25. Single endotherms were observed except for the low molecular weight, (M_v = 8.3 x 10^4) sample crystallized at 43°C which showed an additional overlapping component at lower temperature. Melting temperatures and melting endotherms are also listed in Table 3.2.

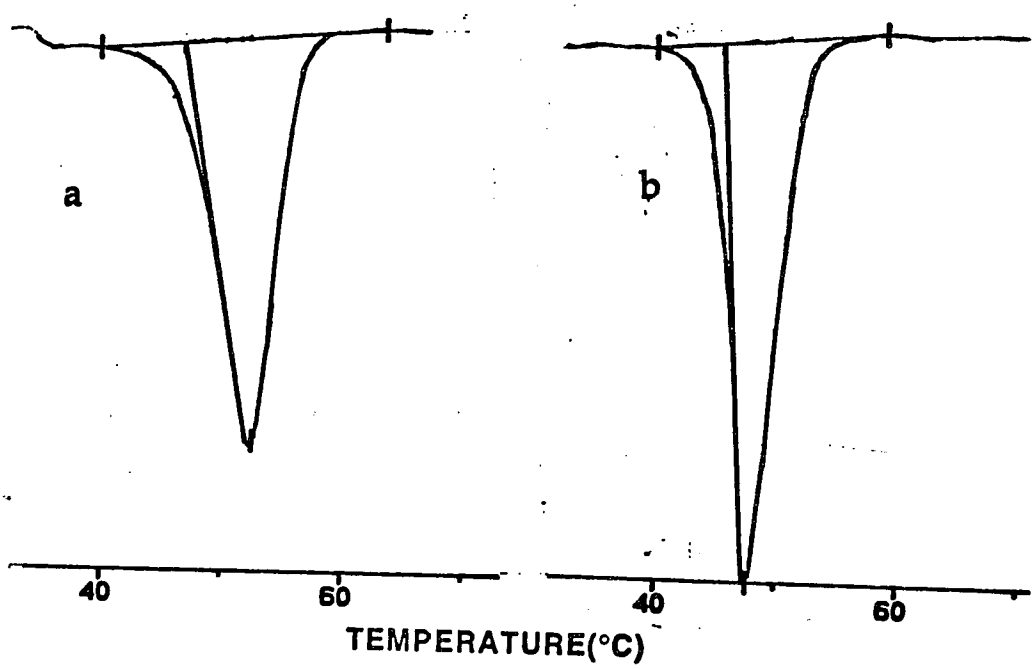

Figure 3.24. DSC scans for melt crystallized TPI: a) beta form crystallized at 43°C and cooled to 25°C, unfractionated sample
b) beta form crystallized at 25°C, heated to 43°C and cooled to 25°C, fractions with Mv = 8.3 x 10^4

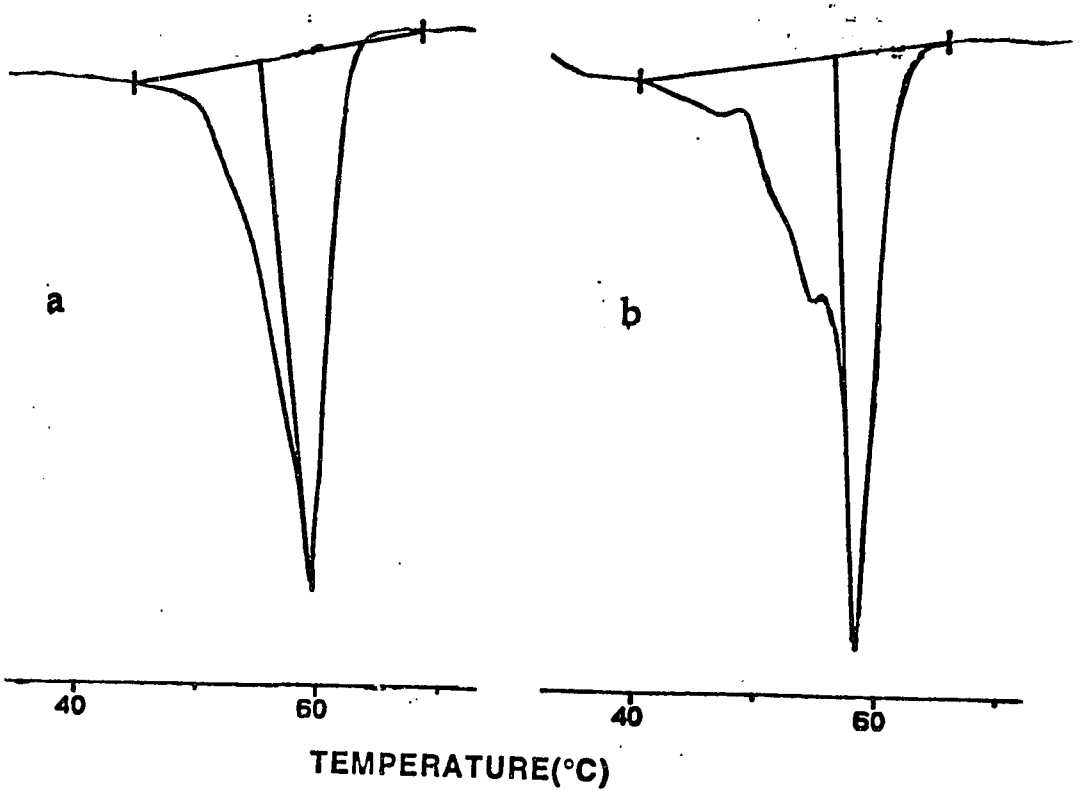

Figure 3.25. DSC scans for melt crystallized TPI: a) alpha form crystallized at 43°C and cooled to 25°C, unfractionated sample
b) alpha form crystallized at 43°C and cooled to 25°C, fractions with Mv = 8.3 x 10^4

Table 3.1. T_m and T_{endo} for beta TPI[a]

Sample	T_c °C	T_m °C	T_{endo} °C
Unfractionated	25	43	47
Unfractionated	36	43	48
M_v=6.1 x 10^5	36	43	47
Unfractionated	43	46	52
M_v=8.3 x 10^4	43	47	51
M_v=6.1 x 10^5	43	45	52
Unfractionated	25/43[b]	46	49
M_v=8.3 x 10^4	25/43[b]	44	48
M_v=6.1 x 10^5	25/43[b]	44	48

a Average of two or more determinations with a precession of ±1 °C

b Sample crystallized at 25°C, annealed at 43°C and cooled to 25°C

Table 3.2. Tm and Tendo for alpha TPI[a]

Sample	Tc-°C	Tm-°C	Tendo-°C
Unfractionated	43	55	60
M_V=8.3 x 10^4	43	56	59
M_V=6.1 x 10^5	43	49	57
Unfractionated	51	61	63
M_V=8.3 x 10^4	51	59	65
M_V=6.1 x 10^5	51	57	64

a Average of two or more determination with a precession of ±1 °C

3.2. FTIR Spectrosopic investigation of bulk crystallized TPI

3.2.1. FTIR Spectroscopy

FTIR spectra were obtained as a function of time for fractionated and unfractionated samples crystallized from the melt by the direct, the annealing and the prenucleation methods between NaCl plates in an IR heating cell. FTIR spectra taken for bulk crystallized TPI samples at various times after cooling from 75°C to 43°C are given in Figure 3.26. The spectra taken at 75°C and immediately after cooling to 43°C are essentially identical. The infrared bands are relatively broad and are representative of an amorphous polymer. One band of particular interest, attributed to out-of-plane C-H vibration, is that centered near 842cm^{-1} but having shoulders at 884 and 860cm^{-1}. Figure 3.26 shows spectra taken after 2 hours which display a sharp band at 876cm-^{1} characteristic of the beta crystal form superimposed on the amorphous spectrum. The amorphous band at 842cm^{-1} decreases in intensity and the sharp crystalline band at 876cm increases in intensity with increasing time; the rate of crystallization decreases and finally approaches zero. Cooling the samples to 25°C leads to a further increase in crystalline band intensity and a decrease in amorphous band intensity. The band at 1665-1670cm^{-1} attributed mainly to C=C stretching remains at constant absorbance within 5% for spectra taken at temperatures from 25°-75°C. FTIR spectra were obtained as a function of time, for the samples crystallized at 25°C and annealed at 43°C. The bands characteristic of the beta crystal form first decrease markedly in intensity, almost disappearing

completely. Then after one hour the intensities of these bands start increasing with time as shown in Figure 3.27.

Infrared spectra at 25°C for the TPI fraction with M_V = 6.1 x 10^5 crystallized at 43°C using direct crystallization and seeded crystallization are given in Figure 3.28. The spectrum at the top (B) is characteristic of a composite of the amorphous and the beta crystalline forms. The other spectrum (A) is characteristic of a composite of the amorphous and the alpha crystalline form. These spectra contain the same number of bands at frequencies within $1cm^{-1}$, as found for solution crystallized samples containing the same crystal form. However, relative intensity differences in some bands occur between solution and melt crystallized samples due to the crystallinity differences.

A 100% crystalline spectrum for each melt crystallized sample is obtained from the semicrystalline spectrum taken at Tc and at 25°C by subtraction of the amorphous spectrum obtained at 70°C. The subtraction is carried out by watching the disappearance of the $842cm^{-1}$ band until the negative component appears throughout the spectrum. The subtracted spectrum of 43°C melt crystallized beta samples for 3 days is shown in Figure 3.29. In order to demonstrate the subtraction method, oversubtracted and undersubtracted spectra are compared with a properly subtracted one in the figure. All of the FTIR spectra obtained for direct bulk crystallized TPI even at short crystallization time can be separated into beta crystalline and amorphous components. The subtracted spectra as a function of time

for unfractionated TPI, crystallized at 25°C and heated to 43°C is given in Figure 3.30. Spectra taken during the first 7 hours cannot be separated into two components. In order to remove all of the 842cm^{-1} band, characteristic of the amorphous component as observed in the melt, over-subtraction of the other part of the spectrum is necessary. At subtraction factors where this over-subtraction is not apparent a band is still evident at 840cm^{-1} and the other bands do not have the same relative intensities as typically found for the beta form. These effects are demonstrated in Figure 3.31.

A FTIR spectrum taken for an alpha form containing sample and the spectrum obtained by subtraction of amorphous component are given in Figure 3.32. A number of differences occur between the spectra for the alpha and beta crystal forms, but one of the most notable is the presence of two bands for the alpha form at 862 and 882cm^{-1} instead of one band at 876cm^{-1}, attributed to the same C-H vibration.

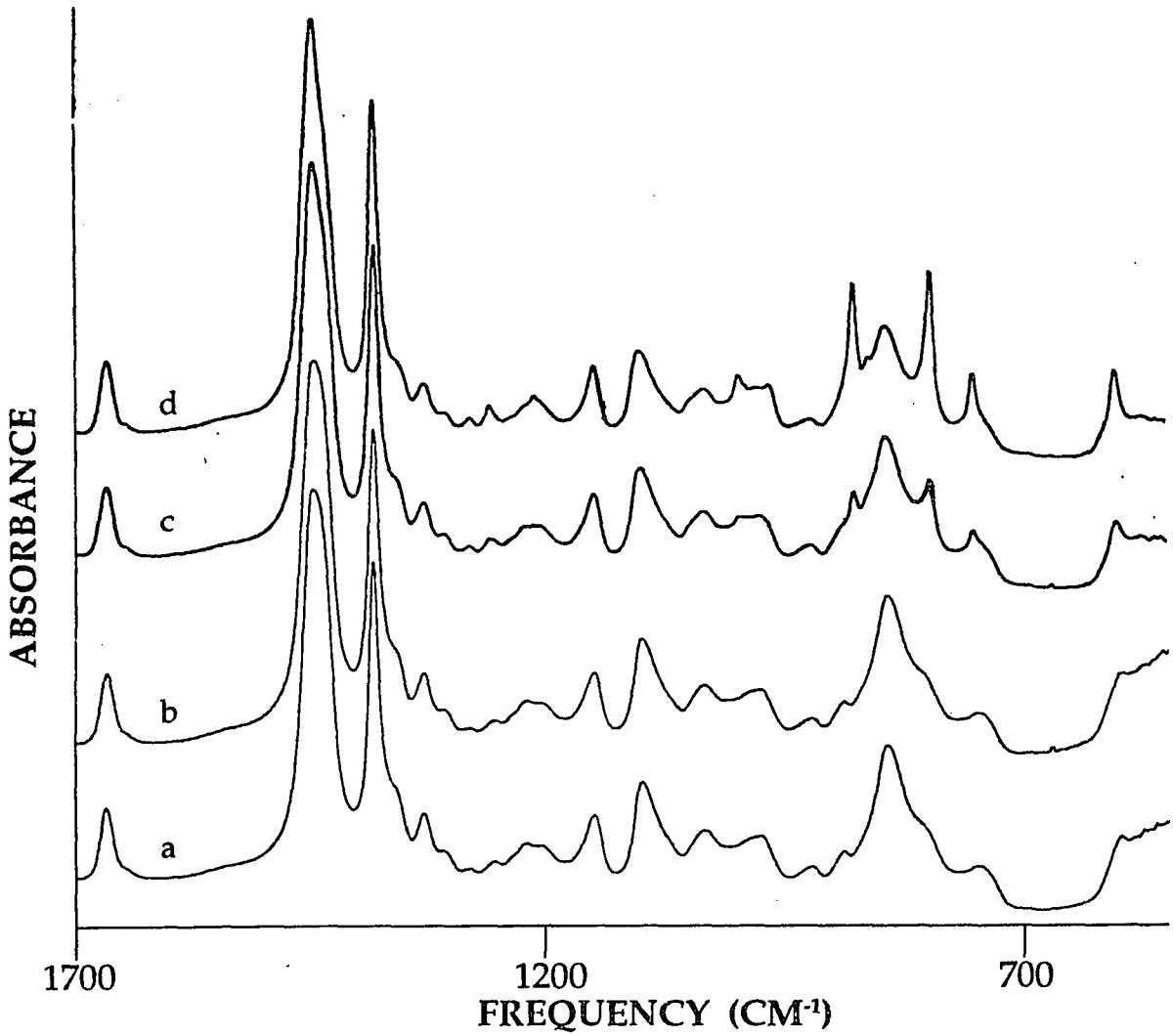

Figure 3.26. FTIR absorbance versus frequency for unfractionated melt crystallized TPI. Spectrum taken at: a) 75°C, b) 43°C, 2 hours later , c) 43°C, 8 hours after taking spectrum a, d) 43°C, 3days after taking spectrum a

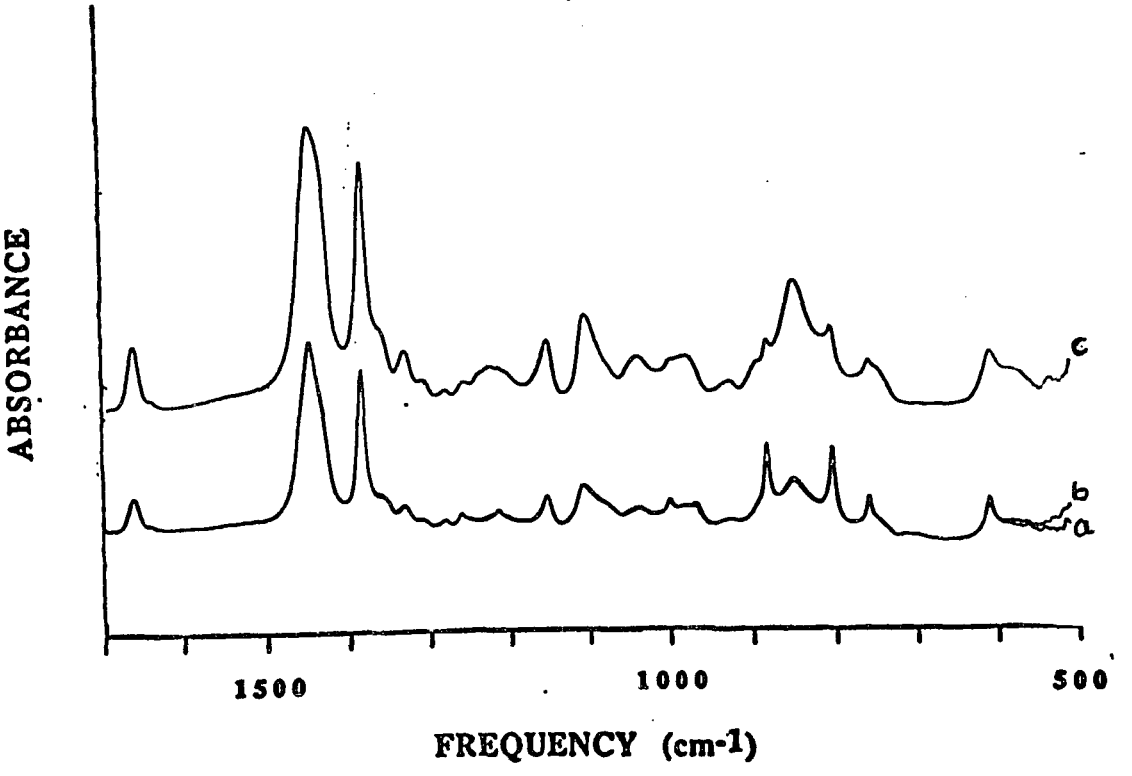

Figure 3.27. FTIR absorbance versus frequency for unfractionated TPI melt crystallized at 25°C and heated to 43°C : a) 43°C, 15min later, b) 43°C, 7hours after taking spectrum a c) 43°C, 58hours after taking spectrum a

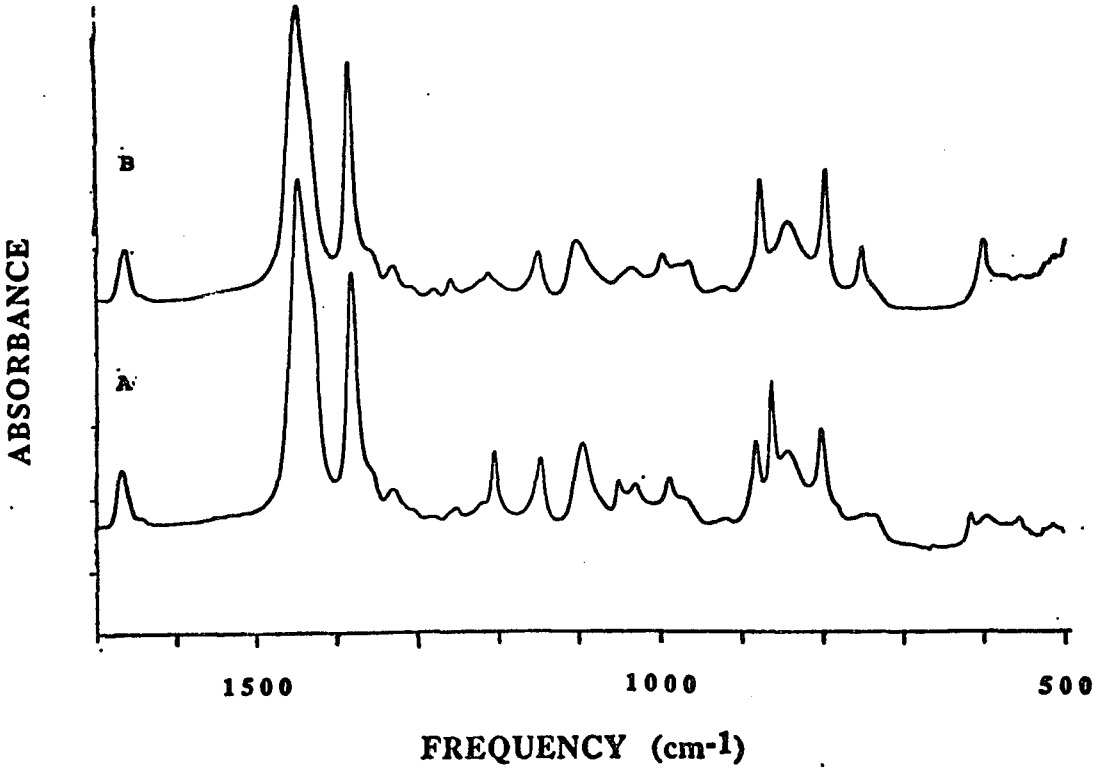

Figure 3.28. FTIR spectra at 25°C for TPI (Mv = 610000) bulk crystallized at 43°C : a) pretreated by cooling from 90°C to 55°C for 2 weeks followed by cooling to 25°C and heating to 65°C ; b) by cooling from 75°C

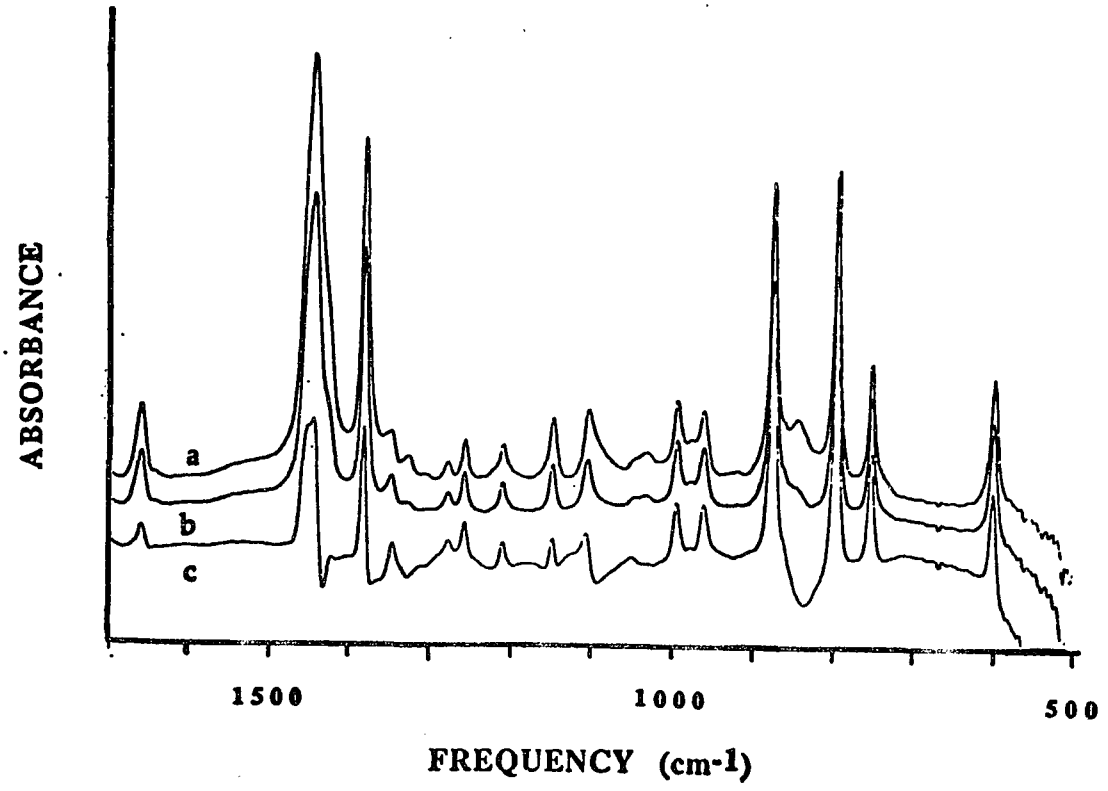

Figure 3. 29. FTIR spectra, for unfractionated TPI crystallized at 43°C for three days, after subtraction of amorphous spectrum:
a) undersubtracted b) correct subtraction, and c) oversubtracted

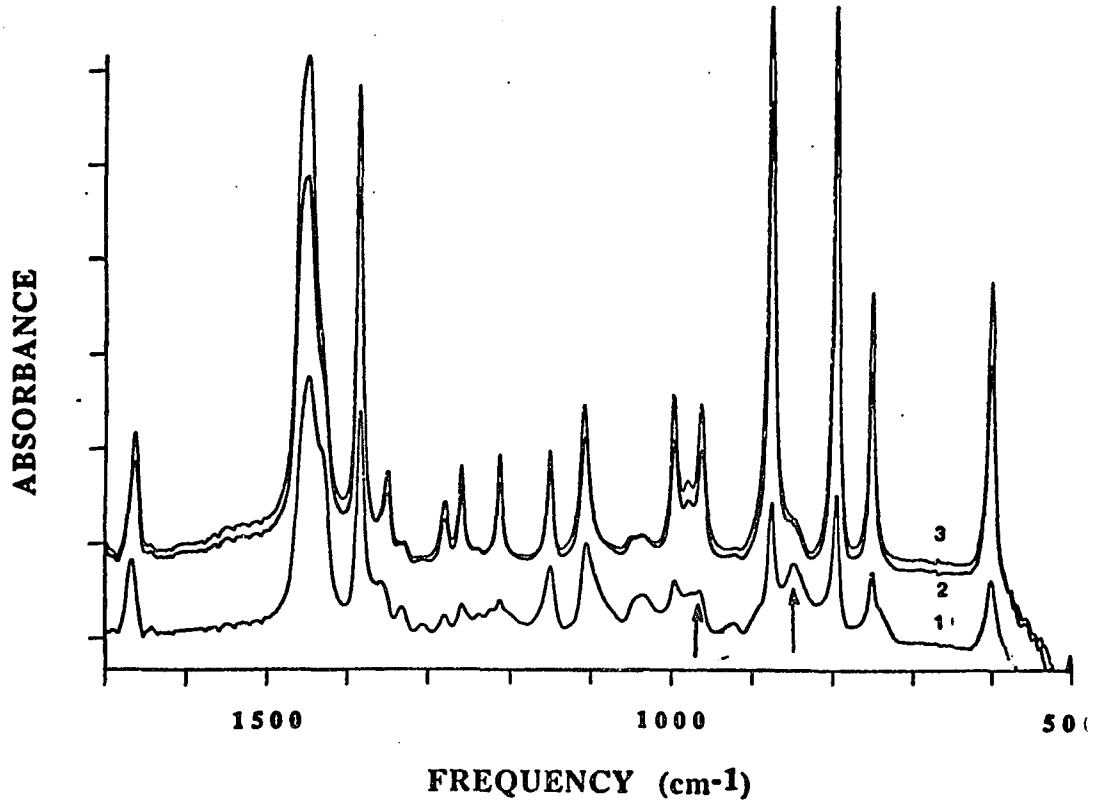

Figure 3.30. FTIR spectra after subtraction (using an amorphous spectrum taken at 60°C) for TPI heated to 75°C, bulk crystallized at 25°C and then heated to 43°C: (1) for 1 h; (2) for 7.3 h; (3) for 58 h (Arrows mark the bands at 840 and 962cm^{-1})

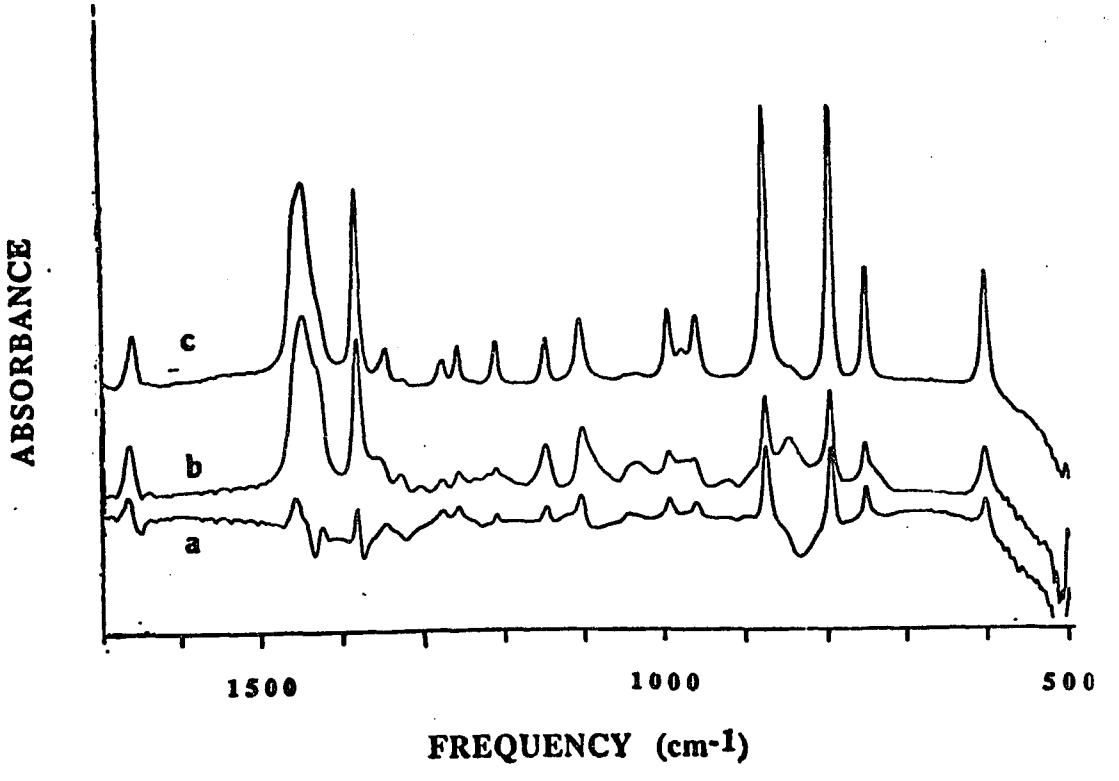

Figure 3.31. FTIR subtraction spectra for unfractionated TPI melt crystallized at 25°C and heated to 43°C for: a) 1 hour, with subtraction necessary to remove 842 cm^{-1} band. b) 1 hour, correct subtraction and c) 4 days, correct subtraction

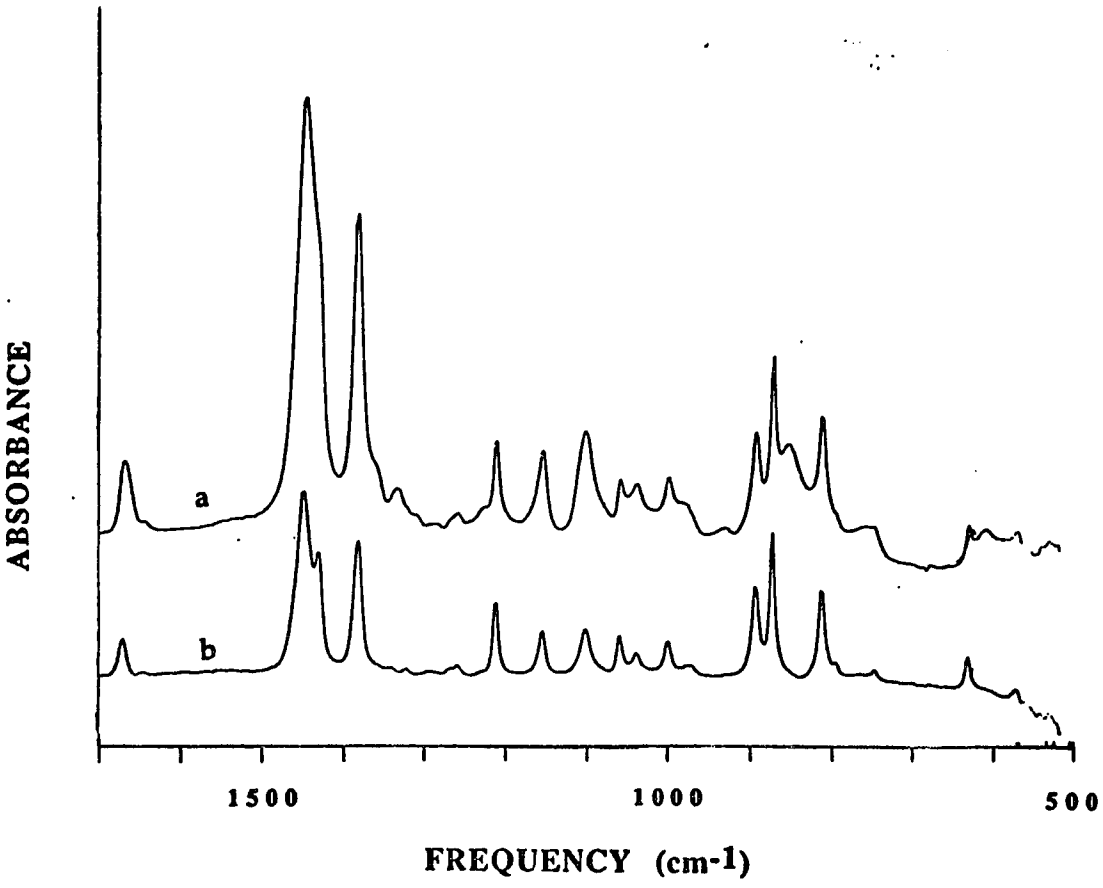

Figure 3.32. FTIR spectra for unfractionated TPI crystallized at 43°C for 47 hours after alpha form seeding: a) before subtraction, b) after subtraction of the amorphous component

3.2.2. Crystallization isotherms

Crystallization isotherms were obtained by plotting subtraction factors against the time for all the melt crystallized samples prepared by the direct, annealing and prenucleation methods. Subtraction factors were obtained by subtracting the amorphous component from the semicrystalline spectrum. Successful subtraction implies that the system is composed of only two components and therefore the computer subtraction factor at each time would be taken as the amorphous or melt-like fraction.

Subtraction factors as a function of time at 36°C and 43°C for melt crystallized unfractionated and fractionated TPI prepared by the direct method are given in Figures 3.33 and 3.34 respectively. The subtraction factor versus time for the 43°C annealed sample is given in Figure 3.35. These crystallization isotherms contain 1) an induction period during which the nucleation process commences, 2) a crystallization period, and 3) a final period where no measurable change in subtraction factor takes place. The final values depends on the molecular weight with unfractionated and the highest molecular weight samples having about the same subtraction factors which are higher than those for the other two molecular weight fractions.

To obtain TPI samples containing the alpha crystal form a prenucleation technique was used. Subtraction factor versus time curves for samples crystallized at 43°C and 51°C are given in Figures 3.36 and 3.37. Crystallization isotherms show both vertical and

horizontal shifts with molecular weight. Rates of crystallization can be obtained from the slope of the curves. The rate of crystallization varies with the molecular weight. The final subtraction factor values increases with increasing molecular weight.

3.2.3. Measurement of amorphous fraction

The amorphous fractions for the various alpha and beta TPI samples at the crystallization temperature are given in Table 3.3. The amorphous fractions at 25°C are given in Table 3.4. Amorphous fractions, obtained from the absorbance ratio method were all lower than the subtraction factors by .03 to .06 units. The values obtained by the latter method must be corrected for the increase in the number of absorbers in the infrared beam upon partial crystallization and cooling the sample. Assuming that the sample volume in the beam remains constant, this correction involves multiplication by the ratio of the amorphous density at 60°C to the sample density at the measurement temperature (see Appendix 1). The corrected amorphous fraction at crystallization temperature and the annealing temperature are given in Table 3.5. The corrected amorphous fraction at 25°C are given in Table 3.6. These corrected values agree with the amorphous fraction obtained by absorbance ratio method within ± 0.01.

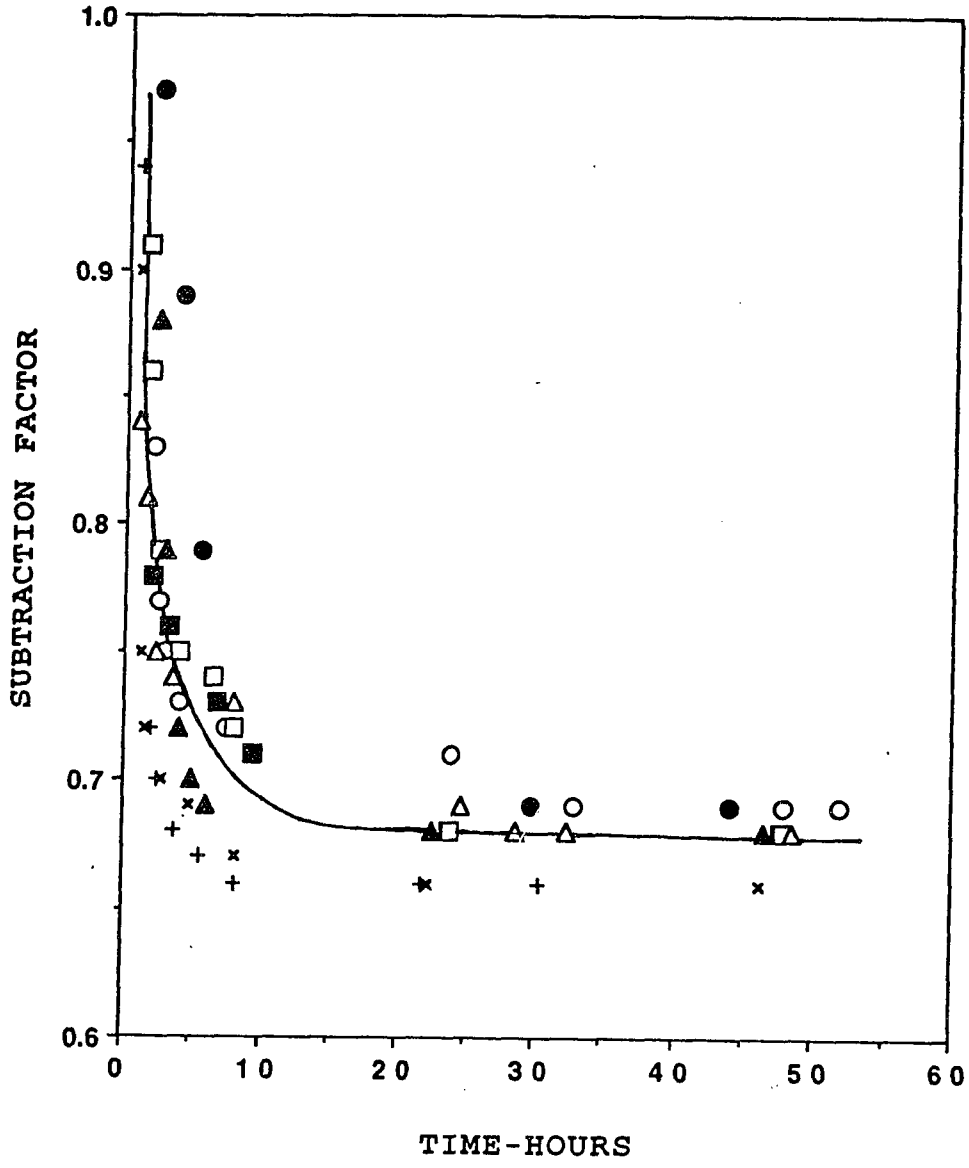

Figure 3.33. FTIR subtraction factor vs time for TPI bulk crystallized at 36°C after cooling from 75°C: (○,●) unfractionated; (+,×) Mv = 83000; (□,■) Mv = 280000; (△,▲) Mv = 610000

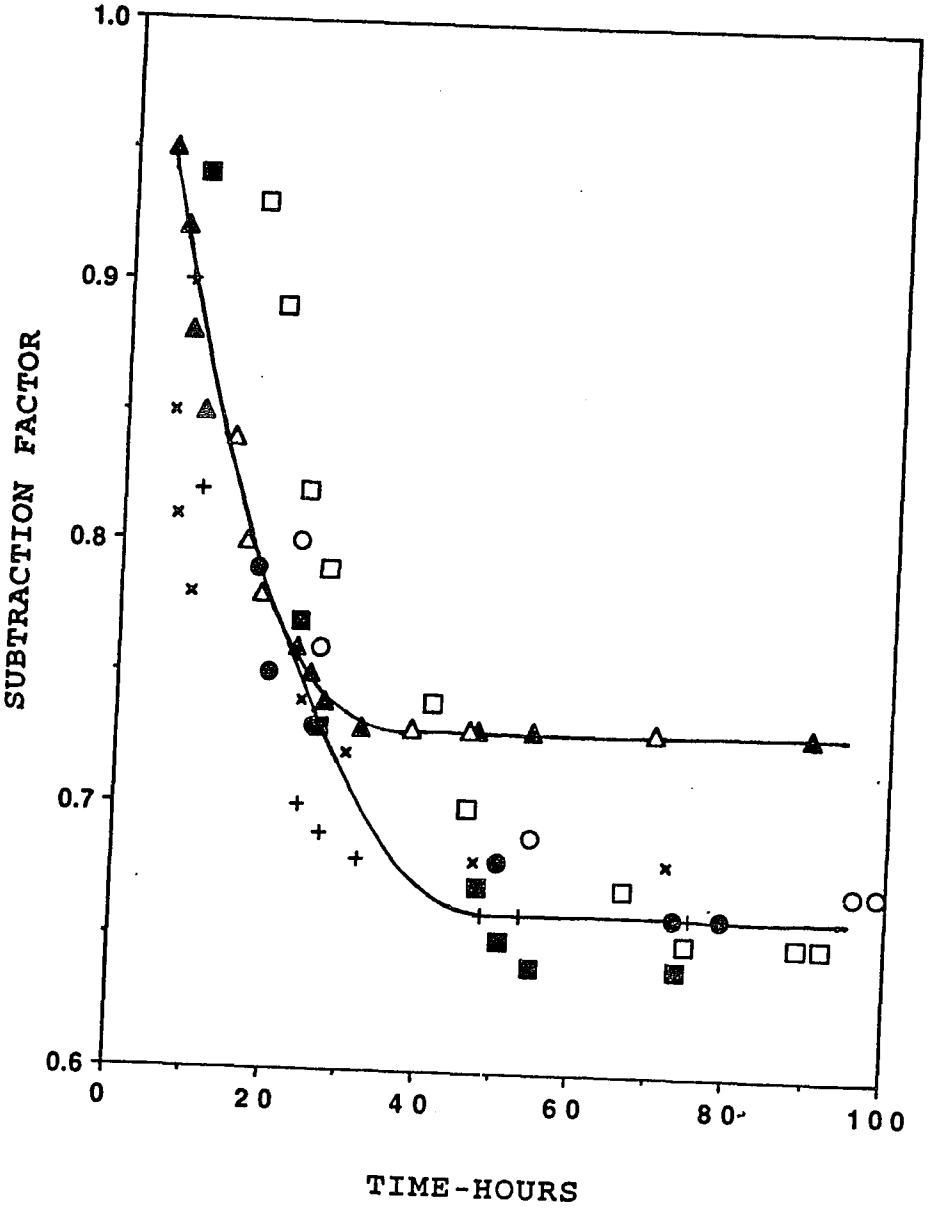

Figure 3.34. FTIR subtraction factor vs time for TPI bulk crystallized at 43°C after cooling from 75°C: (○,●) unfractionated; (+ ,×) Mv = 83000; (□,■) Mv = 280000; (△,▲) Mv = 610000

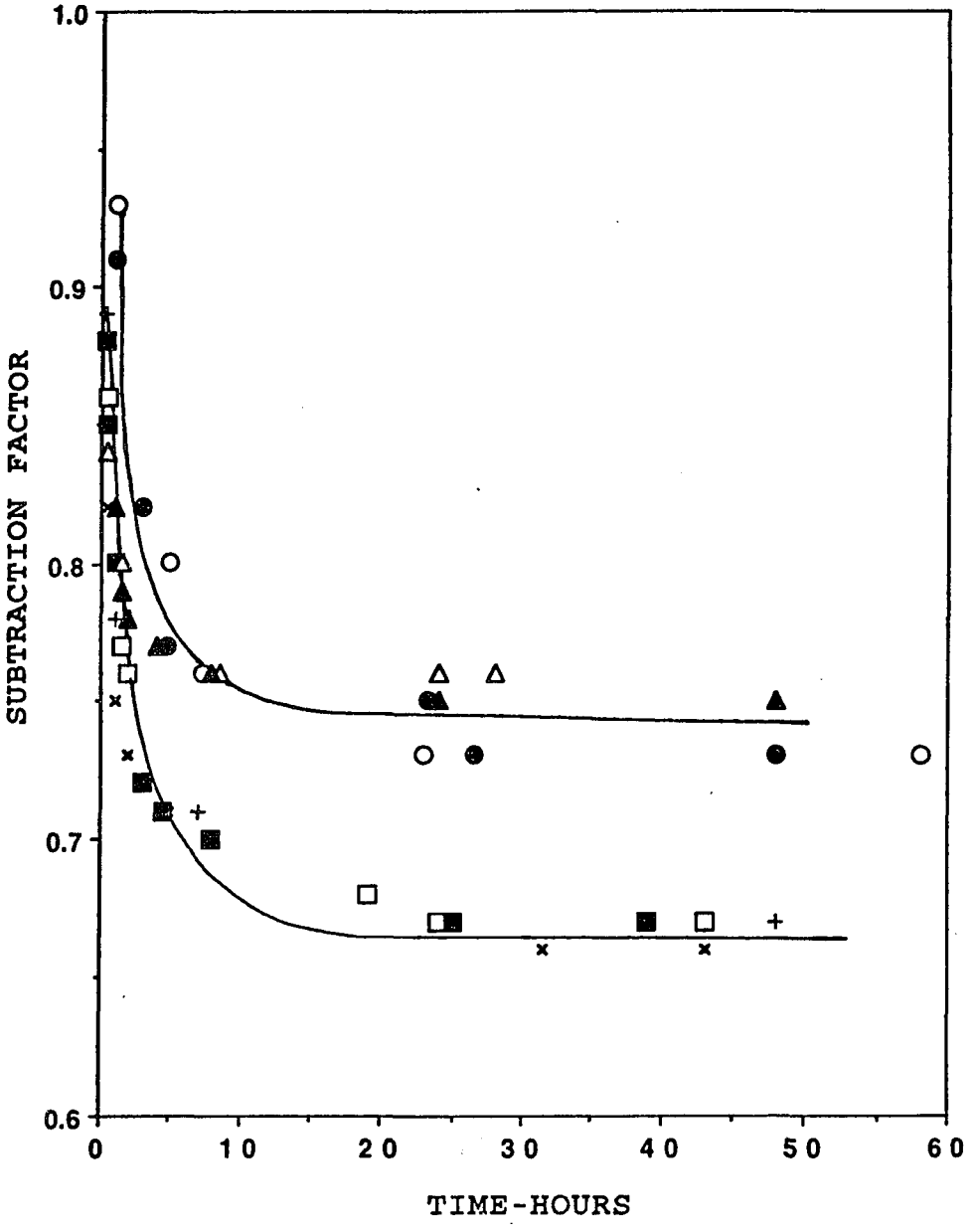

Figure 3.35. FTIR subtraction factor vs time for TPI heated to 75°C, bulk crystallized at 25°C and then heated to 43°C

(○,●) unfractionated; (+,×) Mv = 83000; (□,■) Mv = 280000; (△,▲) Mv = 610000

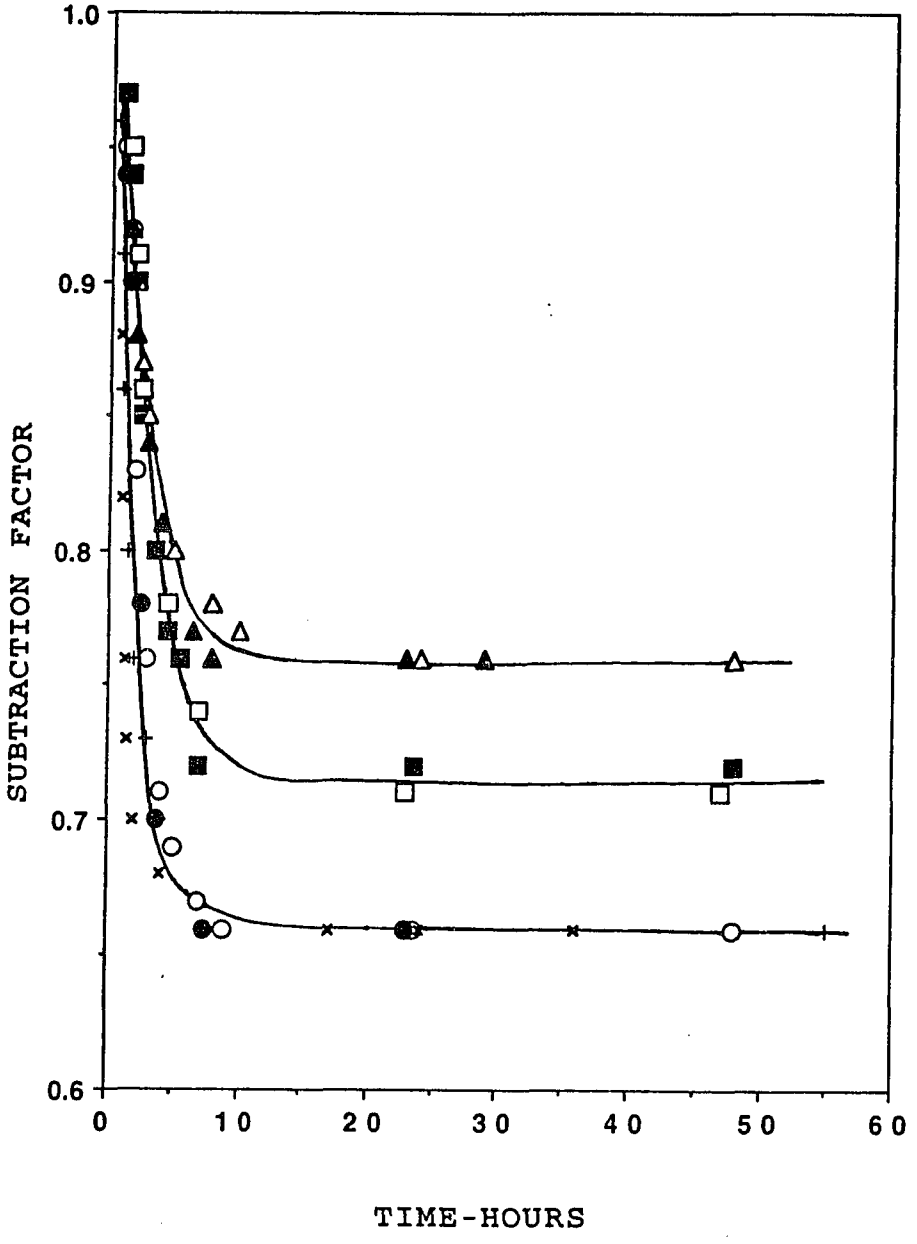

Figure 3.36. FTIR subtraction factor vs time for TPI pretreated by cooling from 90°C to 55°C for 2 weeks followed by cooling to 25°C and heating to 65°C then crystallized at 43°C

(○,●) unfractionated; (+,×) Mv = 83000; (□,■) Mv = 280000; (△,▲) Mv = 610000

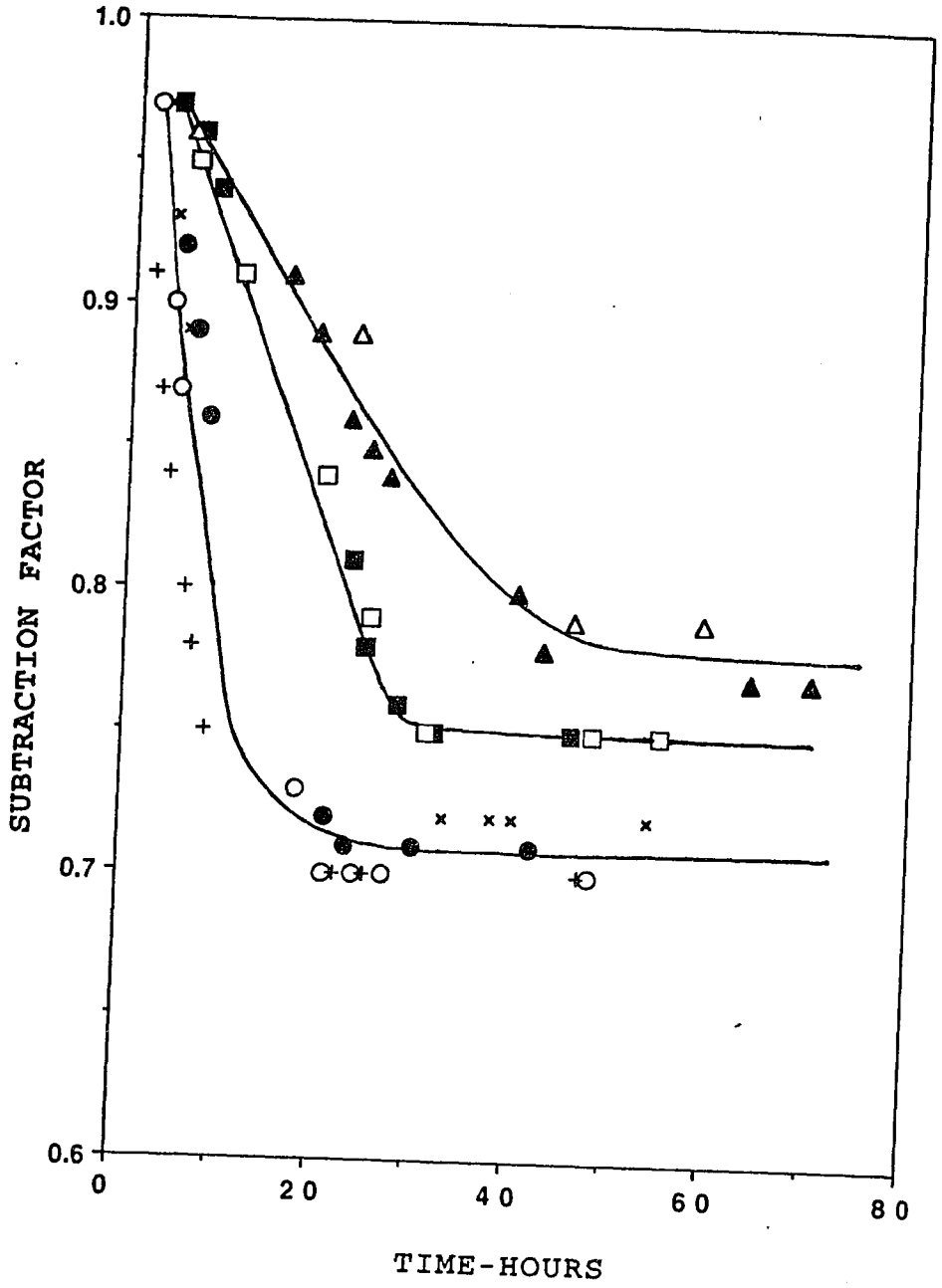

Figure 3.37. FTIR subtraction factor vs time for TPI pretreated by cooling from 90°C to 55°C for 2 weeks followed by cooling to 25°C and heating to 65°C then crystallized at 51°C

(○,●) unfractionated; (+ ,×) Mv = 83000; (□,■) Mv = 280000; (△,▲) Mv = 610000

Table 3.3. Amorphous fraction at Tc

Sample	Tc or Ta	Amorphous fraction	
	°C	Subtraction factor	Absorption Ratio
U.F	25[a]	0.66	0.62
U.F	36[a]	0.69	0.65
8.3 x 10^4		0.66	0.63
2.8 x 10^5		0.69	0.65
6.1 x 10^5		0.68	0.64
U.F	43[a]	0.67	0.62
8.3 x 10^4		0.67	0.63
2.8 x 10^5		0.65	0.61
6.1 x 10^5		0.73	0.70
U.F	25/43[b]	0.73	0.69
8.3 x 10^4		0.66	0.62
2.8 x 10^5		0.66	0.61
6.1 x 10^5		0.75	0.71
U.F	43[c]	0.66	0.61
8.3 x 10^4		0.66	0.62
2.8 x 10^5		0.72	0.67
6.1 x 10^5		0.76	0.71
U.F	51[c]	0.70	0.66
8.3 x 10^4		0.71	0.66
2.8 x 10^5		0.75	0.71
6.1 x 10^5		0.78	0.72

a. melt crys beta form b. annealed beta form

c. pretreated alpha form

Table 3.4. Amorphous fraction at 25°C

Sample	Tc or Ta °C	Amorphous fraction Subtraction factor	Amorphous fraction Absorption Ratio
U.F	25[a]	0.66	0.62
U.F	36[a]	0.64	0.59
8.3 x 10^4		0.58	0.53
2.8 x 10^5		0.62	0.56
6.1 x 10^5		0.62	0.56
U.F	43[a]	0.61	0.56
8.3 x 10^4		0.60	0.52
2.8 x 10^5		0.58	0.53
6.1 x 10^5		0.62	0.57
U.F	25/43[b]	0.67	0.62
8.3 x 10^4		0.67	0.63
2.8 x 10^5		0.65	0.61
6.1 x 10^5			
U.F	43[c]	0.60	0.56
8.3 x 10^4		0.60	0.57
2.8 x 10^5		0.64	0.60
6.1 x 10^5		0.68	0.63
U.F	51[c]	0.58	0.54
8.3 x 10^4		0.58	0.53
2.8 x 10^5		0.62	0.57
6.1 x 10^5		0.64	0.59

a. melt crys beta form b. annealed beta form

c. pretreated alpha form

Table 3.5. Corrected Amorphous Fraction at Tc

Sample	T_c or T_a °C	Amorphous Fraction		
		melt cryst β form	prenucleated α form	annealed β form
unfract	25	0.62	-	-
unfract	36	0.66	-	-
$8.3x10^4$		0.62	-	-
$2.8x10^5$		0.65	-	-
$6.1x10^5$		0.64	-	-
unfract	43	0.63	0.61	0.69
$8.3x10^4$		0.63	0.61	0.63
$2.8x10^5$		0.61	0.67	0.63
$4.9x10^5$		--	--	0.70
$6.1x10^5$		0.70	0.71	0.71
unfract	51	-	0.65	-
$8.3x10^4$		-	0.66	-
$2.8x10^5$		-	0.70	-
$6.1x10^5$		-	0.73	-

Table 3.6. Corrected Amorphous Fraction at 25°C

Sample	T_c or T_a °C	Amorphous Fraction		
		melt cryst β form	prenucleated α form	annealed β form
unfract.	25	0.62		
unfract	36	0.61	-	-
$8.3x10^4$		0.54	-	-
$2.8x10^5$		0.59	-	-
$6.1x10^5$		0.58	-	-
unfract	43	0.56	0.55	0.55
$8.3x10^4$		0.55	0.55	0.56
$2.8x10^5$		0.54	0.59	0.58
$4.9x10^5$		--	--	0.56
$6.1x10^5$		0.58	0.63	0.55
unfract	51	-	0.53	-
$8.3x10^4$		-	0.53	-
$2.8x10^5$		-	0.57	-
$6.1x10^5$		-	0.59	-

3.2.4. Effect of molecular weight on Amorphous fraction.

The amorphous fraction at Tc for all alpha and beta containing samples, obtained from the corrected subtraction factor following complete crystallization is given in Table 3.3. These show a molecular weight dependence for the three types of samples crystallized at 43°C. Upon cooling these samples to 25°C, the amorphous fraction decreases for all samples to 25°C; however, the molecular weight dependence for the amorphous fraction of the beta-TPI samples crystallized at Tc = 43°C is not observed at 25°C. For the alpha samples prepared at Tc = 43 and 51°C and then cooled to 25°C, a molecular weight dependence is observed as shown in Figure 3.38.

3.2.5. Effect of supercooling

Crystalline fractions obtained from the absorbance ratio method for solution crystallized, unfractionated synthetic, balata and gutta percha TPI was reported previously[67]. Beta form samples crystallized at 0°C from amyl acetate and heated slowly in suspension to 30°C have crystalline fractions of 0.61 ± 0.01; for alpha form spherulites crystallized at 20°C and 30°C from hexane the values are 0.55 ± .01. These are larger than the values of 0.38 - 0.46 for beta form and 0.37 - 0.47 for alpha form melt crystallized sample. The differences in crystalline fraction with crystallization method can be correlated with degree of supercooling. which is Tm-Tc for melt crystallized samples and T_d-T_c for solution crystallized samples, where Tm is the equilibrium melting temperature and Td

the equilibrium dissolution temperature in a particular liquid. A plot of crystallinity versus degree of supercooling for beta TPI is given in Figure 3.39. This plot also includes results for stirrer crystallized TPI. The crystallinity decreases with increasing degree of supercooling, as is apparent in the plot.

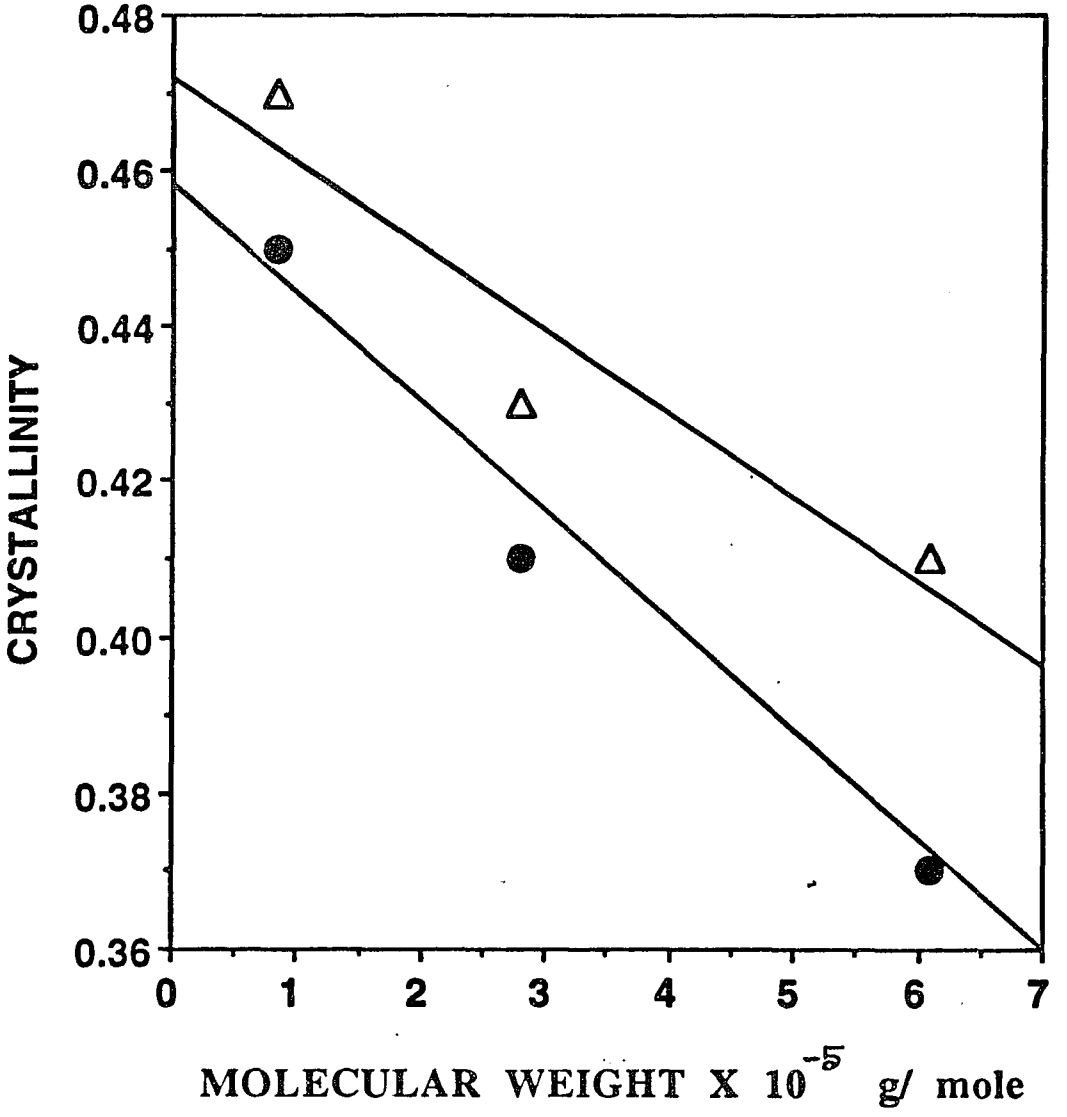

Figure 3.38. Crystalline fraction at 25°C from corrected FTIR subtraction factor for alpha form TPI versus molecular weight: (●) Tc = 43°C ; (△) Tc = 51°C

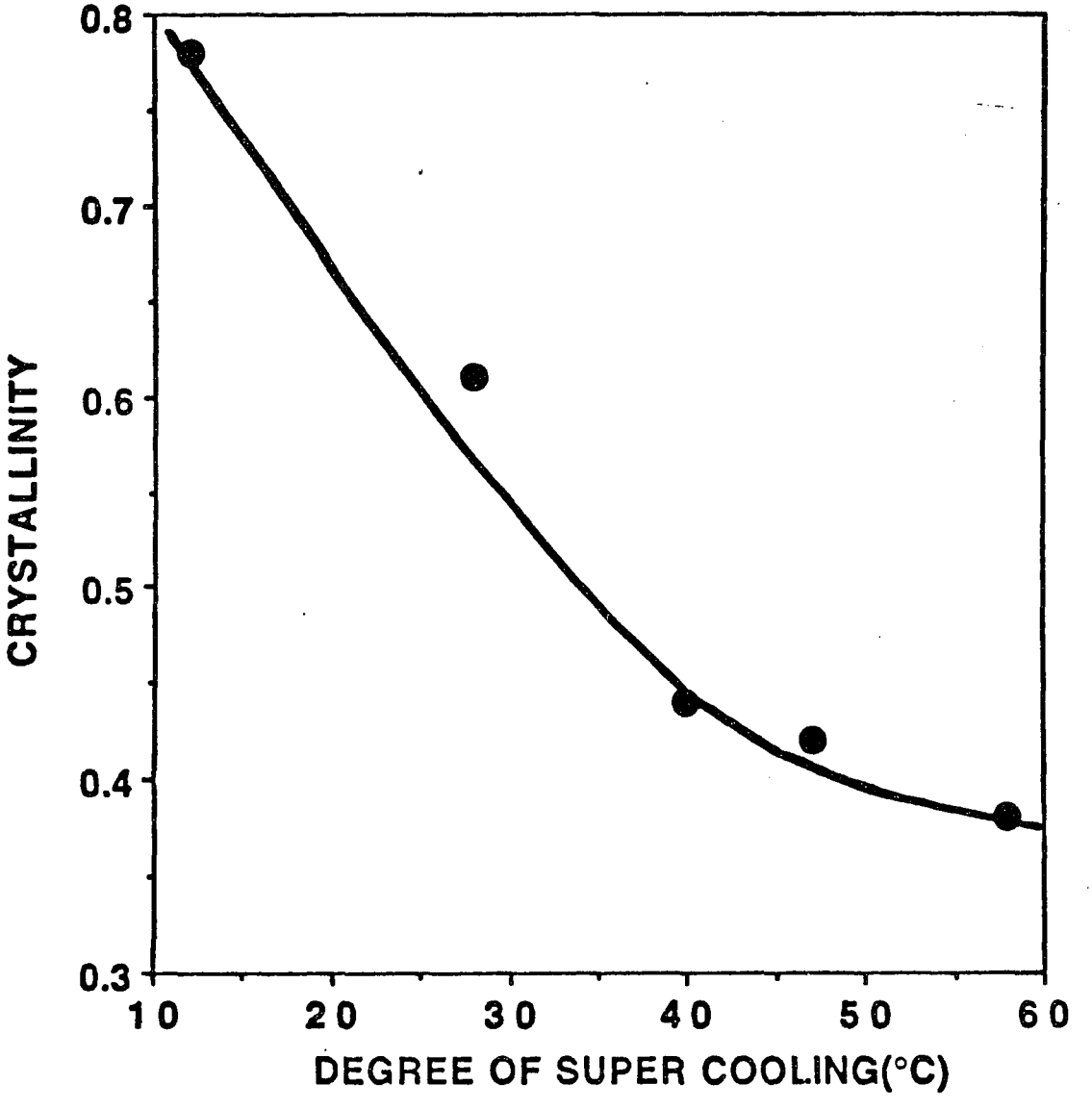

Figure 3.39. Crystalline fraction from FTIR versus degree of supercooling for beta TPI

3.2.6. FTIR spectroscopy at low temperatures

FTIR spectra for melt and solution crystallized unfractionated TPI were taken at 25, 0, -78 and -196° C for alpha and beta form in the FTIR cooling cell. Spectra for alpha and beta melt crystallized TPI are given in Figures 3.40 and 3.41. For samples with either crystal forms many of the crystalline bands increase in intensity with decreasing temperature. Some bands show a shifts in frequency with lowering of the temperature. These shifts in the bands are more easily observed using subtraction spectra. Subtraction of the spectra taken at 25°C from that taken at -196° C for each sample are shown in Figure 3.42. The band shifts taking place are given in Table 3.7. Most of the bands that shift do so to higher frequencies and only one band is shifted to lower frequency as the sample temperature is decreased from 25°C to -196°C. One of the large shifts taking place is in the frequency of the C=C stretching band at 1667cm^{-1} for the alpha form. The absorbance of the C=C band increases linearly when the temperature is lowered from 0°C to -196°C as shown in Figure 3.43. The frequency shifts for the C=C stretching vibration follow a linear relationship with temperature as shown in Figure 3.44. Subtraction factor is plotted against the temperature for alpha and beta containing TPI for both solution and melt crystallized samples in figure 3.45. There is no change in subtraction factor below -78°C for either alpha or beta solution crystallized samples. There is a slight decrease in subtraction factor for the alpha melt crystallized samples and a sudden drop in subtraction factor for beta melt crystallized samples.

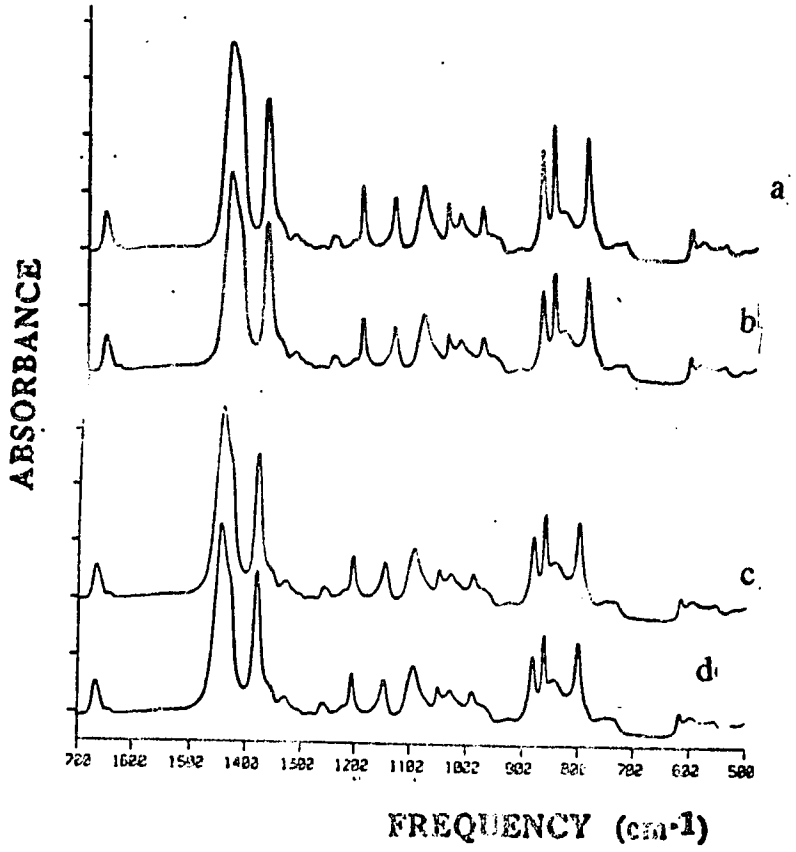

Figure 3.40. FTIR spectra for melt crystallized alpha form containing TPI from 500 to 1700cm^{-1}:

(a) at -198°C (b) -78°C (c) 0°C (d)25°C

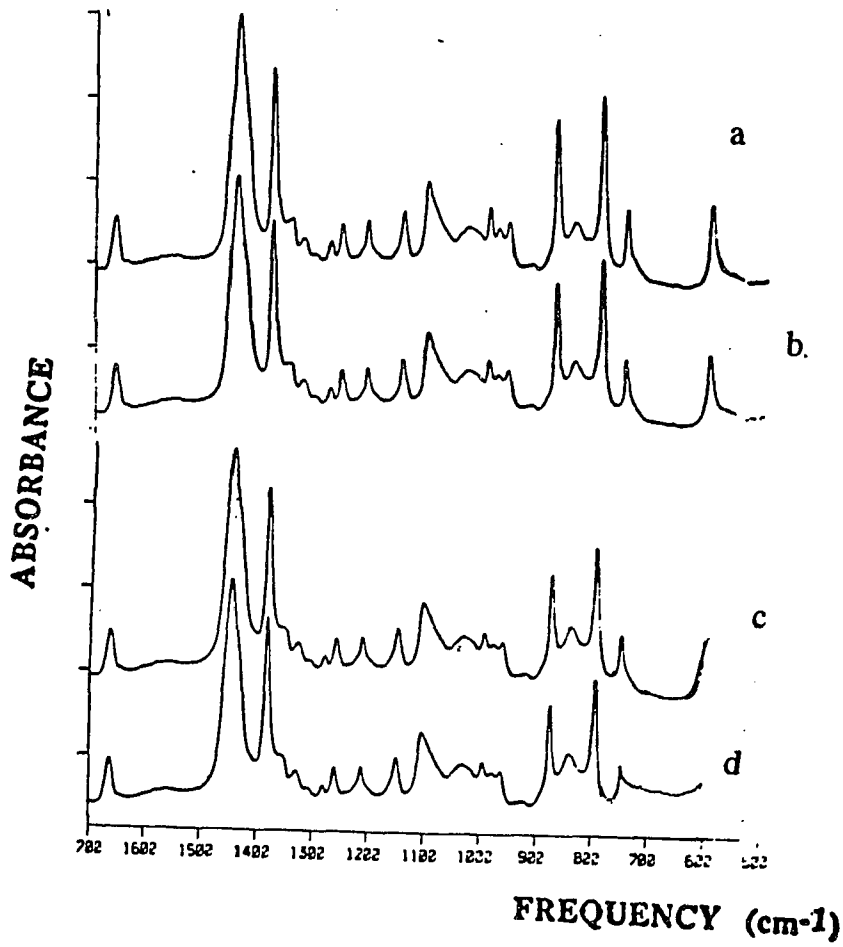

Figure 3.41. FTIR spectra for melt crystallized beta form containing TPI from 500 to 1700cm^{-1}:

(a) at -198°C (b) -78°C (c) 0°C (d)25°C

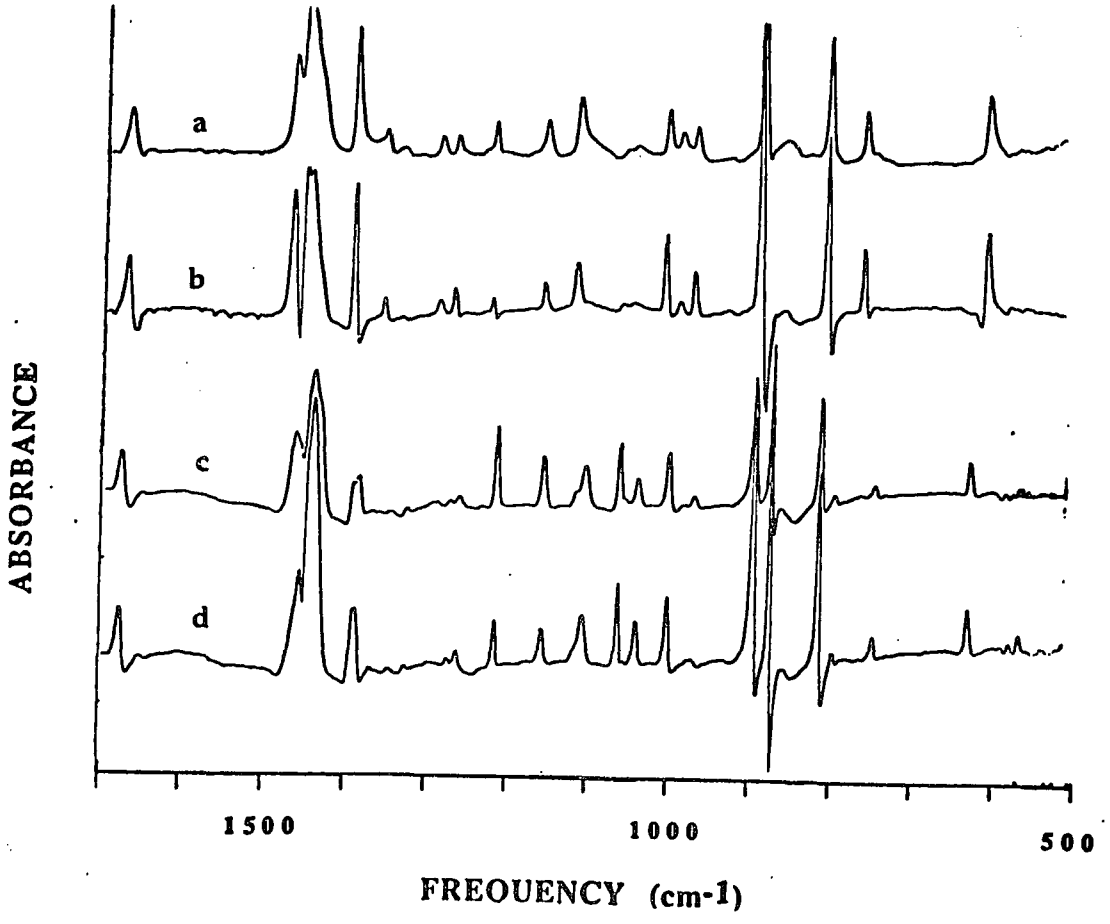

Figure 3.42. FTIR spectra for unfractionated TPI at -196°C after subtraction of spectrum taken at 25°C: a) beta crystal form melt at 90°C,crystallized at25°C; b) beta crystal form from 1% amyl acetate solution heated to 100°C, crystallized at 0°C and heated slowly in suspension to 25°C; c) alpha crystal form from melt at 90°C, crystallized at 55°C for 2 weeks and cooled to 25°C; d) alpha crystal form from 1% amyl acetate solution heated to 100°C, cooled to 0°C, heated to dissolution temperature and crystallized at 25°C

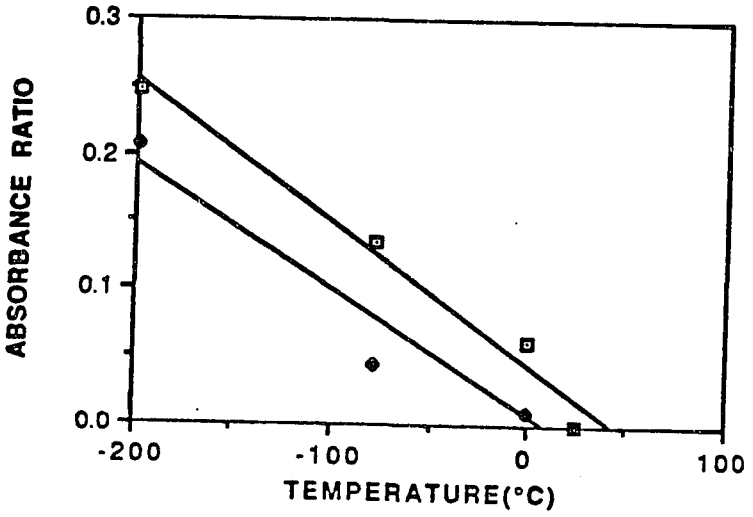

Figure 3.43a. Absorption variation of 1663 cm^{-1} band of beta TPI as a function of measurement temperature

(◆) solution crystallized sample (⊡) melt crystallized sample

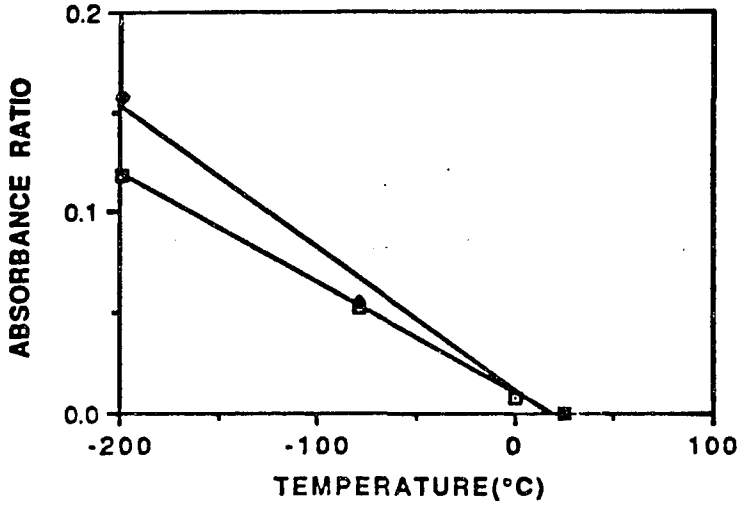

Figure 3.43b. Absorption variation of 1668 cm^{-1} band of alpha TPI as a function of measurement temperature

(◆) solution crystallized sample (⊡) melt crystallized sample

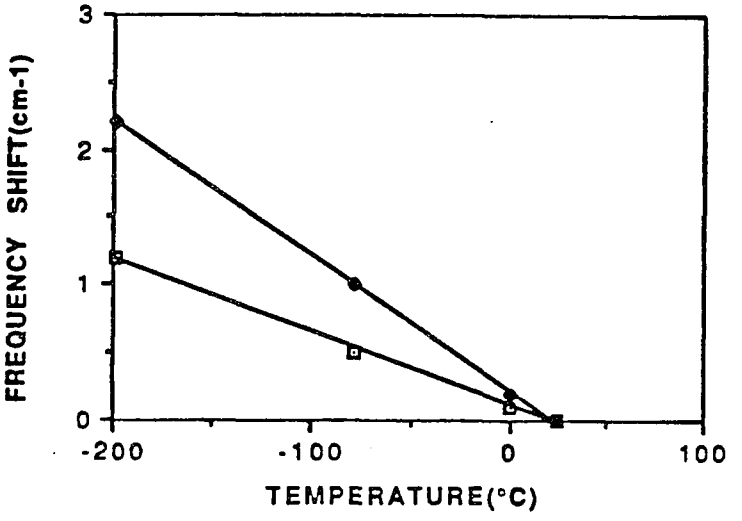

Figure 3.44a. Frequency shift of 1663 cm^{-1} band of beta TPI as a function of measurement temperature

(◆) solution crystallized sample (⊡) melt crystallized sample

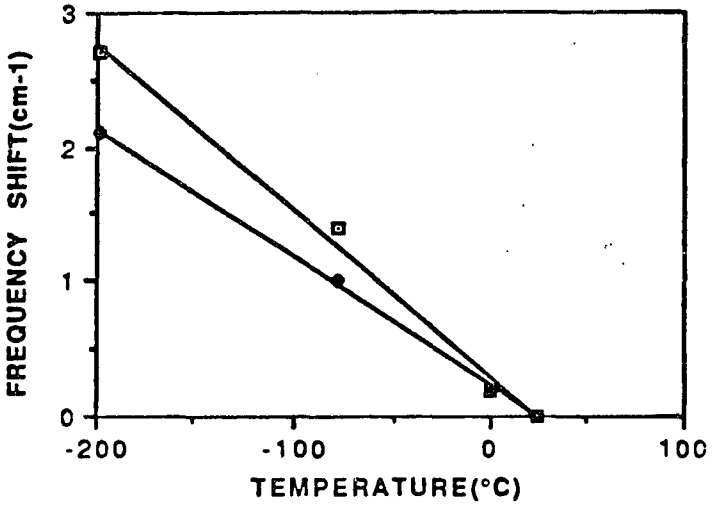

Figure 3.44b. Frequency shift of 1668 cm^{-1} band of alpha TPI as a function of measurement temperature

(◆) solution crystallized sample (⊡) melt crystallized sample

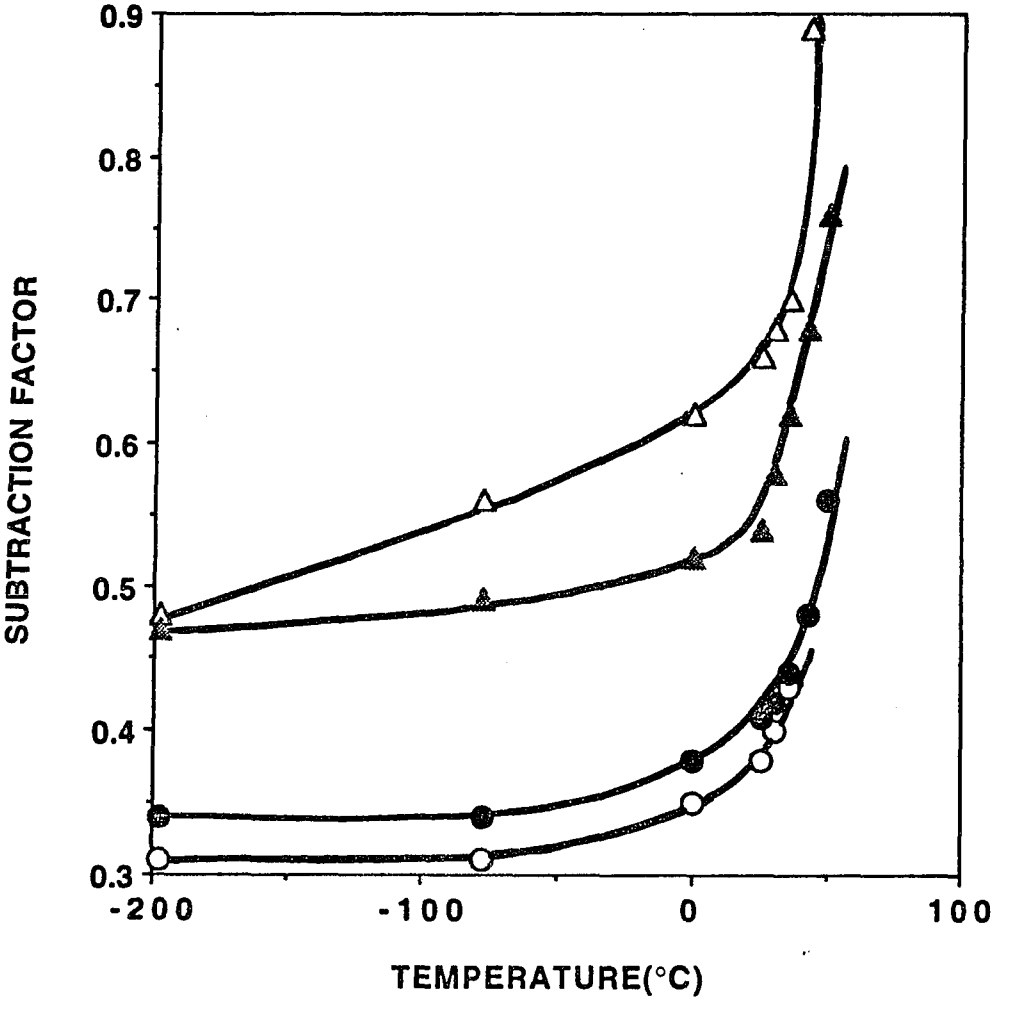

Figure 3.45. FTIR subtraction factor versus temperature for unfractionated TPI: (▲) melt crystallized alpha; (Δ) melt crystallized beta; (●) solution crystallized alpha; (○) solution crystallized beta

Table 3.7. Shift of FTIR frequencies with temperature (25°C to -196°C)

Band cm^{-1}	alpha solution crystallized	alpha melt crystallized	beta solution crystallized	beta melt crystallized
1669	+2	+3	NA	NA
1664	NA	NA	+2	+1
1382	0	0	+1	+1
1212	NA	NA	+1	+1
990	+1	+1	NA	NA
997	NA	NA	+1	0
882	+1	+1	NA	NA
877	NA	NA	+2	+2
862	+2	+2	NA	NA
800	+1	+1	+1	0
600	NA	NA	-1	-1

Where NA is non applicable

3.3 Bulk crystallization of random epoxidized TPI

3.3.1.Morphology

Solution epoxidized TPI crystallized from the bulk exhibit two different types of morphology, hedrite and lamellar. The morphology is dependent on crystallization temperature and the amount of epoxy content. At these crystallization temperatures only the beta crystal form was observed using FTIR spectroscopy. The addition of epoxide units to the TPI chains results in morphologies that appear somewhat different from those observed in unepoxidized bulk crystallized TPI. This depends on the amount of oxirane content. The morphologies of 2.2% epoxidized samples melt crystallized at 25°C are shown in Figures 3.46 and 3.47. Hedrite type structures are apparent in both cases. However the size of the hedrite is smaller and a smaller number of lamellas are involved in its formation compared to unepoxidized samples. Some representative structures obtained for 5% of solution epoxidized TPI crystallized at 25°C is shown in Figure 3.48. Hedrites that are less matured than those crystallized from 2.2% epoxidized TPI appear. The morphology of 9.8% epoxidized TPI crystallized at 25°C is shown in Figure 3.49. These structures are lamellar. A large change in the morphology occurs between 5% to 9.8% epoxidation. The morphologies of 2.2% and 5% epoxidized TPI crystallized at 36°C are shown in Figures 3.50 and 3.51. These structures are also hedrites with fewer lamellas involved in their formation.

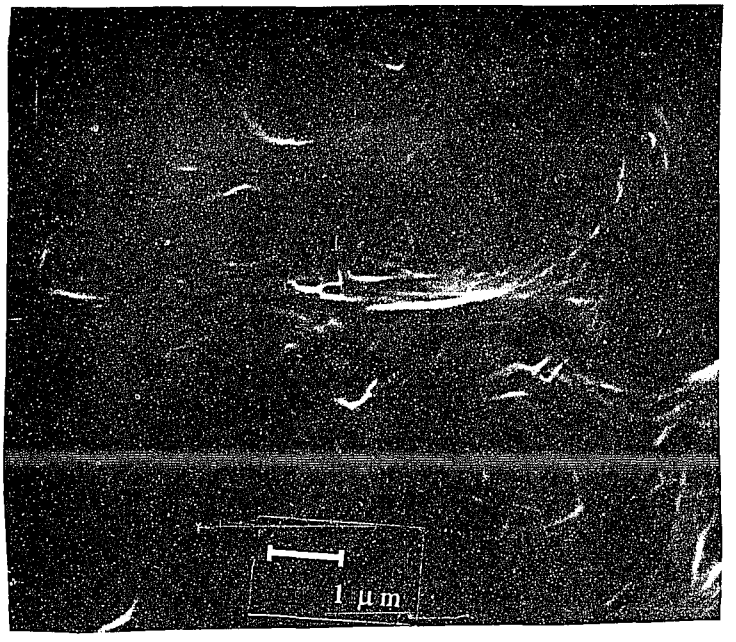

Figure 3.46 Scanning electron micrograph of 2.2% randomly epoxidized TPI crystallized from the melt at 25°C, treated with OsO_4 and Au coated

Figure 3.47. Same as figure 4.1 but different field

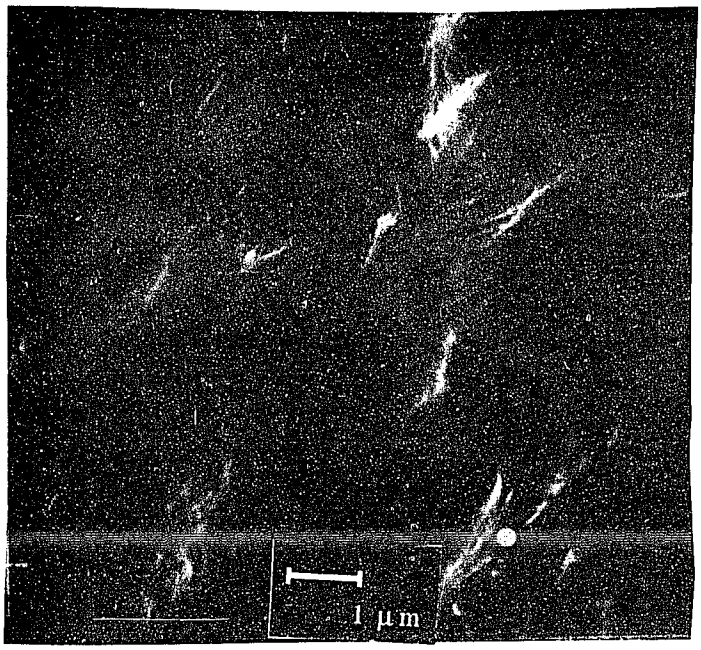

Figure 3.48 Scanning electron micrograph of 5% randomly epoxidized TPI crystallized from the melt at 25°C, treated with OsO_4 and Au coated

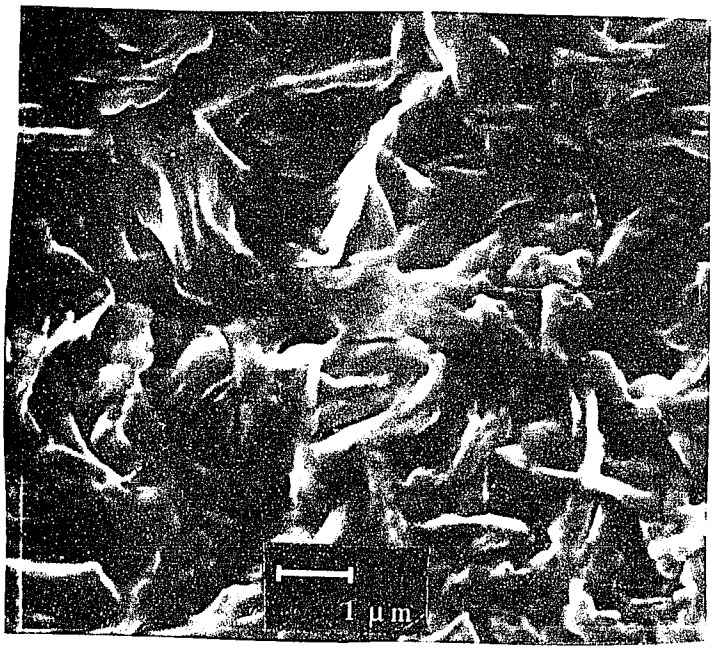

Figure 3.49 Scanning electron micrograph of 9.8% randomly epoxidized TPI crystallized from the melt at 25°C, treated with OsO_4 and Au coated

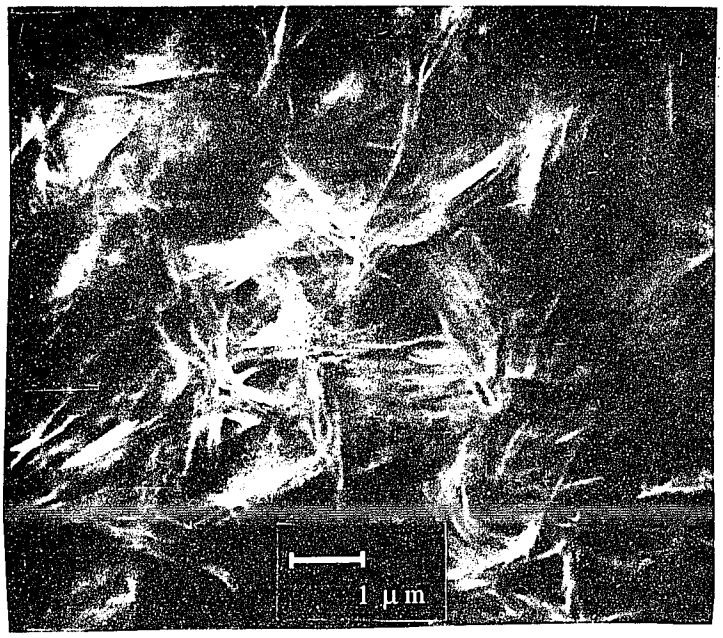

Figure 3.50 Scanning electron micrograph of 2.2% randomly epoxidized TPI crystallized from the melt at 36°C. cooled to 25°C, treated with OsO_4 and Au coated

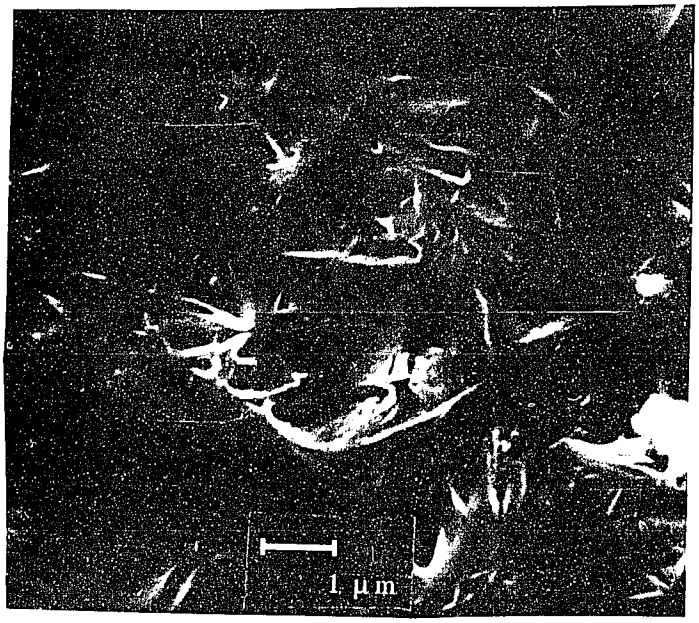

Figure 3.51. Scanning electron micrograph of 5% randomly epoxidized TPI crystallized from the melt at 36°C. cooled to 25°C, treated with OsO_4 and Au coated

3.3.2.FTIR spectroscopy

The FTIR spectra from 500 to 4000cm^{-1} of semicrystalline, randomly epoxidized TPI having different oxirane contents were taken as a function of time at the crystallization temperature(25°,30°and36°C). Semicrystalline beta melt crystallized 9.8% randomly epoxidized TPI crystallized from the melt at 25°C for 30 hours is given in Figure 3.52a. This spectrum shows characteristics of three components; crystalline beta TPI, amorphous TPI and epoxidized TPI. The amorphous spectra were obtained by heating the same sample to 60°C as shown in Figure 3.52b. The crystalline spectrum were obtained by digital subtraction of the amorphous spectrum from the semicrystalline one given in Figure 3.52c.

The subtracted spectrum for 9.8% randomly epoxidized TPI crystallized at 25°C for 30 hours is given in Figure 3.53a, along with a subtracted spectrum for pure TPI (Figure 3.53b). The subtracted spectrum of randomly epoxidized TPI is mainly for crystalline beta TPI; however there are bands for solution epoxidized TPI present at 1250, 1122 and 1068 cm^{-1}. FTIR spectra taken for bulk crystallized solution epoxidized TPI sample at various times during the crystallization process at 30°C are given in Figure 3.54; the sharp bands at 877 and 800 cm^{-1} are first observed after 5 hours for this sample. As time elapsed these bands increased in intensity, finally reaching a constant value. Cooling the sample to room temperature leads to a further increase in crystalline band intensity and a decrease in amorphous band intensity.

The FTIR subtraction factor method was used to obtain the amorphous fraction as a function of time at Tc and the final amorphous fraction at Tc and 25°C. Typical crystallization isotherms were obtained by plotting FTIR subtraction factor against time at Tc of 30° and 36°C as given in Figures 3.55 and 3.56. Attempts to crystallize the 9.8% epoxidized TPI at 36°C were not successful. Melt crystallization of 2.2% epoxidized TPI samples at 43°C was also unsuccessful, although it is possible to melt crystallized unfractionated TPI at that temperature. The final subtraction factor was equated to the amorphous fraction. These values at Tc and 25°C are given in Table 3.8.

The crystallization isotherms contain three major parts: an induction period, a region of constant negative slope during which time crystallization occurs, and a final region of zero slope. The length of the induction period, the slope during the crystallization process and the final subtraction factor depends on the epoxidation amount and crystallization temperature. The nucleation rate of crystallization during that crystallization was obtained from the slope of the subtraction factor/time plot and are given in the Table 3.9. A decrease in rate with increasing epoxy content or with increasing crystallization temperature is observed.

The final subtraction factor at Tc for melt crystallized TPI at 25°C, 30°C and 36°C is plotted versus epoxidation amount as shown in Figure 3.57. The values used here for unepoxidized sample are

averages of values found for unfractionated TPI and fractions therefrom. The final subtraction factor after cooling from Tc to 25°C is also included in Figure 3.57. The latter changes with epoxidation amount in a fashion to changes in the subtraction factor at Tc. However, the curve for the samples crystallized at 36°C and cooled to 25°C is shifted to lower values by 0.06, so that the subtraction factor values for the sample crystallized at 36°C is smaller than that crystallized at 25°C and 30°C at 2.2% epoxidation and larger at 5.0% epoxidation.

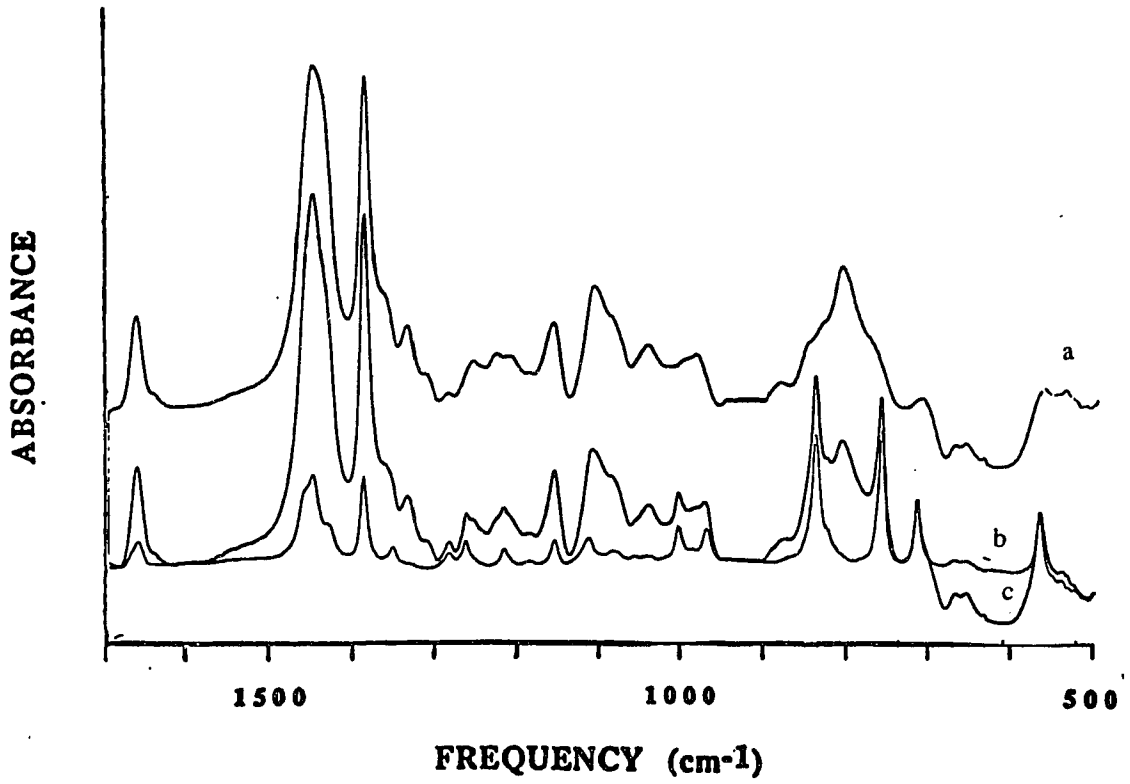

Figure 3.52. FTIR spectra of 9.8% randomly epoxidized melt crystallized TPI

a) amorphous b) semi crystalline c) crystalline

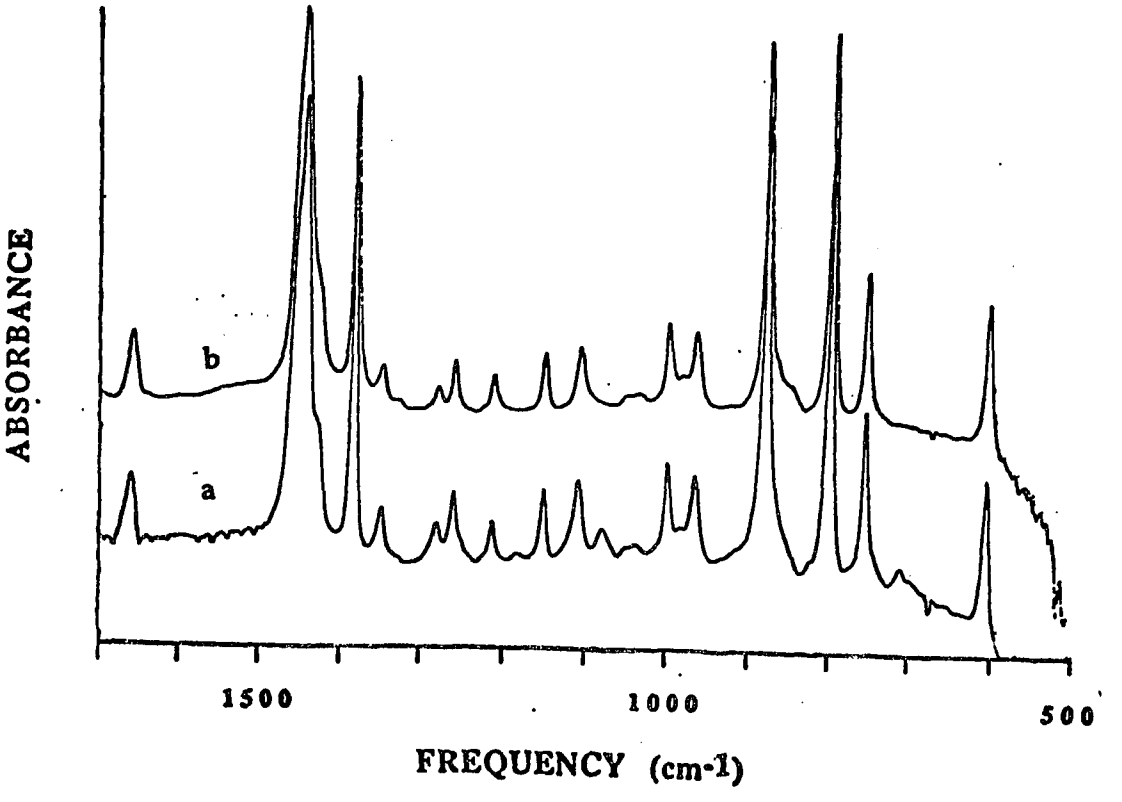

Figure 3.53. FTIR subtraction spectrum for

a) unfractionated TPI melt crystallized at 25°C

b) 9.8 mole% randomly epoxidized TPI melt crystallized at 25°C

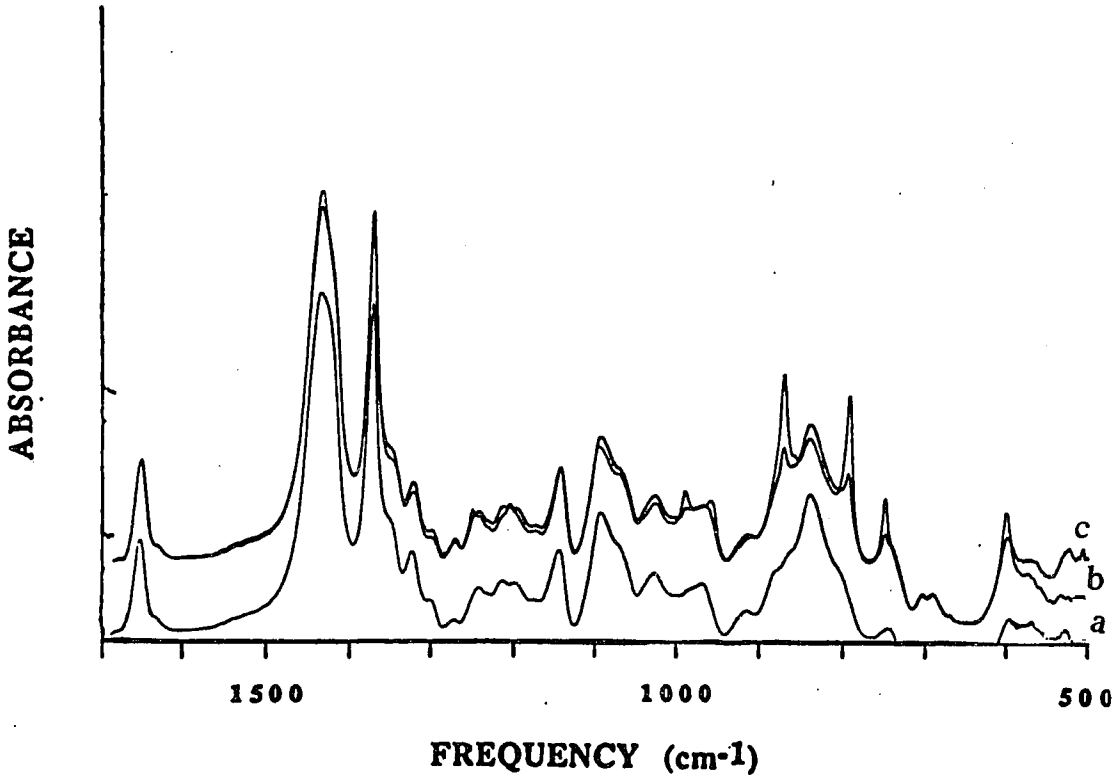

Figure 3.54. FTIR absorbance versus frequency for 9.8% randomly epoxidized melt crystallized TPI at 30°C

a) at 60°C b) at 30°C after 9.5hours c) after 23hours

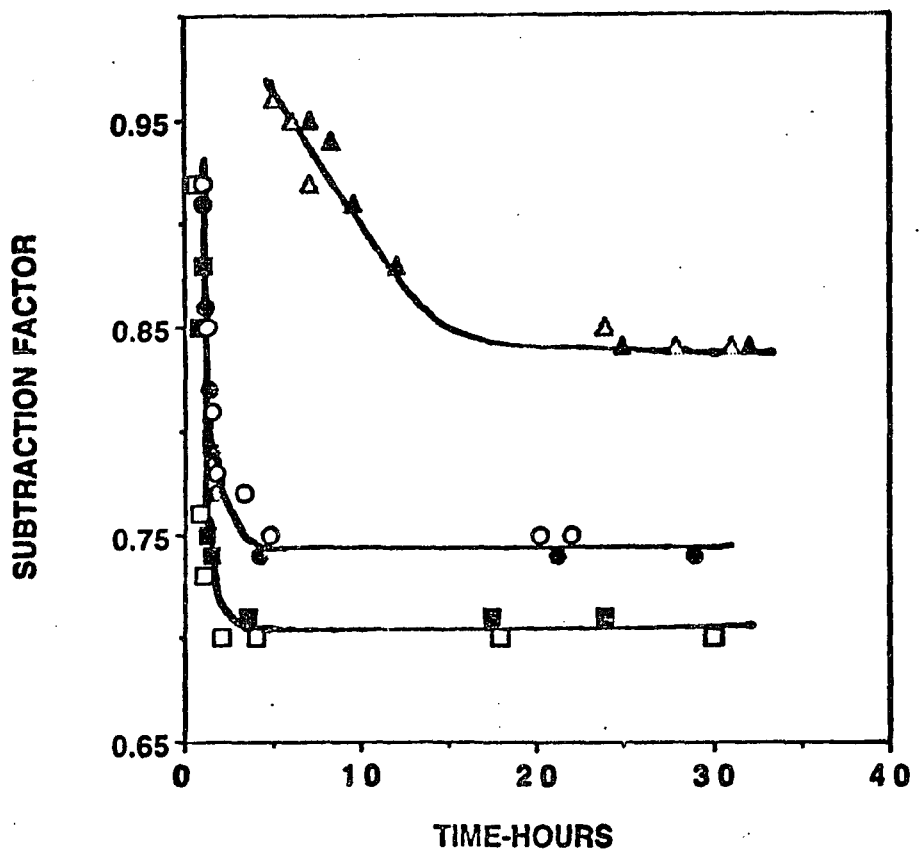

Figure 3.55. FTIR subtraction factor versus time for randomly epoxidized TPI crystallized TPI crystallized from the melt at 30°C epoxidation amount in mole% 2.2 (□,■) 5 (○,●) 9.8 (△,▲)

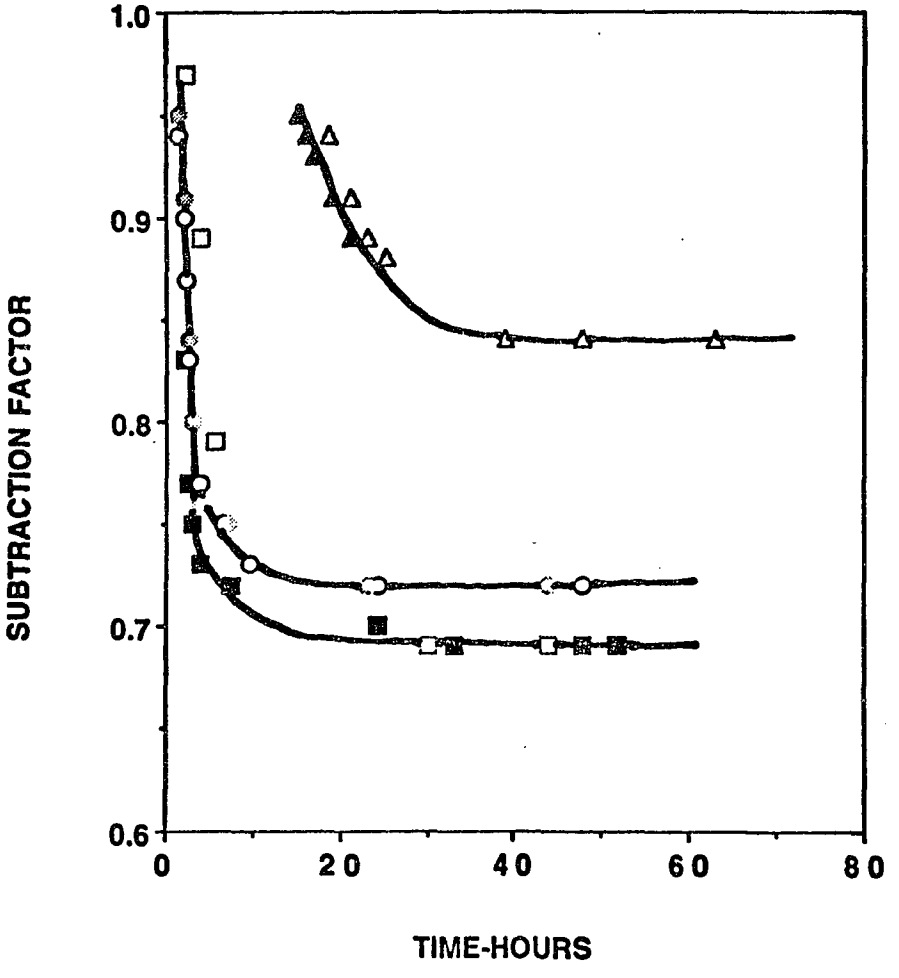

Figure 3.56. FTIR subtraction factor versus time for randomly epoxidized TPI crystallized TPI crystallized from the melt at 36°C epoxidation amount in mole% 0 (□,■) 2.2 (○,●) 5 (△,▲)

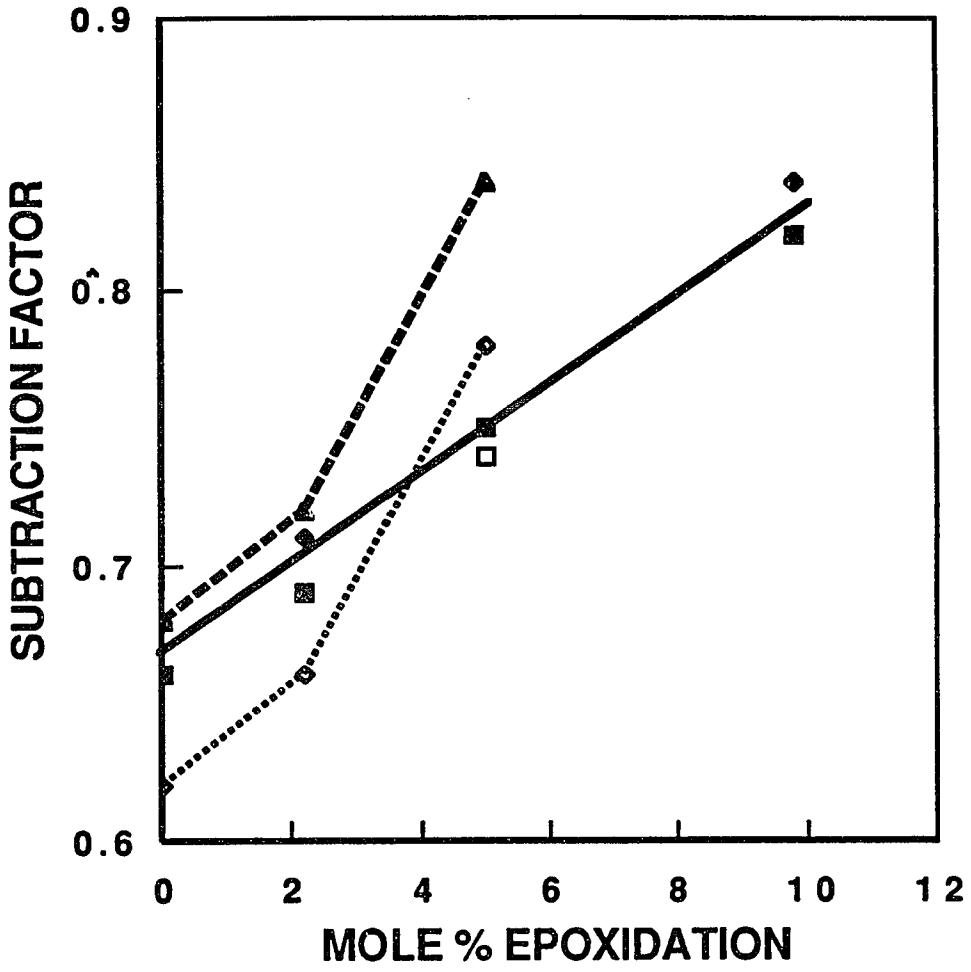

Figure 3.57. Final FTIR subtraction factor versus epoxidation amount: at Tc 25°C (■), 30°C (◆), 36°C (▲) and at 25°C after crystallization at 30°C (□) and 36°C (◇)

Table 3.8. Amorphous Fraction for epoxidized TPI at Tc and 25°C

% epoxy content	Tc (°C)	Amorphous Fraction	
		at Tc	25°C
0	25	0.66	0.66
2.2		0.69	0.69
5		0.75	0.75
9.8		0.82	0.82
0	30	0.68	0.66
2.2		0.71	0.69
5		0.75	0.74
9.8		0.84	0.82
0	36	0.68	0.62
2.2		0.72	0.66
5		0.84	0.78

Table 3.9. Relative melt crystallization Rates from FTIR for solution epoxidized TPI

Epoxidation Amount(mole%)	Tc (°C)	Rate(hr^{-1})
2.2	30	1.0
2.2	36	0.10
5	30	0.22
5	36	0.01
9.8	30	0.014

4. Discussion

4.1. The Morphology

It was demonstrated above that the morphology of trans-1,4-poly isoprene structures grown from the bulk depends on the crystallization temperature, molecular weight and method of crystallization. Two structural types were observed for unfractionated TPI; hedrites and spherulites. The hedrite type morphology is obtained at low crystallization temperature, the spherulitic type morphology at high crystallization temperature. As the crystallization temperature increases, the spherulites formed become larger and more developed. As the crystallization temperature increases, the nucleation rate decreases, leading to larger, more well developed structures.

In earlier work carried out with unfractionated TPI, maltese cross beta spherulites crystallized at 30°C were reported[34-35]. These correspond to the curved and branched sheaf-like structures reported here. A second type of beta form structures crystallized at higher temperatures were also reported earlier. However these are the same sheaf-like stuctures viewed face-on instead of edge-on, as shown by an optical microscopy study of solution crystallized TPI[32]. A micrograph in which both edge-on and face-on views appear for melt crystallized samples is shown in Figure 3.7a. In the present investigation no marked changes in morphology or average size occur for unfractionated TPI crystallized in the beta form at temperatures

from 25°C to 43°C and followed by OsO_4 treatment at 25°C. On the other hand, the fractions, particularly the high molecular weight one, do show changes in morphology as the temperature is changed. For the high molecular weight fraction, when OsO_4 treated at 25°C, more ordered structures appear at high crystallization temperature.

The crystallinity of unfractionated and fractionated TPI was monitored by FTIR spectroscopy for samples crystallized in the beta form between NaCl plates at the crystallization temperature and after cooling to 25°C[121]. An increase in crystalline fraction of 20- 40% is observed in cooling samples crystallized at 43°C to 25°C. The increase in the crystalline fraction is largest for the highest molecular weight fraction, changing from 0.30 to 0.42. In this study appearance of single melting endotherm for bulk crystallized TPI, observed for most samples, is not in agreement with earlier work[122]. The single endotherms observed are in consequence of using isothermal crystallization and only nucleating one form, alpha or beta, in a particular crystallization. Regardless of the morphological differences demonstrated here, the crystallinity of the beta crystal form at 25°C and the DSC melting temperature were found to be independent of molecular weight within experimental error as discussed below. It is belived that the additional crystallization that occurs on cooling from 43°C to 25°C, involves ordering in the chain folds and the interlamellar traverses with an appreciable segregated amorphous component being ruled out. As pointed out above, some morphological changes do occur at the surface upon cooling unfractionated TPI samples crystallized at 43°C. Some of these

changes could be due to the secondary crystallization of some completely amorphous chains present at Tc involving the structures already present. The size of such a component at Tc is not known and may account for only a fraction of the total crystallinity increase. Crystallization of the alpha form by a seeding method yields a spherulitic morphology. The structures obtained at Tc = 43°C for unfractionated TPI in the alpha form are similar in size and appearance to those obtained at the same temperature for the same material in the beta form. Crystallization of a high molecular weight fraction at 43°C gives large spherulites compared to the unfractionated sample. A similar trend was observed at 51°C. The spherulite diameter at Tc = 51°C is from 10 -30 micrometer with the largest values (25 - 30 micrometer) again being found for the high molecular weight fraction. The rate of crystallization, as determined using FTIR, decreases with molecular weight, particularly at Tc = 51°C. A lower rate suggests fewer nuclei which would leads to larger spherulite as observed using SEM. The final crystallinity attained decreases with increasing molecular weight both at Tc and after cooling to 25°C for samples crystallized in the alpha form at 43°C and 51°C.

When the OsO_4 treatment was carried out after cooling to 25°C, smaller sheaf structures were observed on the surfaces of the spherulite structures present at both 43°C and 51°C. These were not observed when the samples were crystallized at 43°C and 51°C and OsO_4-treated at Tc. This suggests the presence of some amorphous

chains at Tc which crystallize as separate structures on cooling to 25°C.

The increase in amorphous fraction with molecular weight for the alpha-containing samples melt crystallized at 43°C is accompanied by a 7°C decrease in melting temperature. The overlapping melting endotherm observed for the lowest molecular weight fraction crystallized at 43°C is indicative of the presence of more than one lamellar thickness. For the alpha-containing samples crystallized at 51°C the amorphous fraction change with molecular weight is similar to those samples crystallized at 43°C, but the melting behavior is different; only one endotherm is present and there is no change of Tm with molecular weight within experimental uncertainty.

Additional crystallization of complete amorphous chains during the cooling process from Tc to 25°C was also observed for the alpha samples prepared by the direct melt crystallization method at 55°C. This yielded spherulitic structures. In some cases spaces between the spherulites, containing multi lamellar structures 2-5 micrometer in length, were observed. These lamellar structures were absent when the OsO_4 treatment was carried out at 55°C.

The effect of crystallization temperature on the morphology that results for melt crystallized thin films is in general agreement with that found in a SEM study for solution crystallized TPI and TEM investigations, melt crystallized polyethylene and melt crystallized poly(ethylene oxide). The morphology of polyethylene and

poly(ethylene oxide) was found to be strongly dependent on polydispersity and molecular weight. In both solution and melt crystallized morphological investigations of polyethylene and poly(ethylene oxide), the size and complexity of the structures obtained increase with temperature. The morphology for solution crystallized TPI changes with molecular weight, particularly at high crystallization temperature where the alpha crystal form is predominant. Melt crystallized alpha-TPI shows little, if any, observable change in morphology with a change in molecular weight.

4.2. FTIR Spectroscopic investigation of bulk crystallized TPI

It was found in the present study that TPI can be crystallized from the bulk up to a temperature of 55°C and that the amorphous fraction for prenucleated alpha samples increases with molecular weight at Tc and after cooling to 25°C. Samples containing the beta crystal form showed a molecular weight dependence at Tc or Ta that disappears upon cooling the samples to 25°C.

Previous investigation of crystallinity for solution crystallized TPI showed a close agreement in values obtained from density measurements and by FTIR, using the ratio of the absorbance of the double bond stretching band at 1665- 1670 cm^{-1} after and before spectral subtraction of the amorphous component[67]. In the present work the 1665-1670 cm^{-1} band was found to be conformationally independent from 0°C to 65°C for melt crystallized TPI samples. It

was also found that the amorphous fraction obtained from the subtraction factor method and the absorbance ratio method, as described in the experimental section, were in close agreement, provided a correction for a change in the number of absorbers is made in the subtraction factor method. The subtraction factor method was used previously to find crystallinities of solution crystallized trans-1,4-polybutadiene[125]. This method for determining crystalline or amorphous fractions should be applicable to any partially crystalline polymers which can be melted without decomposition. Neither the subtraction factor or absorbance methods of determining amorphous fraction depend on calibration. Use of either method does assume that the sample is a two component system with an amorphous part having the same conformational composition as that present in the melt.

In this study, the two component assumption made previously was found to be valid except for annealed samples at short crystallization times. Subtraction of the amorphous component from the spectra obtained after complete crystallization gave the alpha or beta crystal form identical to those for subtracted spectra from solution crystallized samples. However relative intensity differences in some bands occur between solution and melt crystallized samples due to crystallinity differences. The changes in band intensities at constant temperature as a function of time are attributed to the change in chain conformation accompanying the crystallization process. For beta TPI the chain conformation for each repeat unit is STS, starting with the CH_2--CH_2 bond in the skew plus (S) conformation, CH_2--CH_2

bond in a trans conformation and the CH_2--C(CH3) bond in a skew minus(S-) conformation. The repeat units in an amorphous chain can take up this and many other conformations including: CTS, $CT\bar{S}$, CGS, $CG\bar{S}$, SGS and $SG\bar{S}$ where C = cis and G= gauche. The two component assumption does not hold at short crystallization times for beta TPI samples annealed near the melting point. The CH_2-CH_2 bond in amorphous TPI can take up either trans or gauche conformation. The beta and alpha crystal form contain only trans CH_2-CH_2 conformations. Beta TPI (STS conformation) has an infrared band at 877 cm^{-1}, assigned to out of plane =C-H vibration, alpha TPI (CTS CTS- conformation) exhibit a doublet at 862 and 882 cm^{-1} assigned to this vibration[82]. In amorphous TPI a broad band at 842 cm^{-1} with shoulders at 860 and 884 cm^{-1} are observed. The 842 cm^{-1} band has been attributed to the various conformations containing gauche CH_2-CH_2 bonds. Therefore, the additional band obtained at 840 cm^{-1} in the subtracted spectrum for 43°C annealed beta TPI in the present work is believed to be indicative of an excess of gauche CH_2-CH_2 conformations over those usually present in amorphous TPI samples. At later times the excess of gauche conformations in the annealed beta TPI samples are converted to trans and the extra spectral component after subtraction diminishes in relative intensity.

Crystallization isotherms are obtained by plotting the FTIR subtraction factor against time. These isotherms follow the conformational conversion from the amorphous state to a particular crystal form. The rate of this crystallization is obtained from the slope of the plot. The appearance of these plots was found in this

work to depend on the crystallization, the method of crystal nucleation and in some cases the molecular weight. For all samples in either crystal form the higher molecular weight fraction has the largest amorphous fraction at 43°C. In light of the behavior on cooling to 25°C and the reversibility on reheating to 43°C, the higher amorphous fraction for beta samples at Tc is most likely caused by differences at the fold surface or in the interlamellar parts. The presence of a segregated low molecular weight amorphous component at Tc and Ta for the higher molecular weight samples could also lead to a larger amorphous fraction for these. However, this presence would be expected in both of the unfractionated samples. Since the amorphous fraction for these samples is clearly different (see Table 3.5), the presence of a significant segregated amorphous component is not considered likely. The molecular weight dependence of the amorphous fraction for the alpha containing samples at Tc is still apparent on cooling the sample to 25°C and therefore is possibly partially due to a different cause than that responsible for the differences with molecular weight for beta samples at Tc.

The effect of molecular weight on crystallinity at Tc and 25°C for narrow polyethylene fractions was reported earlier[102]. At Tc the crystallinity becomes strongly molecular-weight-dependent between 10^5 and 10^6 g/mole and the increase in crystallinity on cooling to 25°C changes markedly in that range and above. The results of this investigation on melt crystallized TPI are consistent with that work. The lamellar thickness distribution for polyethylene was investigated

using transmission electron microscopy as a function of molecular weight and crystallization temperature[126]. This distribution was shown to be strongly dependent on these parameters for that polymer. However, to date this type of study has not been carried out for TPI in either crystal form.

Of particular interest is that at 25°C, the beta crystal containing specimens exhibit no clear dependence of amorphous fraction on molecular weight. Apparently all of these samples have similar lamellar thickness distributions. In agreement with this explanation the beta containing TPI samples prepared at 43°C have a Tm that is independent within the experimental uncertainty of molecular weight and thermal history . The morphologies of the alpha and beta crystal containing samples cooled to 25°C have been reported in section 3.1 and are found to be different[121]. The alpha form yields spherulites while the beta form gives hedrite type structures. It is possible that the morphological differences are causing some of the observed changes of crystallinity with molecular weight.

FTIR crystallinities previously reported for both alpha and beta solution crystallized specimens of unfractionated TPI show an increase in amorphous fraction upon heating from 25°C to 50°C and a decrease on cooling to -30°C[83]. The decrease in amorphous fraction taking place on cooling melt crystallized TPI samples from Tc to 25°C is in general agreement with the increase in this parameter previously observed upon heating the dried solution crystallized mats. During solution crystallization any completely amorphous

chains present after the crystallization process at 30°C is over should have been removed in the extensive washing that preceded collection of the samples by filtration. Therefore the crystallinity increase observed on cooling those samples after drying must be due to fold or interlamellar traverse ordering. Fold surface ordering is therefore one possible cause of the crystallinity increase observed upon cooling melt crystallized samples from Tc to 25°C. A segregated amorphous component at Tc could also crystallize on cooling to 25°C. The possible presence of a substantial segregated amorphous component in melt crystallized TPI samples at Tc was discussed above and was considered unlikely. Further evidence for the absence of an appreciable amount of segregated amorphous component is the observation of single melting endotherms for all beta crystal form samples subsequently cooled to 25°C and the alpha containing samples crystallized at 51°C. Lamellas resulting from crystallization of a segregated amorphous component would be expected to have smaller thickness than the lamellas crystallizing at Tc, particularly for those crystallized at the highest Tc, and therefore to have a lower melting temperature. This would lead to two DSC endotherms if the lamellar thicknesses of the two components are significantly different.

A comparison of the amorphous fraction for unfractionated beta TPI crystallized from the melt with those obtained without and with stirring shows differences that can be related to supercooling taking place. The degree of super cooling for melt crystallized samples is T^*_m— T_c and T^*_d-T_c where T^*_m is the equlibrium melting point and

taken as 83°C[117] and T^*_d is the equilibrium dissolution temperature and is approximated by Td found for stirrer crystallized TPI[127]. Amorphous fractions for stirrer crystallized, solution crystallized and melt crystallized are 0.22, 0.39 and 0.56, while the supercoolings are 12, 28 and 40°C, respectively. As expected an increase in amorphous fraction with increasing degree of supercooling is observed.

In the present work, the effect of temperature below 25°C on the semicrystalline FTIR spectra and amorphous fraction were investigated for solution crystallized and melt crystallized samples. Increases in band intensity with decreasing temperature were observed. Some of the bands show shifts in frequency (see Table3.7). Most of the bands that shift do so to higher frequency except one band at 600cm^{-1} for beta TPI, which shifts to lower frequency. This band has been previously assigned as a C=C-C deformation band. One of the larger shifts taking place is in the frequency of the C=C stretching band at 1667`cm^{-1} for the alpha form. The different frequencies observed for this band for the two crystal forms at 25°C is due to small differences in C=C bond length[82]. Therefore a change in the C=C bond length with the temperature, particularly for the alpha form could be the cause of the frequency shifts observed. As the temperature is lowered from room temperature all bands increase in height while some of them narrow as well. This phenomenon had been reported previously for other polymers[76-80]. This has been explained in terms of the change in intermolecular spacing that causes an increase in the dipole-dipole interaction. Another reason for the increase in intensity is the change in lattice

potential as the molecules get closer to each other, which increases the vibrational force constants. These changes also cause small shifts in some of the bands.

The amorphous fraction of melt crystallized TPI decreases when samples are cooled from Tc to 25°C as discussed above. Further decrease in amorphous fraction occurs below 25°C as shown by plots of subtraction factor versus temperature for melt and solution crystallized alpha and beta TPI given in Figure 3.45. There is no change in amorphous fraction below -78°C for all samples except for the beta melt crystallized sample. Changes in amorphous fractions are not expected to occur below the glass transition temperature. No reasonable explanation is available at this time for this behavior of the beta melt crystallized samples.

4.3. Crystallization of Random Epoxidized TPI

In this study oxirane units were placed in the TPI chain in amounts of 2.2, 5.0 and 9.8% and the polymers were crystallized from the melt using the direct method. The morphology of randomly epoxidized TPI copolymers crystallized from the melt depends on the crystallization condition and the amount of oxirane content. The increases in amorphous fraction observed in this study with increasing epoxidation amount at Tc=25°C is approximately reflected in the morphology with fewer lamellas and less regular structures being seen by SEM, particularly at 9.8% epoxidation. The morphologies for the 2.2% and 5% epoxidized samples, crystallized at

36°C and subsequently cooled to 25°C, show fewer distinguishable structures than those samples with the same epoxy content crystallized by cooling directly to 25°C. However, the amorphous content obtained by the FTIR subtraction factor method at constant epoxidation is not very different.

The final subtraction factor used in figure 4.57 refers to the TPI components of the copolymer. The final subtraction factor for crystallization by cooling to 25°C or to 30°C at each epoxy content is the same within the experimental error of 0.01 and increases linearly with epoxy content. At 36°C the plot deviates significantly from linearity with a sharp increase in subtraction factor occuring between 2.2 and 5% epoxidation. Due to this strong deviation, the sample with 9.8% epoxy content was not expected to crystallize at 36°C, as confirmed experimentally. The final subtraction factor, corrected for the change in number of absorbers in the samples upon cooling and partial crystallization, has been equated in section 3.2.3 to the amorphous fraction for melt crystallized TPI. In this part the uncorrected subtraction factor values are used since the densities necessary to apply the correction are not known for epoxidized samples. The difference in the corrected and uncorrected subtraction factor for the unepoxidized samples is 7%. This difference decreases with increasing subtraction factor. The fraction of units in the chain present in amorphous parts of the sample includes the epoxidized units rejected from the crystal core during the crystallization process. These materials were previously crystallized from solution. Using the combination of suspension epoxidation followed by C-13 NMR

spectroscopy of the product in solution, it was concluded that no detectable epoxidized units were present in the crystal core of the solution crystallized samples for epoxidations up to 5%; there was a evidence of a small number of these units in the crystal core for the 9.8% epoxidized sample. Assuming that the number of epoxidized units included in the crystal core during melt crystallization is negligibly small, the fraction of TPI units in the amorphous regions would be given by multiplication of the subtraction factor by the fraction of TPI units present in the sample. This gives values of 0.68, 0.71, and 0.74 for the fraction of amorphous TPI units in the samples for epoxidations of 2.2, 5.0 and 9.8%, respectively, for Tc =25°C . For Tc = 36°C these values are 0.71 and 0.80 at Tc and 0.65 and 0.74 after cooling to 25°C for epoxidations of 2.2 and 5.0% respectively. The average values for the uncorrected subtraction factor for unepoxidized TPI are 0.66 for Tc = 25°C, 0.68 for Tc =36°C and 0.62 for the samples crystallized at 36°C and subsequently cooled to 25°C. The trends in this corrected subtraction factor with epoxidation amount and temperature are still the same as those evident in figure 3.57.

The rejection of a comonomer unit from the crystal core during the crystallization process should also lead to the rejection of crystallizable units adjacent to the comonomer unit. The number of TPI units rejected would be expected to increase with increasing crystal stem length. This effect was observed to occur for 99% trans, 1% cis-1,4-poly butadiene[114-115,128] crystallized from solution and

for segmented block copolymers of TPI and epoxidized TPI crystallized from solution.

In the study of solution epoxidized TPI crystallized from solution[128] the crystal stem length and the average fold length were determined. The amorphous fraction, equated to the fraction epoxidized and containing the epoxidized units present in the copolymers, was determined to be 0.35, 0.35, 0.37 and 0.38 for samples with 0, 1.4, 2.2 and 5.0 mole % epoxidation, respectively, at T_c = 20°C. For T_c = 10°C values of 0.38 and 0.39 for the 2.2% and 5.0% epoxidized samples, respectively, were obtained. The amorphous fraction for solution crystallized samples is about one-half those for melt crystallized samples having the same amount of epoxy content. The unepoxidized solution-crystallized samples are prepared at a smaller degree of supercooling than the melt crystallized samples. The average lamellar thickness is expected to increase with decreasing amount of supercooling and this should lead to a decrease in the amorphous fraction, as observed for the unepoxidized sample. It is reasonable to assume that this difference in supercooling will prevail for the solution epoxidized TPI samples. The change in amorphous fraction with an increase in epoxidation amount up to 5% is about three times larger for melt-crystallized samples than for solution-crystallized samples. Since the lamellar thickness for the melt crystallized samples is significantly less than for the solution crystallized ones, TPI unit ejection due to epoxy unit ejection is expected to be less. Therefore the larger change in amorphous fraction with increasing epoxidation amount for melt crystallized

samples cannot be attributed to epoxy group ejection but must be due to the intrinsic differences of chain mobility and in the progress of the crystallization process in the two media.

In the FTIR study on the melt crystallization of unfractionated TPI and fractions therefrom it was concluded that the decrease in amorphous fraction upon cooling samples crystallized at 43°C and 36°C in the beta crystal form was largely due to changes in the amorphous parts at lamellar surfaces of structures already formed. This conclusion was supported by similar changes observed upon cooling solution crystallized lamellas. The presence of up to 5.0 mole % epoxidation has no effect on this decrease in amorphous fraction on cooling from Tc = 36°C to 25°C, although the amorphous fraction measured at Tc = 36°C increases in a nonlinear fashion with epoxidation amount.

5. Conclusions

The following conclusions have been drown from the above investigations

1. The morphology of unfractionated synthetic TPI and two fractions therefrom crystallized from the melt in either the alpha or beta crystal form was investigated at Tc and 25°C by SEM.

2. The morphology is found to be lamellar and the organization depends on miolecular weight, crystal form and the crystallization temperature. For the alpha crystal form the size of the structures observed increases with increasing crystallization temperature.

3. Morphology of TPI was studied at T_c and 25°C. Morphological changes did occur when the samples cooled down from T_c to 25°C. Some of this change could be due to secondary crystallization of some completly amorphous chains present at T_c involving the structures already present.

4. Morphology of bulk crystallized solution epoxidized TPI was investigated. Differences in morphology with epoxy content and T_c were observed.

5. The two component assumption was found to be generally valid; subtraction of the amorphous component from spectra obtained after compleate crystallization gave alpha or beta crystal spectra identical to those for the subtracted spectrum from solution crystallized samples.

6. The 1665-1670 cm-1 band was found to be conformationally independent from 0°C to 65°C for melt crystallized TPI sample. It was also found that the amorphous fractions obtained from the subtraction factor and absorbance ratio method were in close agreement, provided a correction for a change in the number of absorbers is made in the subtraction factor method.

7. The rate of crystallization depends on crystallization temperature, method of crystallization and in some cases the molecular weight.

8. The beta crystal containing samples exhibit no clear dependence of amorphous fraction on molecular weight. Therefore all these samples expected to have simillar lamellar thickness distribution.

9. Molecular weight dependence of the amorphous fraction for the alpha form samples at Tc and after cooling to 25°C was observed. This suggests that a difference in lamellar thickness distribution is occuring.

10. The effect of amount of epoxidation and crystallization temperature on crystallization rate and final amorphous fraction also was investigated.

11. A decrease in rate and increase in amorphous fraction with increasing epoxy content was observed.

6. APPENDIX 1

Let AF_r = the true amorphous fraction,

AF_m = the measured amorphous fraction,

x = the number of absorbers at 75°C and x +Δx = the number of absorbers at Tc

$$AF_r/AF_m = x/(x+\Delta x) = m/(m+\Delta m)$$
$$= d_a V_a/d_{pc} V_{pc}$$

where m = mass of amorphous sample

m + Δm = mass of crystallized sample

d_a and V_a are the amorphous density and the amorphous sample volume and d_{pc} and V_{pc} are the density and volume of the crystallized sample

If the sample thickness remains constant,

Va = Vpc and $AF_r/AF_m = d_a/d_{pc}$

7. REFERENCES

1. Meyer, K.H. "Natural Synthetic High Polymers," 2nd Ed; Interscience, New York (1950).

2. Keller, A. J. Polym. Sci, Symp; 1975, 7, 51; 1977, 1, 59.

3. Sharples, A. " Crystallinity " Chap.4 in "Polymer Science" Vol 1, A.D. Jenkins, Ed, North Holland, Amsterdam 1972.

4. Sperling, L.H. " Introduction to Polymer Science " Wiley, New York, 1986.

5. Woodward, A.E. " Atlas of Polymer Morphology," Hanser verlag, Munich, 1989.

6. Kuo, C. Ph.D. Thesis, CUNY, 1984.

7. Keller, A. Kolloid Z u Z. Polym. 1964, 197, 98.

8. Keith, H.D.; Padden, F.J.; Vadimsky, R.G. J. Polym. Sci. A2 1966, 4, 267.

9. Bunn, C.W.; Alcock, T.C. Trans. Faraday. Soc. 1945, 41,317.

10. Keith, H. D in " Physics and Chemistry of the Organic Solid State", (Fox, D etal. Ed) pp 461, Interscience, New York, 1963.

11. Keller, A. Rep. Prog. Phys. 31, part 2, 623, 1968.

12. Keller, A. Phys. Today. 1970, May, Page 42

13. Keller, A.; Keith, H. D.; Bonart, R.; Fischer, E. W. Kolloid Z. 231, 1969

14. Xu, J. PhD. Thesis, CUNY, 1988.

15. Young, R. J. " Introduction to Polymers " Chapman and Hall, 1981.

16. Munk, P " Introduction to Macromolecules Science " Wiley, New York, 1986.

17. Khoury, F. J. Res. Nat. Bur. Std (U.S) 1966, 70A, 29.

18. Keller, A. Phil. Mag. 1957, 2, 1171.

19. Jaccordine, R. Nature. 1955, 176, 305.

20. Fisher, G.W. Z. Naturforsh. 1957, 12a, 753.

21. Till, P.H. J. Polym. Sci. 1957, 24, 301

22. Maxfield, J.; Mandelkern, L. Macromol. 1977, 10, 1141.

23. Natta, G.; Corradini, P. Rubber Chemistry Tech. !960, 33, 703.

24. Niegish, W.D.; Swan, P.R. J. Appl. Phys. 1960, 31, 1906.

25. Basset, D.C.; Keller, A.; Matsuhashi, S. J. Polym. Sci. 1963, A1, 763.

26. Keith, H.D. J. Polym Sci. A2, 1964, 4339.

27. Keith, H.D.; Padden, F.J.Jr. J. App. Phy. 1964, 35, 1270.

28. Keith, H.D.; Padden, F.J.Jr. J. App. Phy. 1964, 35, 1286.

29. Basset, D.C. " Principles of Polymer Morphology " Cambridge University. Press, London, 1981.

30a. Maxfield, J.; Mandelkern, L. Macromolecules. 1977, 10, 1141.

30b. Mandelkern, L.; Go, S.; Peiffer, D.; Stein, R.S. J. Polym. Sci. Polym. phys. Ed. 1977, 15, 1189.

31. Allen, R.C.; Mandelkern, L. J. Polym. Sci, Phy. Ed. 1982, 20, 1465.

32. Kuo, C..; Woodward, A.E. Macromol. 1984, 17, 1034.

33. Xu, J.R.; Woodward, A.E. Macromol. 1986, 19, 1114.

34. Davies, C.; K.L, Long, O.E. J. Mater. Sci. 1977, 12, 2165.

35. Davies, C.; K.L, Long, O.E. J. Mater. Sci. 1979, 14, 2529.

37. Keller, A.; Martuscelli, E. Makromol. chem. 1972, 151, 189.

39. Wunderlich, B. "Macromolecular Physics" Vols 1,2 Academic Press, 1975.

40. Geil, P. H. " Polymer Single Crystals" Wiley, New York, 1963.

41. Yoon, D.J.; Flory, P.J. Polymer. 1977, 18, 509.

42. Vogl, R.; Sillescie, H. Macromolecule.1979, 12, 162.

43. Mandelkern, L. J. Polym. Sci; Polym. Rev. 1975, 50, 457.

44. Jackson, J. F.; Mandelkern, L. Macromolecule. 1968, 1, 547.

45. Illers, K. H.; Kanig, G. Colloid and Polymer. Sci. 1982, 260, 564.

46. Bank, M.I.; Krimm, S. J. Polym. Sci. A2, 1969, 7, 1785.

47. Cheam, T.C.; Krimm, S. J. Polym. Sci; Polym Phys Ed. 1981, 19, 423.

48. Iso.Ando, Sato. H. Polymer. 1985, 26,1864.

49. Calvert, P. Nature. 1976, 263, 371.

50. Hendrix, C.; Whiting, D.A.; Woodward, A.E. Macromol. 1971, 4, 57.

51. Keller, A.; Matreeyek, W.; Winslow, F.H. J. Polym. Sci. 1962,62, 291.

52. Guzman, J.; Fatou, J.G.; Perena, J.M. Makromol. Chem. 1980, 181, 1051.

53. Basset. D.C. Polymer; 1964, 5, 457.

54. Equiluz, M.; Ishida, H.; Hiltner, A. J. Polym. Sci, Polym. Phy. Ed. 1979, 17, 893.

55. Equiluz, M.; Ishida, H.; Hiltner, A. J. Polym. Sci, Polym. Phy. Ed. 1980, 18, 2295.

56. Patel, G. N.; Keller, A. J. Polym. Sci. Polym. Phy. Ed. 1975, 13.

57. Keller, A.; Udagawa, Y. J. Polym. Sci, A2. 1971, 9, 1793.

58. Harrison, I.R.; Baer, E, J. Polym. Sci. A2; 1971, 9, 1305.

59. Wichacheewa, P.; Woodward, A.E. J. Polym. Sci, Polym. Phys. 1978, 16, 1849.

60. Stellman, J.M.; Woodward, A.E. J. Polym. Sci. 1967, B, 7, 755.

61. Stellman, J.M.; Woodward, A.E. J. Polym. Sci. 1971, A2, 9, 59.

62. Tseng, S.; Herman, W.; Woodward, A.E. Macromol. 1982, 15, 3338.

63a. Wang, P.G.; Woodward, A.E. Macromol. 1987, 20, 1818.

63b. Wang, P.G.; Woodward, A.E. Macromol. 1987, 20, 2718.

63c. Wang, P.G.; Woodward, A.E. Macromol. 1987, 20, 1823.

64. Anandakumaran, K.; Herman, W.; Woodward, A.E. Macromol. 1983, 16, 563.

65. Chang, B. H.; Seigmann, A.; Hiltner, A. J. Polym. Sci, Polym. Phys. Ed. 1984, 22, 255.

66. Tishler, F.; Woodward, A.E. Macromol. 1986, 19, 1328.

67. Gavish, M.; Corrigan,J.P.; Woodward, A.E. Macromol.1988, 21, 2079.

68. Koenig, J.L. Appl. Spec. 1975, 29, 293.

69. Methods in Experimental physics, 16A, Chap 3.

Snyder, Infrared and Raman spectra of polymers (Academic Press, New York,1980)

70. Coleman, M.M.; Painter, P.C. J. Macromol. Chem C16. 1978, 2,197

71. Coleman, M.M.; Painter, P.C.; Tabb, D.L.; Koenig, J. L. Polym. Lett. 1974, 12, 577.

72. Painter, P.C.; Koenig, J.L. J. Polym. Sci. Polym. Phy. 1977, 15, 1885.

73. Koenig. J.L.; Antoon, M.K. J. Polym. Sci. Polym. Phy.1978, 15, 1357.

74. Lin, S.B.; Koenig. J.L. J. Polym. Sci. Polym. Phy. 1980, 20, 2277.

75. Orander, L.N. Opt. Spectroscopy (USSR). 1961, 11,68.

76. Hannon, M.J. J. Polym. Sci, A2, 1969, 7,

77. Huang, Y.S.; Koenig, J.K. J. Appl. Polym. Sci, 1971, 15, 1237.

78. Frank, W.; Schmidt, H.; Wuff, W. J. Polym. Sci, Polym. Symp. 1977, 61, 317.

79. Frank, W.; Strohemire. Prog. Colloid and Polym. Sci. 1979, 66, 205.

80. Boreio, E.G.; Koenig, J.K. J. Chem. Phys. 1970, 52, 3425.

81. Petcavich, R. J.; Coleman, M. M. J. Polym. Sci. Polym. Phys. Ed. 1980, 18, 2097.

82. Gavish, M.; Brennan, P.; Woodward, A.E. Macromol. 1988, 21, 2083.

83. Gavish, M.; Woodward, A.E. Polymer. 1989, 30, 905.

84. Mandelkern, L.; Flory, P.J. J. Am. Chem. Soc. 1951, 73, 3206.

85. Mandelkern, L.; Quinn, F. A.; Flory, P.J. J. Appl. Phys. 1954, 25, 830.

86. Flory, P.J.; Mandelkern, L.; Hall, H.K. J. Am. Chem. Soc. 1951, 73, 2532.

87. Gobalan, M.; Mandelkern, L. J. Phys. Chem. 1967,12, 3823.

88. Mancarella, C.; Martucelli, E. Polymer. 1977, 18, 1240.

89. Hay, J.N.; Mills, P.J. Polymer.1982,23,1380.

90. Hay, J.N. J. Polym. Sci. A3 1965, 4, 433.

91. Beech, D. R.; Booth, C.; Hillier, I. H.; Picles, C.J. Europ. Polym. J. 1972, 8, 799.

92. Avrami, M. J. Chem. Phys. 1939, 7, 1103.

93. Avrami, M. J. Chem. Phys. 1940, 8, 212.

94. Avrami, M. J. Chem. Phys. 1941, 9, 177.

95. Hoffman, J. D. Polymer. 1983, 24, 3.

96. Hoffman, J. D. Polymer. 1982, 23, 656.

97. Dimarzio, E.A.;. Guttman, C.M.; Hoffman, J.D. Faraday. Discuss. Chem. Soc, 1979, 68, 210.

98. Hay, J. N.; Sabin, M. Polymer. 1969, 10, 203.

99. Cooper, W.; Vaughan, G. Polymer. 1963, 4, 329.

100. Keith, H. D.; Padden, J. R. J. Appl. Phys. 1964, 35, 1286.

101. Palys, L. H.; Phillips, J. J. Polym. Sci. Polym. Phys. Ed. 1980, 18, 829.

102. Ergoz, E.; Fatou, J. G.; Mandelkern, L. Macromol. 1972, 5, 147.

103. Walter, E.R.; Reding, F.P. J. Polym. Sci. 1958, 20, 561.

104. Swan, P.R. J. Polym. Sci. 1962, 56, 409.

105. Wunderlich, B.; Poland, D, J. Polym. Sci. A 1963, 1, 357

106. Bodely, D.M.; Wunderlich, B.; J. Polym. Sci. A-2 1966, 4, 25

107. Roe, R.J.; Gerniewski, C. Macromolecules. 1972, 6, 212

108. Mandelkern, L.; Baker, C. H. Polymer. 1966, 7, 71

109. Holidsworth, P.J.; Keller, A. Makromol. Chem. 1969, 125, 70

110. Harrison, I.R.; Baer, E. J. Polym. Sci, Polym. Phy. Ed. 1971, 9, 843

111. Briber, R.M.; Thomas, E.L. Polymer. 1985, 26, 8.

112. Briber, R.M.; Thomas, E.L. Polymer. 1986, 27, 66.

113. Marchetti, A.; Martuscelli, E, J. Polym. Sci, Polym. Phy. Ed. 1976, 14, 157

114. Corrigan, J.P.; Zemel, I.S.; Woodward, A.E. J. Polym. Sci, Part B. 1989, 27, 1135.

115. Corrigan, J.P.; Zemel, I.S, Corrigan, J.P, Woodward, A.E. J. Polym. Sci, Part B; 1989, 27, 2479.

116. Cooper, W.; Vaughan, G. Polym 1963, 4, 329.

117. Flangan, R. D.; Rijke, A. M. J. Polym. Sci, Part A-2 1972, 10, 1207

118. Takehashi, Y.; Sato, T.; Tadokoro, H.; Tanaka, Y. J. Polym Sci, Polym. Phys. Ed. 1973, 11, 233.

119. Bunn, C. W. Proc. R. Soc. London. 1942, 180, 40.

120.Patterson, D. J.; Koenig, J. L. Polymer 1988, 29, 240.

121. Vasanthan, N.; Corrigan, J. P.; Woodward, A.E. Polymer, 1993, 34, 2270

122. Lovering, E. G.; Wooden, D. C. J. Polym. Sci-A2. 1969, 7, 1639.

123. Maxfield, J.; Madelkern, L. Macromol. 1977, 10, 550.

124. Allen, R. C.; Mandelkern, L. J. Polym. Sci. Polym. Phys. Ed. 1982, 20, 1465.

125. Wang, P.; Woodward, A. E. Makromol Chem, 1989, 190, 875.

126. Vogiet-Martin, I. G.; Mandelkern, L. J. Polym. Sci. Polym. Phys. Ed. 1984, 22, 1901

127. Mukherji, S.; Woodward, A. E. J. Polym. Sci. Polym. Phys. Ed. 1984, 22, 793.

128. Xu, J.; Woodward, A. E. Macromol. 1988, 21, 1988.